

7-2-2012

Evaluation of the laboratory resilient modulus test using a New Mexico subgrade soil

Anthony Cabrera

Follow this and additional works at: https://digitalrepository.unm.edu/ce_etds

Recommended Citation

Cabrera, Anthony. "Evaluation of the laboratory resilient modulus test using a New Mexico subgrade soil." (2012).
https://digitalrepository.unm.edu/ce_etds/63

This Thesis is brought to you for free and open access by the Engineering ETDs at UNM Digital Repository. It has been accepted for inclusion in Civil Engineering ETDs by an authorized administrator of UNM Digital Repository. For more information, please contact disc@unm.edu.

Anthony Sebastian Cabrera

Candidate

Civil Engineering

Department

This thesis is approved, and it is acceptable in quality and form for publication:

Approved by the Thesis Committee:

Dr. Rafiqul A. Tarefder, Chairperson

Dr. Mahmoud R. Taha

Dr. Tang-Tat Ng

**EVALUATION OF THE LABORATORY RESILIENT
MODULUS TEST USING A FINE-GRAINED NEW MEXICO
SUBGRADE SOIL**

by

ANTHONY SEBASTIAN CABRERA

**B.S. CIVIL ENGINEERING, UNIVERSITY OF NEW MEXICO,
DECEMBER 2009**

THESIS

Submitted in Partial Fulfillment of the
Requirements for the Degree of

**Master of Science
Civil Engineering**

The University of New Mexico
Albuquerque, New Mexico

May 2012

ACKNOWLEDGEMENTS

I would like to acknowledge my advisor and the chair of my committee, Dr. Rafi Tarefder, for funding me as a research assistant and providing me the opportunity to conduct this study. I also would like to thank the other members of my committee, Dr. Mahmoud Taha and Dr. Tang-Tat Ng. Your participation is greatly appreciated.

Thanks to the Civil Engineering staff. Yolanda, Candyce, Josie, Ambrose, and Rebekah.

I would also like to thank the New Mexico Department of Transportation Research Bureau for project funding and equipment used in this study. I specifically would like to thank the members of my project technical panel: Virgil Valdez, Jeff Mann, Robert McCoy, Parveez Anwar, Bob Meyers, and Bryce Simons.

I must give credit to Dr. John Stormont and Lary Lenke, for giving me my first opportunity in geotechnical materials testing as an undergraduate student. Those projects provided valuable experience. The quality and attention to detail you taught me by example helped me with this research and will no doubt benefit me in my future career. Jacob Hays, your knowledge and hard work were invaluable to the projects we worked on together. Ken Martinez, thanks for your support and lending me equipment to use in this study. Also, thanks to Naomi Waterman, Gahzanfar Barlas, and Tahmid Rahman for your participation in the lab.

Last but not least, Mekdim Weldegiorgis and Damien Bateman, it was great working with you guys and it has been a blessing having you as friends.

EVALUATION OF THE LABORATORY RESILIENT MODULUS TEST USING A NEW MEXICO FINE-GRAINED SUBGRADE SOIL

by Anthony Sebastian Cabrera

B.S. Civil Engineering, University of New Mexico, 2009
M.S. Civil Engineering, University of New Mexico, 2012

Abstract

Resilient modulus (M_r) is a laboratory determined parameter, where a cylindrical specimen is subjected to dynamic axial stresses under confining stresses, while axial deformations are measured. By definition M_r is the ratio of the peak axial stress to the corresponding recoverable axial strain. Currently, there are two accepted laboratory testing protocols for determining M_r , namely AASHTO T 307 and NCHRP 1-28A. These two standards differ from one another in ways that are known to affect M_r , namely in location of load and deformation transducers.

One focus of this study is the determination of resilient modulus for an A-6 subgrade soil at varying moisture conditions (± 2 -3% relative to optimum). Specimens of 2.8 inch and 4 inch diameters are reconstituted using modified proctor compaction. Resilient modulus values are determined using internal and external deformation measurement techniques. Comparative analyses are performed, and based on the results a multivariate regression equation has been developed which estimates resilient modulus as a function of gravimetric moisture content and maximum cyclic axial stress for this soil.

A second focus of this study is aimed at addressing the potential for reducing the time and complexity required to determine M_r of a cohesive fine-grained subgrade soil. An experimental study is conducted, where unconfined dynamic testing is performed. In this study, load pulse forms and durations differ from standardized tests. Test sequence durations are also reduced. Resilient Modulus values determined from this alternate testing experiment match well with values determined from the standardized test results. Alternate and Standard M_r values are within 15% of each other for 35 of 40 test comparisons, with an average magnitude difference of 9%.

TABLE OF CONTENTS

LIST OF FIGURES	ix
LIST OF TABLES	xi
CHAPTER 1	1
INTRODUCTION.....	1
Introduction.....	1
1.2 Evaluating Testing Methods for Cohesive Fine-Grained Soils	4
1.3 Reducing Testing Time for Cohesive Fine-Grained Soils	9
1.3 Objectives	10
1.4 Thesis Outline	11
CHAPTER 2	13
LITERATURE REVIEW	13
2.1 Introduction.....	13
2.2 Resilient Modulus Standards	14
2.2.1 AASHTO T307-99.....	14
2.2.2 NCHRP 1-28A.....	18
2.2.3 Summary of Current Test Protocols	22
2.3 Equipment Effects and Deformation Measurement Techniques	23
2.3.1 Load Cell.....	23
2.3.2 Effect of Deformation Measurement on Mr	24
2.3.3 Triaxial Cell	29
2.4 Resilient Modulus of Fine Grained Soils.....	30
2.4.1 Effect of Moisture Content	30
2.4.2 Testing Influences	31
2.4.3 Constitutive Models	32
CHAPTER 3	35
MATERIALS, SPECIMEN PREPARATION, AND TESTS METHODS	35
3.1 Introduction.....	35
3.2 Materials and Classifications	35

3.3 Moisture-Density Relationship	38
3.4 Specimen Preparation	40
3.4.1 Specimen Compaction	40
3.4.2 End Treatments	45
3.5 Test Methods.....	46
3.5.1 Resilient Modulus Testing	48
3.5.2 Alternate Mr Testing Experiment	55
CHAPTER 4.....	57
RESILIENT MODULUS RESULTS AND DISCUSSION.....	57
4.1 Introduction.....	57
4.2 Objective.....	57
4.3 Resilient Modulus Testing	58
4.3.1 2.8 inch Diameter Specimens	58
4.3.2 4 inch Diameter Specimens	66
4.3.3 Resilient Modulus Results Discussion.....	68
4.4 Static Testing Results.....	84
4.4.1 Unconfined Compression Testing Results.....	84
4.4.2 Elastic Modulus Testing	87
4.5 Multivariate Linear Regression.....	88
4.6 Resilient Modulus Testing Summary.....	93
CHAPTER 5	94
EXPERIMENTAL ALTERNATE Mr TEST RESULTS.....	94
5.1 Introduction.....	94
5.2 Objective.....	96
5.3 Alternate Method Results of 2.8 inch Diameter Specimens	97
5.3.1 Dry of Optimum.....	97
5.3.2 Optimum	99
5.3.3 Wet of Optimum	100
5.3.4 Discussion of 2.8 inch diameter Alternate Mr Method Results.....	101
5.4 Alternate Experiment Results of 4 inch Diameter Specimens.....	103
5.4.1 Dry of Optimum.....	104

5.4.2 Optimum	105
5.4.3 Wet of Optimum	105
5.4.4 Discussion of 4 inch diameter Alternate M_r Experiment Results	106
5.5 Comparison of 2.8 and 4 inch Diameter Alternate M_r Method Results	107
5.6 Comparison of M_r Results Using Alternate and Standard Method	108
5.6.1 Comparison to Standardized M_r Using Linear Regression of Test Sets	109
5.6.2 Comparison to Standardized M_r Using Segmented Regression Prediction.....	111
5.7 Alternate M_r Test Summary	113
CHAPTER 6.....	115
CONCLUSIONS AND RECOMMENDATIONS.....	115
6.1 General.....	115
6.2 Conclusions.....	115
6.3 Recommendations.....	117
REFERENCES	121

LIST OF FIGURES

Figure 1.1 Cylindrical M_r Specimen Stress Illustration	2
Figure 1.2 Example M_r Cycle Illustrating Axial Stress and Strain.....	2
Figure 1.3 Example M_r Setup Schematic Illustrating Transducer Locations	5
Figure 2.1 Example T 307 Test Setup (Source: AASTHO T 307-99).....	17
Figure 3.1 U.S. 491 Gallup to Shiprock.....	36
Figure 3.2 Backhoe Loader Removing Soil Used In This Study.....	36
Figure 3.3 Sample of Soil Used in Study.....	37
Figure 3.4 Determining Atterberg Limits	38
Figure 3.5 Example of Mixing Procedure.....	38
Figure 3.6 Moisture-Density Relationship.....	39
Figure 3.7 Compaction Size and Lift Illustration (Not to Scale).....	42
Figure 3.8 Split Molds Used for Compaction.....	43
Figure 3.9 Mold Setup with Membrane and Applied Vacuum.....	44
Figure 3.10 Example of Gypsum Cement Capping Method.....	46
Figure 3.11 Universal Testing Systems Used in Study.....	48
Figure 3.12 Load Cell for Used For Resilient Modulus and Alternate Testing.....	49
Figure 3.13 Haversine Load Pulse (Source: AASHTO T 307-99 protocol).....	50
Figure 3.14 Example of Stress during Last Five Resilient Modulus Cycles	51
Figure 3.15 Example Strain Behavior during Last Five Resilient Modulus Test Cycles	51
Figure 3.16 LVDT Setup for Glued Button Deformation Measurement.....	52
Figure 3.17 Epoxied Button Examples	53
Figure 3.18 Ring Clamp Method Examples	54
Figure 3.19 External LVDT Setup Clamped to Loading Piston.....	54
Figure 3.20 Example of Alternate Test Stress-Strain Response Form and Consistency	56
Figure 4.1 M_r Plot 2.8 inch Diameter Dry of Optimum MC, $\sigma_3 = 4$ psi	59
Figure 4.2 M_r Plot 2.8 in. Diameter @ Optimum MC, $\sigma_3 = 4$ psi.....	61
Figure 4.3 M_r Plot 2.8 in. Diameter Wet of Optimum MC, $\sigma_3 = 4$ psi.....	63
Figure 4.4 Dry of Optimum M_r including Higher Stress Sequences 2.8 inch Diameter Specimens	65
Figure 4.5 Optimum M_r including Higher Stress Sequences 2.8 inch Diameter Specimens.....	65
Figure 4.6 Wet of Optimum M_r including Higher Stress Sequences 2.8 inch Diameter Specimens	66
Figure 4.7 M_r Plot 4 inch Diameter, $\sigma_3 = 4$ psi	68
Figure 4.8 Load Cell Output vs. Deflection.....	72
Figure 4.9 Example of Deformation Accounts 2.8 inch Diameter Specimens	74

Figure 4.10 Internal Deformation Measurement Comparison Plot	79
Figure 4.11 Internal Deformation Measurement Comparison Plot 2	79
Figure 4.12 Resilient Modulus Size Comparison	80
Figure 4.13 Dry of Optimum 2.8 inch vs. 4 inch Plot	81
Figure 4.14 Optimum 2.8 inch vs. 4 inch Plot	82
Figure 4.15 Wet of Optimum 2.8 inch vs. 4 inch Plot	83
Figure 4.16 2.8 inch Diameter UCS Plot	85
Figure 4.17 4 inch Diameter UCS Plot	86
Figure 4.18 Elastic Modulus Results 4 in. Diameter Specimens	88
Figure 4.19 Predicted vs. Measured M_r as a function of $\sigma_{\max\text{cyclic}}$ and Moisture Content	92
Figure 4.20 Predicted vs. Measured M_r as a function of $\sigma_{\max\text{cyclic}}$ and Moisture Content	92
Figure 5.1 Stress and Strain vs. Time	98
Figure 5.2 Alternate Experimental Test Stress-Strain Plot	99
Figure 5.3 Alternate Experiment Resilient Modulus vs. Moisture Content	101
Figure 5.4 2.8 inch Diameter Alternate Experiment and Standard Resilient Modulus Results.	102
Figure 5.5 Alternate Experiment Method Stress and Strain versus Time	103
Figure 5.6 4 inch Diameter Wet of Optimum Stress-Strain Plot	104
Figure 5.7 Alternate Method Resilient Modulus vs. Moisture Content for 4 in. Diameter	106
Figure 5.8 Alternate Method Resilient Modulus vs. Moisture Content for All Specimens	107
Figure 5.9 Alternate Method Resilient Modulus Specimen Size Comparison	108
Figure 5.10 Example of Method 1 Prediction Fits for Standard M_r Results	110
Figure 5.11 Test Method Comparison Plot 1	111
Figure 5.12 Test Method Comparison Plot 2	113

LIST OF TABLES

Table 1.1 AASHTO T 307 Subgrade Test Sequences for Fine-Grained Soils.....	3
Table 1.2 Resilient Modulus Compaction Methods according to Test Standard and Size.....	8
Table 2.1 AASHTO T 307 Load Cell and LVDT Capacity and Range Requirements	16
Table 2.2 AASHTO T307 Subgrade Sequence for Type 2 Soils	18
Table 2.3 NCHRP 1-28A Testing Sequence for Fine-Grained Subgrades	19
Table 2.4 NCHRP 1-28A Load Cell Requirements.....	21
Table 2.5 Various M_r Test Protocol Differences	22
Table 3.1 Gradation Information	37
Table 3.2 Equivalent blows per lift using modified compaction effort	42
Table 3.3 Moisture Contents at Fabrication and Post-Testing for 2.8 inch Diameter Specimens	45
Table 3.4 Test Matrix for 2.8 inch Diameter Specimens.....	47
Table 3.5 Test Matrix for 4 inch Diameter Specimens	47
Table 4.1 2.8 in. Diameter @ 2% Dry of Optimum MC M_r Results.....	59
Table 4.2 2.8 in. Diameter @ Optimum MC M_r Results	61
Table 4.3 2.8 in. Diameter Wet of Optimum MC M_r Results.....	63
Table 4.4 4 inch Diameter M_r Results.....	67
Table 4.5 Confining Pressure Effect 2.8 inch Diameter Dry of Optimum	70
Table 4.6 Confining Pressure Effect 2.8 inch Diameter Optimum.....	70
Table 4.7 Confining Pressure Effect 2.8 inch Diameter Wet of Optimum.....	70
Table 4.8 Confining Pressure Effect 4 inch Diameter	71
Table 4.9 Extraneous Deformation Estimation 2.8 inch Diameter Specimens.....	73
Table 4.10 Internal Deformation Measurement Comparison 2.8 in. Dry of Optimum	76
Table 4.11 Internal Deformation Measurement Comparison 2.8 in. Optimum.....	77
Table 4.12 Internal Deformation Measurement Comparison 2.8 in. Wet of Optimum.....	77
Table 4.13 Internal Deformation Measurement Comparison 4 in. Specimens.....	78
Table 4.14 Dry of Optimum 2.8 inch vs. 4 inch Diameter Comparison.....	81
Table 4.15 Dry of Optimum 2.8 inch vs. 4 inch Diameter Comparison.....	82
Table 4.16 Wet of Optimum 2.8 inch vs. 4 inch Diameter Comparison	83
Table 4.17 2.8 inch Diameter UCS Values.....	85
Table 4.18 4 inch Diameter UCS Results	86
Table 4.19 Elastic Modulus Values from Static Test on 4 inch Diameter Specimens	87
Table 4.20 Prediction Equation and ANOVA Table Using 3 Predictors (Cyclic Stress, Moisture Content, and Confining Pressure).....	90

Table 4.21 Prediction Equation and ANOVA Table Using 2 Predictors (Cyclic Stress and Moisture Content)	90
Table 4.22 Prediction Equation and ANOVA Table Using 4 Predictors (Cyclic Stress, Moisture Content, Confining Pressure, and UCS)	91
Table 4.23 Prediction Equation and ANOVA Table Using 4 Predictors (Cyclic Stress, Moisture Content, Confining Pressure, and UCS)	91
Table 5.1 Dry of Optimum Alternate Experiment Test Results	98
Table 5.2 Optimum Alternate Experiment Test Results	100
Table 5.3 Wet of Optimum Experiment Test Results.....	100
Table 5.4 Alternate Method Results for 4 inch Diameter Dry of Optimum	104
Table 5.5 Alternate Method Results for 4 inch Diameter at Optimum.....	105
Table 5.6 Alternate Method Results for 4 inch Diameter Wet of Optimum.....	105
Table 5.7 Size Comparison of Alternate Method Resilient Modulus Results	108
Table 5.8 Standard vs. Alternate Experiment Test Results Method 1 Comparison	110
Table 5.9 Standard vs. Alternate Experiment Test Results Method 2 Comparison	112

CHAPTER 1

INTRODUCTION

Introduction

Resilient modulus is a measure of stiffness corresponding to resilient strains due to cyclic loads at various stress combinations designed to simulate traffic loads a soil element would experience based on its respective location within the pavement structure. Mathematically M_r is defined by Eq. (1.1):

$$M_r = \frac{\sigma_{cyclic}}{\epsilon_r} \quad (1.1)$$

where σ_{cyclic} is the maximum axial cyclic stress, and ϵ_r is the resilient strain associated.

Resilient modulus is an input used in the recently developed Mechanistic Empirical Pavement Design Guide (MEPDG) (NCHRP 1-37A (2004)). The input is used to characterize stress-strain behavior in unbound base, subbase, and subgrade materials which support an asphalt pavement surface layer. Resilient modulus is determined in laboratory, and is a stress controlled test. MEPDG currently recommends two laboratory protocols for determining resilient modulus, NCHRP 1-28A and AASHTO T 307-99. In these protocols, a cylindrical specimen with a 2:1 height to diameter ratio is subjected to various axial and confining stress combinations within a triaxial confining chamber. Figure 1.1 shows a general illustration of the stresses applied to a test specimen, where $\sigma_1 - \sigma_3$ represents the axial deviatoric stress and σ_3 is the confining stress applied by air pressure. Figure 1.2 illustrates a typical axial loading cycle, where stress and

strain are plotted to show the two parameters used for determining a respective M_r value for the cycle.

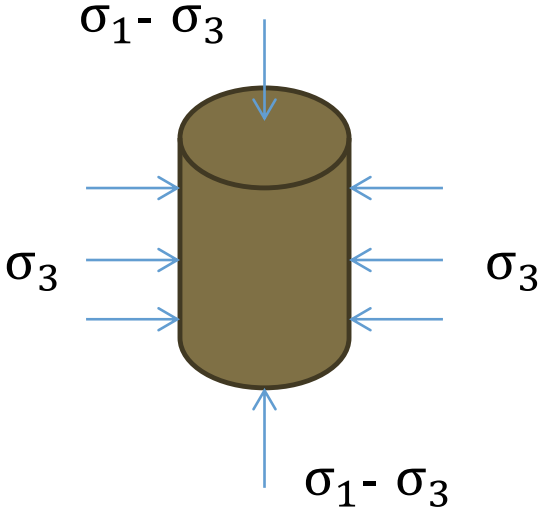


Figure 1.1 Cylindrical M_r Specimen Stress Illustration

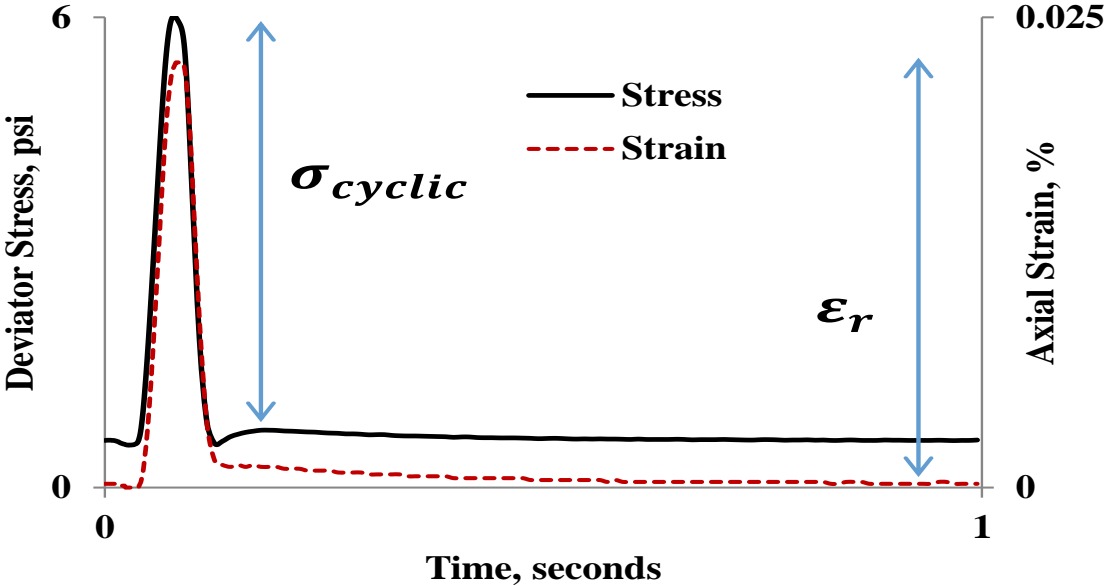


Figure 1.2 Example M_r Cycle Illustrating Axial Stress and Strain

It is noted that in Figure 1.2, the minimum stress is not zero, but rather a constant contact stress that is applied throughout the test which is 10% of the deviatoric stress as shown Table 1.1. For fine-grained subgrade testing, the most common test sequencing used follows AASHTO T 307-99 “Determining the Resilient Modulus of Soils and Aggregate Materials.” Table 1.1 lists the test sequences of AASHTO T 307, where an initial conditioning sequence is typically applied for 500 cycles followed by 15 stress combinations each lasting 100 cycles. The test sequences combine 6, 4, and 2 psi confining stresses with 2, 4, 6, 8, and 10 psi maximum cyclic axial stresses. For each of the 15 test sequences an M_r value is determined as the average M_r of the last 5 cycles (cycles 95-100).

Table 1.1 AASHTO T 307 Subgrade Test Sequences for Fine-Grained Soils

Sequence No.	Confining Pressure, σ_3	Deviator Stress, σ_d	Cyclic Stress, σ_{cyclic}	Seating Stress, $0.1\sigma_d$	No. of Loading Cycles
	psi	psi	psi	psi	
0	6	4	3.6	0.4	500
1	6	2	1.8	0.2	100
2	6	4	3.6	0.4	100
3	6	6	5.4	0.6	100
4	6	8	7.2	0.8	100
5	6	10	9.0	1.0	100
6	4	2	1.8	0.2	100
7	4	4	3.6	0.4	100
8	4	6	5.4	0.6	100
9	4	8	7.2	0.8	100
10	4	10	9.0	1.0	100
11	2	2	1.8	0.2	100
12	2	4	3.6	0.4	100
13	2	6	5.4	0.6	100
14	2	8	7.2	0.8	100
15	2	10	9.0	1.0	100

It was introduced that there are two recommended protocols for laboratory determination of resilient modulus, and it is noted that there are various differences and similarities between the two standards related to stress sequences, load pulse form, deformation measurement, and compaction methods, which are further detailed in Chapter 2. The main concentration of this study, in regards to the differences between test protocols, relates to deformation measurement and compaction method. Determining resilient modulus is a complex and time consuming test, sensitive to many variables, both equipment and material related. Resilient modulus testing includes small deviator stresses and measuring small deformations, therefore it is critical that measurements are accurate and any erroneous deformations be eliminated. That being said, ultimately with any complex laboratory test, it is desirable to determine if a more efficient test can produce the same results. The first problem this research seeks to evaluate is the difference in resilient modulus results produced by using deformation measurement methods of the two different testing protocols. The second problem is the time it takes to run a test, thus the need exists to evaluate if a faster alternate test relative to standard M_r protocols can produce comparable results for a cohesive fine grained soil. What follows is a more detailed account of the two problems introduced.

1.2 Evaluating Testing Methods for Cohesive Fine-Grained Soils

The current accepted standards for determining resilient modulus are:

- Determining the Resilient Modulus of Soils and Aggregate Materials (AASHTO T 307-99 (2003))
- Harmonized Test Methods for Laboratory Determination of Resilient Modulus for Flexible Pavement Design. (NCHRP 1-28A)

While there are many differences between the two standards, one difference that this study focuses on is the location of the LVDTs used to measure axial deformation. Figure 1.3 is a general schematic of the laboratory setup for determining resilient modulus, where the respective locations of the transducers used to determine M_r are called out according to their associated test protocols.

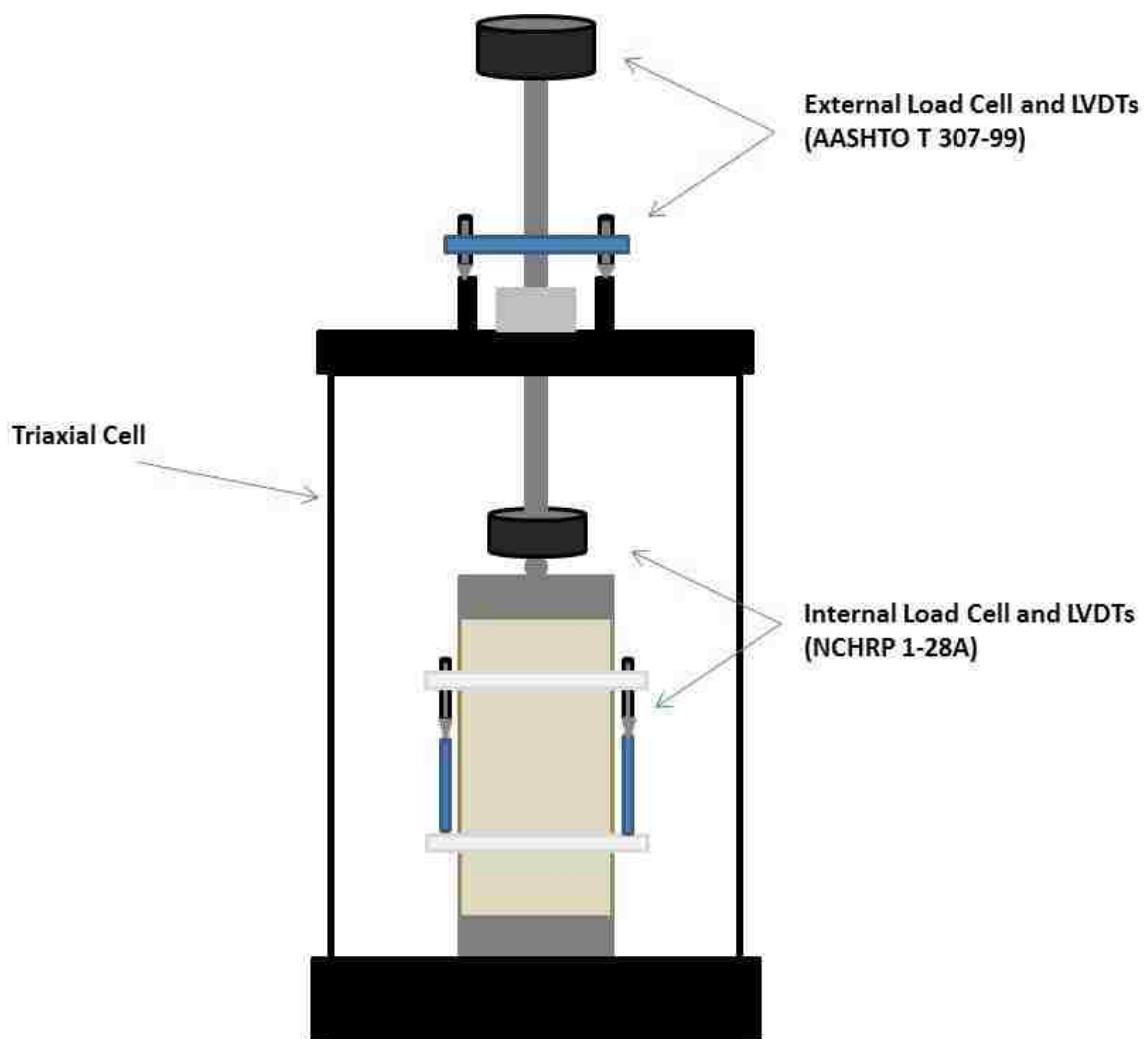


Figure 1.3 Example M_r Setup Schematic Illustrating Transducer Locations

Boudreau and Wang (2003) concluded that though internal measurements for stress and strain can eliminate or reduce the errors associated with the equipment variation, internal instrumentation is very difficult and time consuming. AASHTO T 307 requires externally mounted spring type LVDTs, while NCHRP 1-28A calls for internal LVDTs where deformations are measured on the test specimen. External LVDTs make test setup less difficult than mounting internal LVDTs, however many publications have pointed out the difference in values between the two measurement methods and/or the potential influence of erroneous deformations on resilient modulus values when using external LVDTs (Greoger et al. (2003), Beharano et al. (2003), Konrad and Robert (2003), Boudreau and Wang (2003), Mohammad et al. (1994) Kim and Drabkin (1994), Burczyk et al. (1994), Barksdale et al. (1990)). Many of these studies use comparisons of measurements on specimen using spring-type LVDTs located in ring clamps on the specimen versus actuator mounted external LVDTs. Other researchers have found that in regards to deformation measurement the best method to determine resilient modulus, though more difficult, is fixing buttons to the specimen (Barksdale et al. (1997), Andrei (2003)). Of the two studies introducing fixing buttons to a specimen, one included a comparison to results using ring clamp LVDTs holders where resilient modulus tests were conducted on synthetic specimens with known stiffness values. It is believed, based on review of the literature, that no study has been conducted comparing the fixed button spring type LVDTs to ring clamped hollow core LVDTs. In addition to comparing these two methods, the current study also compares results from external LVDTs i.e. the influence of system compliance on resilient modulus. The method for fixing the buttons to the specimen is also believed to be previously untested in such a comparison study, where the buttons are similarly epoxy glued, a portion of the specimen is scraped out and filled with glue followed by placement of the button. The void is completely

filled by the epoxy and the button becomes fixed in place. Another difference between the two standards is the type of compaction method when reconstituting specimens. AASHTO T 307, mentions multiple methods compaction for fabricating resilient modulus specimens namely, vibratory, static, and kneading compaction. However, regarding compaction, the standard method for determining moisture-density relationships of soils is to use impact compaction due to a standard or modified proctor compaction effort (AASHTO T 99 or T 180). While AASHTO T 307 requires a standard or modified compaction effort to determine the optimum moisture content and maximum dry density of a remolded resilient modulus specimen, it does not mention standard or modified compaction efforts as method for fabricating test specimens. NCHRP 1-28A does allow for impact compaction, however only specimens of 4 inch and 6 inch diameters are considered. In general there are three standard sizes of resilient modulus specimens: 2.8, 4, and 6 inch diameters with 2:1 height to diameter ratio. Fine grained cohesive soils meet the AASHTO T 307 criteria for being reconstituted into a 2.8 inch diameter specimen size according to the largest particle diameter being smaller or equal to one-fifth the size of the mold diameter. However, NCHRP 1-28A does not include reconstituted 2.8 inch diameter specimens, only undisturbed specimens of this size are considered. Table 1.2 shows the size and compaction methods followed by AASHTO T307 and NCHRP 1-28a methods.

Table 1.2 Resilient Modulus Compaction Methods according to Test Standard and Size

Resilient Modulus Test Protocol Compaction Methods			
Test Standard	Reconstituted M_r Specimen Diameter (in.)		
	2.8	4.0	6.0
AASHTO T 307	Vibratory, Static, Kneading	Vibratory, Static, Kneading	Vibratory, Static, Kneading
NCHRP 1-28A	N/A	Vibratory, Kneading, Impact	Vibratory, Kneading, Impact

A 2.8 in. diameter specimen at 2:1 height to diameter ratio requires approximately one third the amount of material compared to that required by 4 in. diameter specimens. Also, the time needed to compact is significantly less for the smaller specimen. Past studies have shown the effect of impact versus kneading compaction do not significantly influence resilient modulus of cohesive subgrade soils, particularly those compacted at optimum and wet of optimum conditions (Muhanna et al. (1999), Barksdale et al. (1997)). In addition, these researchers have commented on the difficulty in obtaining target densities and moisture contents when using kneading compaction as well as the fact that impact compaction is the standard which dictates in-situ values. In the interest of using less material, time, and effort, and because compaction by the proctor hammer is used for characterizing the moisture-density relationships of soils, the potential of effect of compaction for determining resilient modulus of 2.8 inch diameter specimens should be examined.

1.3 Reducing Testing Time for Cohesive Fine-Grained Soils

According to Marr et al. (2003) three issues have deterred researchers from running resilient modulus tests, these include: test complexity, equipment cost, and variations in results. This presents the need for a laboratory method of determining resilient modulus that is both more simple and efficient in setup and test duration. While a majority of time to generate resilient modulus results may lie in specimen preparation and equipment setup, reducing the testing time itself would be beneficial, especially if large amounts of tests need to be performed to build up material databases used for design.

For cohesive fine-grained soils, it is believed the potential exists to reduce the testing time by half or more by eliminating testing sequences or developing an alternate test. Several researchers have found that confining pressure does not significantly affect M_r of cohesive fine grained soils. That is to say, unconfined testing is adequate for resilient modulus characterization (Muhana et al. 1999, Thompson and Robnett 1979, Fredlund et al. 1977). Li and Qubain (2003) point out that cohesive soils in AASHTO T292-96 were only tested at a single confining pressure because the range of confining pressure expected within subgrades are small and have minimal effect on M_r values obtained from cohesive specimens. It is important to evaluate if a second dynamic test, which is faster and unconfined, can yield results comparable to those of the standard resilient modulus test for cohesive fine grained soils. Based on the literature, such faster unconfined or single confining pressure tests have been performed in Illinois and Indiana (Kim and Siddiki (2006), Tutumuler and Thompson (2005)). However, these tests have been limited to using standardized sequences. In this study a test is introduced

which includes differences from standardized sequences such as load pulse form, duration, and elimination of contact stresses and rest period.

1.3 Objectives

Specific objectives of this study are the following:

1. To evaluate various deformation measurement methods and determine the feasibility of using impact compaction for preparing 2.8 inch diameter specimens for M_r testing. This specifically includes determining resilient modulus testing for impact compacted specimens of 2.8 in. and 4 in. using two internal deformation methods and one external deformation method. Specimens at varying moisture contents, because resilient modulus of cohesive fine-grained subgrade soils are known to be affected by moisture content, this will provide a larger range of stiffness values for comparison. In addition, the resilient modulus values at various moisture contents of this specific New Mexico subgrade soil can benefit design considerations.
2. Evaluate an alternate testing technique for determining M_r , which is more efficient. In particular, a test is set up where confining pressure is eliminated and sequences are 60 cycles rather than 100 cycles is examined. Additionally the load pulse form and duration are changed. Based on the stress and strain behavior of specimens during alternate testing, resilient modulus values are then determined and compared to results from the standardized sequences tested for as part of Objective 1. For this method the reference

deformation measurement method (fixed glued button LVDTs) is used for both testing and standard results comparison.

1.4 Thesis Outline

Chapter 1 introduced resilient modulus as well as some areas this research will attempt to investigate. Chapter 2 is a technical literature review focused on previous research relevant to the scope of this thesis. Chapter 2 focuses on testing standards, test equipment effects and deformation measurement techniques, and resilient modulus of cohesive fine-grained soils. Chapter 3 introduces the reader to the materials used in this study, including preliminary soil information (such as gradation, moisture density relationship, Atterberg limits etc.). This chapter also includes information on specimen preparation, as well as the testing equipment and test methods used. Chapter 4 provides the results of the completed tasks of Objective 1. Results are presented in tabular and graphical forms and are generally separated by specimen size, moisture contents, standard/deformation measurement type, and test method. Chapter 4 includes discussions on comparisons between deformation measurement methods and specimen sizes. An initial look at Chapter 4 results shows that for the selected deformation measurement method, resilient modulus shows a decreasing linear trend with increasing deviator stresses and moisture contents have a significant effect, while not showing significant variation due to confining pressure. To examine this, a multivariate linear regression analysis is performed analyzing the effects and significance of these variables and a prediction equation is generated as a function of deviator stress and moisture content. Chapter 5 provides results from the alternate method for determining resilient modulus that are determined from the completion of tasks in the second objective. This includes discussion and comparison of results based on moisture contents and

sizes. Chapter 5 concludes with a comparison of alternate test method results to standard resilient modulus values at equivalent maximum axial cyclic stresses.

Chapter 6 summarizes the findings of this study, and culminates with conclusions and recommendations.

CHAPTER 2

LITERATURE REVIEW

2.1 Introduction

Resilient modulus is an input parameter for unbound pavement layers in the Mechanistic Empirical Design Guide (MEPDG) and is defined as the stress divided by strain that is recoverable due to repeated axial loads. Direct measurement of resilient modulus is determined in the laboratory by applying a combination of deviator and confining stresses while measuring the corresponding axial strain. This chapter focuses mainly on three topics:

- The current standards for performing resilient modulus tests
- Test equipment effects and deformation measurement techniques
- Resilient modulus of fine grained soils

Many sources of this literature review come from *Resilient Modulus Testing or Pavement Components ASTM STP1437*, a compilation of papers for a June 2002 symposium (Durham et al. (2003)). Though many of the publications referenced in this review are 10 to 20 years old, they are relevant to this study. Many current resilient modulus studies focus on modeling, empirical predictive equations, or field correlations. Such studies are necessary, however it is very possible to neglect the fact that the data used for development or validation can come from different protocols producing that produce different results.

This chapter provides the reader with a background understanding resilient modulus as it applies to subgrade soils, as well as an appreciation of the intricacies of the test and factors that can influence results.

2.2 Resilient Modulus Standards

Many authors have discussed the history of resilient modulus testing, from its inception to the evolution of standards. Andrei (1999) went into great depth in detailing and comparing the four recent standards at the time: AASTHO T 292-91, AASHTO T 294-92, AASHTO TP46-94 and NCHRP 1-28 Draft-96. The objective was to harmonize existing standards into a single protocol. Many key differences were found between the existing protocols including: deformation and load measurement locations, stress magnitudes and sequences, confining stresses and unconfined resilient modulus testing, material type characterizations, and compaction methods. The result of the study was the development of the NCHRP 1-28A protocol. Currently, two protocols are considered accepted standards in determining resilient modulus by MEPDG: AASHTO T 307-99 and NCHRP 1-28A.

2.2.1 AASHTO T307-99

AASHTO T 307-99 was implemented from LTPP Protocol P46/AASHTO TP46-94. This section will detail the T 307 standard with a focus on fine-grained subgrade soils.

Material Type

This standard has two material type definitions, where materials are characterized as Type 1 or Type 2. Type 1 soils materials must have less than 70 percent passing the No. 10 sieve and less

than 20 percent passing the No. 200 sieve as well as have a PI of 10 or less. Any soils that do not meet these criteria are characterized as Type 2.

Specimen Size

Reconstituted specimen sizes are determined by material type and maximum particle size.

Reconstituted Type 2 materials are to be fabricated into a mold size where the diameter is at least five times the maximum particle size. The standard also calls out scalping particles 25 percent of the largest diameter mold available. Height to diameter ratio is at least 2 to 1.

Compaction Methods

Type 2 soils may be compacted using one of two methods, static or kneading. The general method is considered static compaction using a plunger method where equal weights of lifts are compacted to fixed heights using plugs, thereby compacting to desired densities. Kneading compaction is done using a manual or mechanical compactor.

Test Equipment

Testing system requirements covered in T 307 include load cell and LVDT maximum capacities/ranges which depend on specimen size. A list of maximum load cell capacities and LVDT ranges corresponding to specimen diameter is shown in Table 2.1. LVDTs for this standard are required to be spring-loaded. Two LVDTs are fixed to the loading piston rod outside of the triaxial cell. The load cell is also located outside of the confining chamber. Figure 2.1 shows the typical test set up provided by AASHTO T 307.

Table 2.1 AASHTO T 307 Load Cell and LVDT Capacity and Range Requirements

Specimen Diameter (mm)	Load Cell		LVDT Range (mm)
	Maximum Capacity (kN)	Required Accuracy (N)	
71	2.2	+/- 4.5	+/- 1
100	8	+/- 10.0	+/- 2.5
152	22.24	+/- 22.24	+/- 6

The duration of the rest period of the loading cycles is determined by the loading device. The standard requires a top-loading, closed loop, electro-hydraulic or pneumatic system. For both systems the duration of the haversine loading cycle is 0.1 seconds, however for pneumatic systems the rest period is 0.9 to 3.0 seconds while for hydraulic systems the rest period is 0.9 seconds. It is this author's opinion that nearly all of current resilient modulus testing systems being currently used are servo-hydraulic systems, i.e. the standard test cycle for this standard will be a 0.1 second load pulse followed by a 0.9 second rest period.

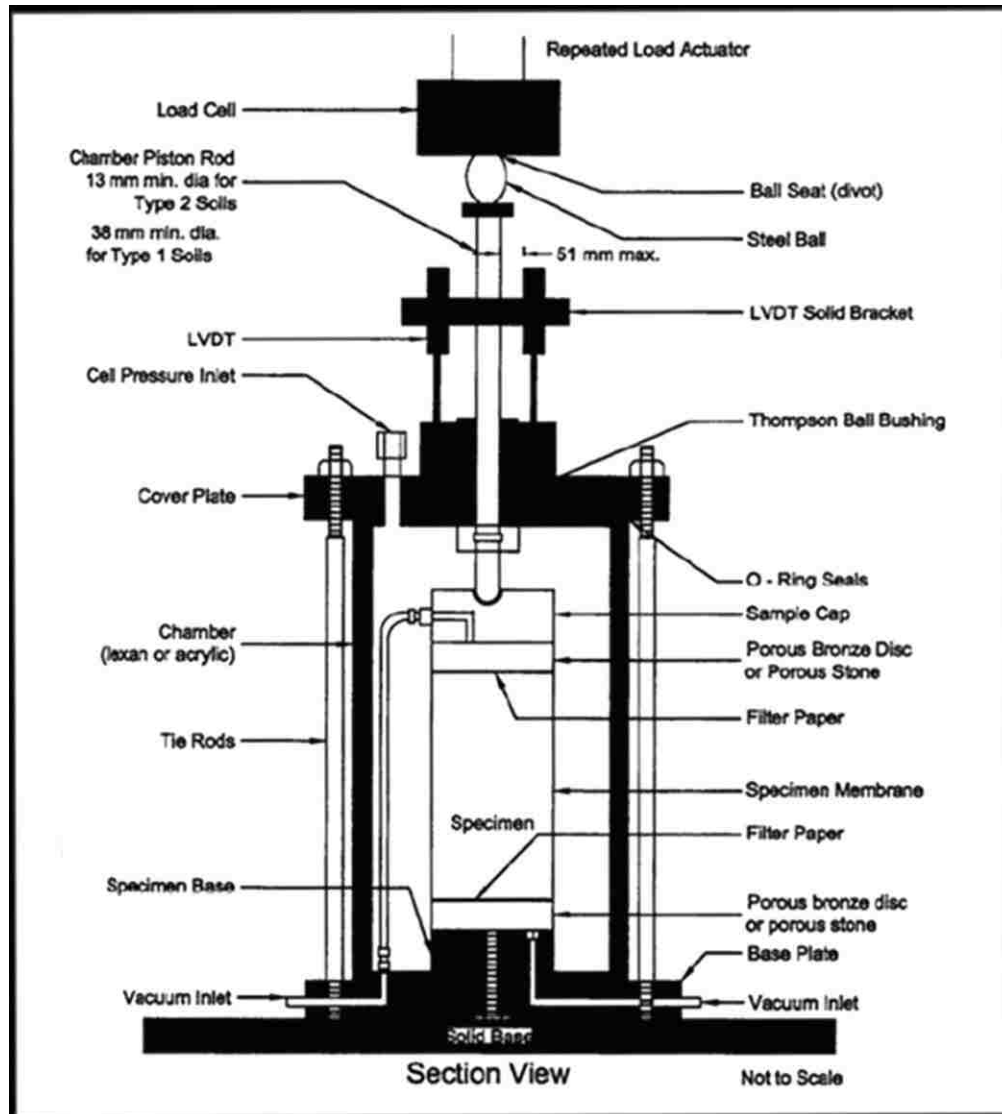


Figure 2.1 Example T 307 Test Setup (Source: AASTHO T 307-99)

Testing Sequences

The subgrade testing sequence for AASHTO T 307 of Type II soils consists of a conditioning sequence and 15 test sequences. Confining stresses range from 2 to 6 psi and deviator stresses range from 2 to 10 psi. Test sequence information can be seen in Table 2.2.

Table 2.2 AASHTO T307 Subgrade Sequence for Type 2 Soils

Sequence No.	Confining Pressure, σ_3	Deviator Stress, σ_d	Cyclic Stress, σ_{cyclic}	Seating Stress, $0.1\sigma_d$	No. of Loading Cycles
	psi	psi	psi	psi	
0	6	4	3.6	0.4	500-1000
1	6	2	1.8	0.2	100
2	6	4	3.6	0.4	100
3	6	6	5.4	0.6	100
4	6	8	7.2	0.8	100
5	6	10	9.0	1.0	100
6	4	2	1.8	0.2	100
7	4	4	3.6	0.4	100
8	4	6	5.4	0.6	100
9	4	8	7.2	0.8	100
10	4	10	9.0	1.0	100
11	2	2	1.8	0.2	100
12	2	4	3.6	0.4	100
13	2	6	5.4	0.6	100
14	2	8	7.2	0.8	100
15	2	10	9.0	1.0	100

2.2.2 NCHRP 1-28A

NCHRP 1-28A is a test standard that was developed to harmonize research findings from Project 1-28 with existing AASHTO standards TP46, T 292, T 294 and the FHWA LTPP *Laboratory Start-Up and Quality Control Procedure* (NCHRP Research Results Digest 2004). There are numerous differences between AASHTO T 307 and NCHRP 1-28A, especially in regards to testing sequences, deformation measurement, and specimen size and preparation. This portion of Chapter 2 covers some of these areas where NCHRP 1-28A differs from AASHTO T307 in regards to fine-grained subgrade soils.

Testing Sequences

Similar to AASHTO T 307, NCHRP1-28A uses a haversine loading pulse, however the duration of the pulse is 0.2 seconds followed by a 0.8 second rest period, rather than a 0.1 second pulse followed by a 0.9 second rest period. While groupings of test sequences 1-5, 6-10, and 11-15 have confining pressures of 6, 4, and 2 psi respectively for AASHTO T307, NCHRP 1-28A vary from sequence to sequence. Table 2.3 shows the NCHRP 1-28a testing sequence for fine-grained subgrades. Here we see that there are 16 test sequences compared to 15 for AASHTO T307 and the cyclic stresses keep values that can be grouped in sequences, i.e. sequences 1-4, 5-8, 9-12, and 13-16 have cyclic stresses of 4,7,10, and 14 psi respectively. Also note that the contact stress is not 10% of the deviator stress and that the minimum and maximum cyclic stresses during the test are higher for NCHRP 1-28A than for AASHTO T307.

Table 2.3 NCHRP 1-28A Testing Sequence for Fine-Grained Subgrades

Sequence No.	Confining Pressure, σ_3	Deviator Stress, σ_d	Cyclic Stress, σ_{cyclic}	Seating Stress	No. of Loading Cycles
	psi	psi	psi	psi	
0	4	7.8	7.0	0.8	1000
1	8	5.6	4.0	1.6	100
2	6	5.2	4.0	1.2	100
3	4	4.8	4.0	0.8	100
4	2	4.4	4.0	0.4	100
5	8	8.6	7.0	1.6	100
6	6	8.2	7.0	1.2	100
7	4	7.8	7.0	0.8	100
8	2	7.4	7.0	0.4	100
9	8	11.6	10.0	1.6	100
10	6	11.2	10.0	1.2	100
11	4	10.8	10.0	0.8	100
12	2	10.4	10.0	0.4	100
13	8	15.6	14.0	1.6	100
14	6	15.2	14.0	1.2	100
15	4	14.8	14.0	0.8	100
16	2	14.4	14.0	0.4	100

Material Type

NCHRP 1-28A breaks materials into four material types: 1, 2, 3, or 4. Type 1-3 materials are remolded. Type 1 materials are all unbound granular base and subbase materials and all untreated subgrade soils with maximum particle sizes larger than 0.375 inches, noting that all particles greater than 1 inch shall be scalped. Type 2 materials have a maximum particle size less than 0.375 inches and less than 10% passing the No. 200 sieve. Type 3 materials are all untreated subgrade soils with maximum particle size less than 0.375 inches with greater than 10% passing the No. 200 sieve. Finally, materials which are undisturbed (i.e. thin-walled tube samples of untreated subgrades) are characterized as Type 4 materials.

Specimen Size

All remolded specimens are compacted to either 4 or 6 inch diameter sizes. Type 1 materials are compacted to a 6 inch diameter if the maximum particle size is greater than 0.75 inches; otherwise they are compacted to a 4 inch diameter. Type 2 and 3 materials are compacted to 4 inch diameters. Type 4 materials are tested as 2.8 inch diameter undisturbed specimens.

Compaction Methods

Compaction method is dictated by material type. Type 1 materials are compacted by impact or vibratory compaction. Type 2 materials are compacted by vibratory compaction. Type 3 materials are compacted by impact or kneading compaction.

Test Equipment

The load cell and deformation measurement sensors are placed inside the triaxial cell in NCHRP 1-28A. For axial deformation measurements, measurements are made on the specimen and three

types of sensors are specified: (1) Clamp mounted LVDTs, (2) non-contact sensors, or (3) optical extensometers. Standard gauge lengths are $\frac{1}{4}$ diameter points, i.e. for 2:1 height to diameter specimens this is the middle half of the specimen. The standard includes notes on maximum ranges, and minimum sensitivities. Regarding very soft specimens the standard notes that deformations may be taken between the top and bottom platens. For stiff to very stiff specimens the standard states to consider grouting ends because of small displacements at small deviator stresses. Though the standard recommends different techniques for if specimens are soft or stiff to very stiff, there are no threshold values of modulus that separate test specimens into this category. Regarding load cells, the maximum load capacity and required accuracy are listed in Table 2.4.

Table 2.4 NCHRP 1-28A Load Cell Requirements

Specimen Diameter mm (in)	Load Cell	
	Maximum Capacity kN (lb)	Required Accuracy N (lb)
71 (2.8)	2.2 (500)	+/- 4.5 (+/- 1)
102 (4.0)	8.9 (2000)	+/- 17.8 (+/- 4)
152 (6.0)	22.24 (5000)	+/- 22.24 (+/- 5)

While AASHTO T307 allows for testing to be done using either a pneumatic or hydraulic loading device, NCHRP 1-28A states that the loading system shall be electro-hydraulic, thus pneumatic loading devices are not considered. In regards to the confining chamber, it is to be made of a suitable transparent material such as polycarbonate or acrylic. Many triaxial chambers

are cylindrical. The standard notes that for cylindrical triaxial cells optical extensometers cannot be used because the sight line must pass through a flat face.

2.2.3 Summary of Current Test Protocols

Differences between the AASHTO T 307 and NCHRP -28A protocols for fine-grained subgrades include: deformation and load cell location, stress sequences (number, load duration, magnitudes), and compaction methods. A summary of these differences are listed in Table 2.5. It is noted these are not all the differences between the two standards.

Table 2.5 Various M_r Test Protocol Differences

Topic	Test Protocol	
	AASHTO T 307	NCHRP 1-28A
Load Cell Location	Outside Cell	Inside Cell
LVDT Location	Outside Triaxial Cell, Mounted on Loading Piston	Inside Triaxial Cell, Attached to Specimen
Option of 2.8 in. Diameter Reconstituted Specimen?	Yes	No
Option of Impact Compaction?	No	Yes
Testing Sequences for Fine-Grained Subgrades	15 ea. 2,4,6,8,10 psi deviator stresses and 2,4,6 psi confining stresses	16 ea. 4,7,10,14 psi deviator stresses and 2,4,6,8 psi confining stresses
Load Pulse Form, Duration	Haversine, 0.1 s	Haversine, 0.2 s

2.3 Equipment Effects and Deformation Measurement Techniques

The two main pieces of equipment discussed in this section are deformation sensors (in this case LVDTs) and load cells. Resilient modulus is a stress controlled test where the two values used to calculate M_r are stress and strain, so naturally accurate measurements of load and deformation are critical to successful testing. In addition, extensive literature exists on the influence of load cells and deformation measurement in resilient modulus testing. Other physical hardware, such as the triaxial cell, will be discussed briefly.

2.3.1 Load Cell

Primary physical issues concerning the load cell in resilient modulus testing are concerned with the location of the load cell, inside or outside the triaxial cell.

In a paper focused on the background and discussion of AASHTO T 307, Groeger et al. (2003) pointed concerns for using both external and internal load cells. When using an external load cell, they point out that attention must be paid to ensure that friction (between the loading piston and confining chamber) is minimized. If friction is a concern and an internal load cell is preferred, then it is unnecessary to correct for the uplift force due to the confining pressure within the cell, however a new source of error in the deformation of the load cell is introduced. Most load cells used in resilient modulus testing are strain gauge type load cells, with a design stiffness and linear deflection range up to maximum load output. Therefore as the authors point out, the load cell will need to deform to control and read loads. This deformation becomes a concern with T307 because test deformation measurements are being taken outside the triaxial cell, thus load cell deformation will contribute directly to strain values and reduce the M_r value.

Assuming no other erroneous deformation contributions, the internal load cell deformation with external LVDT measurements will introduce errors in results increasing with increasing stiffness of the specimen.

A study performed by Bejarano et al. (2003) supports concern for frictional forces influencing load cell readings when the load cell is placed externally. Results showed that at higher loads external load readings could reach 15% higher than internal. According to authors the difference between external and external load readings did not appear constant and the variation “indicates that while many triaxial test apparatus use only an external load cell, this may not yield acceptable results.”

In conclusions to a study on triaxial cell interaction examining drag forces on the loading rods, Boudreau and Wang (2003), recommended that internal load and deformations measurements can “eliminate or reduce the inherent errors associated with equipment variation.” They go on to point out that such a decision will introduce a tester to the difficulty and time associated with implementing internal instruments.

2.3.2 Effect of Deformation Measurement on Mr

In section 2.2, it was introduced that there are two standardized options for measuring resilient modulus, each with different specifications on deformation sensor location. Historically these two methods have been shown to produce results which can differ greatly from one another. This section introduces literature studies related to effects of deformation measurement on resilient modulus.

Barksdale et al. (1997) found that to perform reliable resilient modulus tests, axial deformation should be measured on the specimen. The comprehensive study, titled NCHRP 1-28, included tests on synthetic, cohesive, and granular specimens, using external, and different internal deformation measurement methods. A significant portion of the NCHRP final report is dedicated to system compliance and axial deformation measurement. Significant findings as they relate to deformation measurement of cohesive fine-grained subgrade soils are:

- Satisfactory results are not reliable when measuring deformations externally with conventional triaxial cells, especially when M_r exceeds 10,000 psi.
- Even after accounting for system compliance using dummy samples, the threshold for reliable M_r values is 60,000 psi.
- Deformation measurements on specimens using plugs epoxied to specimen were considered reference compared to rings clamped around the specimen because “extraneous displacements and potential slip was eliminated.”

In the report, Barksdale et. al repeatedly highlight the amount of effort taken to remove compliance from the test system in order to minimize the amount of error using external measurements. In a multi-lab study that was part of NCHRP1-28, large variations in results between labs when using external LVDTs lead the authors to conclude that regarding the amount of time and effort necessary to account for extraneous deformations and calibrate test systems accordingly, it is doubtful the required resources (expertise, time, effort) are available in production or even research labs to accurately measure M_r with external deformations.

Groeger et al. (2003) published a background and discussion paper on T 307, where it is stated that external deformation measurement should be examined. The authors state that reasons for measurements outside the cell are that externally mounted LVDTs are more efficient and slip may occur when deformations are measured on the specimen. The authors continued defense is that internally mounted LVDTs remove what they call “slop” (compliance issues) in the system, which contributes to strain in calculating resilient modulus values.

Bejarano et al. (2003) found when comparing M_r results determined using on sample, top-platen, and external LVDT measurements, that on sample measurements consistently produced the highest results, followed by top-platen, then external measurements. The reason given for the difference is that top-platen includes end effect deformation contributions, and the external value is affected by end effects plus compliance (due to actuator, frame, and load cells). As the stiffness increases the difference is greater. The authors add that compliance is not considered in resilient modulus testing, and while some laboratories attempt to account for compliance empirically, since end effects are inconsistent correcting compliance is not expected to be accurate.

Boudreau and Wang (2003) concluded that for efficiency of production external deformation is allowed, while internal measurements can remove or decrease errors associated with equipment variation. They list compliance issues including: load rod compression and bending, porous stone compression, unfixed connection points (platens), and base bending. In regards to internal instrumentation, the authors point out that it is both difficult and time-consuming.

Konrad and Robert (2003) concluded that axial strain must be measured with gauges on the sample, at least over a diameter length, typically over the middle third. Another conclusion was in regards to accuracy of gauges must be considered when measuring very small strains at the smallest deviator stresses, where discussion on the concern of deformations below the non-linearity error of the LVDT were introduced. The example LVDT is for a 200 mm high specimen with a range of ± 2.5 mm, which results in a ± 0.00625 mm precision. At the lowest stress sequence level, this would correspond to a maximum resilient modulus of roughly 200 kPa (about 29 ksi) outside of the non-linearity error threshold. Recommendations by the authors concerning modifications to AASHTO T307-99 included LVDT location and elimination of lower stress levels.

Andrei (2003) found when comparing internal measurement setups using synthetic specimens of varying stiffness values found that results in the range of the non-linearity ranges produced questionable results. He also points out that the existing testing standards do not provide what to do with modulus values measured smaller than the non-linearity range. One synthetic sample evaluated has a modulus value of 210 ksi which the author points out is achievable by a subgrade soil in a dry state, yet even when the resolution was increased 10 times (from a 0.2 to 0.02 in range), still one-quarter of the data fell below the non-linearity range. In defense of the non-linearity behavior affecting the resilient modulus the authors shows that in one instance the modulus values are decreasing and eventually stabilizing when the deformation is beyond the non-linearity range while in another instance it increases then stabilizes. Since the synthetic specimen used as an example should behave elastically and should not show stress-strain

dependency in this case, the author states that the values at the low strain levels should equal the stabilized values outside the non-linear portion of the LVDTs.

Burczyk et al. (1994) found that for undisturbed Shelby tube samples of A-4 and A-6 subgrade soils that resilient modulus value determined on the specimen using a ring clamp setup gave consistently higher results than external LVDTs.

Mohammad (1994) studied the influence of internal deformation measurements made on cohesive and granular materials at specimen ends and middle one-third of the specimens. The authors' reason for internal measurement is that it is subjected to fewer compliance errors. Recommendations included a multiplier for clays for resilient modulus in unconfined conditions of 1.5 to 1.6 when measurements are made at the ends of a specimen (on platens) compared to middle measurements. Basically, values were higher when measurements were made over the middle third than on the ends.

Kim (1994) cited complexities in local strain measurement recommendations made to eliminate errors in small to intermediate strains of 0.01 to 1 percent, as a motive to study the influence of grouting ends of specimens to platens (i.e. will grouting specimens improve external deformation measurements). The study found that for resilient modulus tests external deformation measurement can be used reliably when specimen stiffness is below 50 ksi stiffness, but at higher M_r values external measurements are smaller than the reference value and as stiffness increases so does the difference.

2.3.3 Triaxial Cell

In Section 2.2.1 it was discussed that the load cell is located outside of the cell in the AASHTO T 307, while this can be advantageous in eliminating the load cell deformation when placed inside the cell and keeping LVDTs located outside, it can neglect influences from the triaxial cell which can have a significant effect when applying small loads like those during a resilient modulus subgrade test. One correction which is accounted for in the T307 protocol is the resultant force due to the uplift force from the confining pressure, and the weight of the piston rod. This is implemented by the force adjustment defined by Eq. (2)

$$F = (A * P) - W \quad (2)$$

Where F is the resultant force, A is the piston rod cross-sectional area, P is the confining pressure, and W is the weight of the piston rod plus the externally mounted deformation measurement setup.

Boudreau and Wang (2003) investigated triaxial cell influence and found that by comparing two triaxial cells and recording loads for while applying pulse deformations without a specimen that one cell produced 0.5 lb. of friction while another produced 2.0 lb. of friction. Note that for Sequence 1 of the T307 Subgrade test the deviator stress is 2 psi, for a 2.8 inch diameter specimen this results in about a 12.3 lb. load, where a cell producing seal drag of 2 lbs. represents about 16% of the stress that is supposed to be applied. Bejarano et al. (2003) found due to load rod friction between the cell and loading piston and uplift forces, external load cell readings higher for external load cells. Groeger et al. (2003) commented on the influence of

triaxial cell on the resilient modulus test in regards to frictional forces on the loading piston, emphasizing the amount of effort that must be spent to ensure friction is removed.

2.4 Resilient Modulus of Fine Grained Soils

Unlike granular base and subbase materials which show increasing to confining stresses, resilient modulus values of fine grained subgrade soils are known to decrease with deviator stresses (Huang (2004)). In regards to material influences, fine grained soils are influenced by moisture changes, with the difference in M_r between wet and dry conditions being 100% or larger (Barksdale (1997)).

2.4.1 Effect of Moisture Content

Liang et al. (2008) citing numerous studies documenting the effect of moisture content on resilient modulus including (Wolfe and Butalia (2004), Drumm et al. (1990), Mohammad et al. (1996) and Pezo et al. (1992)), as a reason for developing a prediction model which shows variation in resilient modulus with moisture content. The model incorporates matric suction, a value directly related to moisture content, and is further described in Section 2.4.3. The authors note that the model which MEPDG uses for moisture seasonal variation is very general and does not illustrate stress and moisture effects and that only one other predictive model published at that time incorporated stress effects and suction.

Li and Qubain (2003) examined moisture effects on the resilient modulus of three subgrade soils, ranging from 2-3 dry and wet of optimum and optimum. The authors note that resilient modulus tests are generally performed at optimum moisture content, and this may neglect in situ moisture

variations subgrade soils experience throughout the year. All three soils showed a decreasing trend in resilient modulus with increasing moisture content. The trend for a clayey sand showed from about 8% moisture content to 15% moisture content M_r values decreased from about 120 MPa to 70 MPa (roughly 17 ksi to 10 ksi). For a lean clay with moisture contents ranging from from approximately 7% to 18% M_r values decreased from about 110 MPa to 40 MPa (roughly 16 ksi to 6 ksi). It is noted that the tests performed, the axial deformations were measured externally.

2.4.2 Testing Influences

Studies dating to over 30 years ago on cohesive soils were showing confining stresses had little effect on their resilient modulus values. Thompson and Robnett (1979) found that repeated loading testing with no confining pressure was acceptable for resilient modulus testing of cohesive soils. Fredlund et al. (1977) found that for a soil with a PI of nearly 17 percent, confining stresses from 3 to 6 psi were insignificant.

Muhanna et al. (1999) found by performing resilient modulus tests on 4 in. diameter A-6 and A-5 specimens at varying moisture contents that there is was no significant effect due to the number of load applications, rest period, or load sequence. The authors concluded that confining pressures in the range of 0 to 10 psi had less than a 5% effect on resilient modulus. It can be mentioned in this regard that confining pressures in the AASHTO T 307 standard are 2, 4, and 6 psi respectively for subgrade soils and 2, 4, 6, and 8 psi in NCHRP 1-28A.

While past studies have shown the insignificant effect of confining pressures in the ranges tested for resilient modulus, to date cohesive fine-grained soils are still being subjected to multiple confining pressures in the testing protocols. This results in longer testing time as well as increased cost, setup time, and complexity that comes with the physical triaxial chamber.

2.4.3 Constitutive Models

Li and Selig (1994) reported that many constitutive models have been introduced to define the resilient modulus of fine-grained soils, two of the main ones being the bilinear model and power model which are both functions of deviator stress along with constant parameters. The bilinear model proposed by Thompson and Robnett (1976) is shown in Eqs. (3a) and (3b) and characterized modulus before and after a breakpoint where the slope changes with respect to deviator stress. In the bilinear model K_1 and K_2 are model constants dependent on soil conditions and K_3 and K_4 typically are negative, and σ_{di} is the break point deviator stress and σ_d is the deviator stress.

$$M_r = K_1 + K_2\sigma_d \quad \text{when } \sigma_d < \sigma_{di} \quad (3a)$$

$$M_r = K_3 + K_4\sigma_d \quad \text{when } \sigma_d > \sigma_{di} \quad (3b)$$

A power model is shown by Eq. (4). Where k and n are constants which depend on soil type/state, n is usually negative, and σ_d is the deviator stress.

$$M_r = k\sigma_d^n \quad (4)$$

A model taking into account moisture effects was developed by researchers incorporation soil suction (Liang et al. 2008). The proposed model, shown in eq. (5) applies to cohesive soils in unsaturated conditions and introduces matric suction as a variable affecting the resilient modulus.

$$M_R = K_1 P_a \left(\frac{\theta + \chi_w \psi_m}{P_a} \right)^{K_2} \left(\frac{\tau_{oct}}{P_a} + 1 \right)^{K_3} \quad (5)$$

where $\theta = \sigma_1 + \sigma_2 + \sigma_3$ is the bulk stress, $\sigma_1, \sigma_2, \sigma_3$ are three principal stresses; τ_{oct} is octahedral shear stress, ψ_m is matric suction; χ_w is Bishops parameter; P_a is atmospheric pressure; and K_1, K_2, K_3 are regression constants.

The current constitutive model proposed by NCHRP 1-28A and used for calculations by MEPDG is shown in Eq. (6) and is known as the generalized or “universal model.”

$$M_r = k_1 P_a \left(\frac{\theta}{P_a} \right)^{k_2} \left(\frac{\tau_{oct}}{P_a} \right)^{k_3} \quad (6)$$

where $\theta = \sigma_1 + \sigma_2 + \sigma_3$ is the bulk stress, $\sigma_1, \sigma_2, \sigma_3$ are three principal stresses; τ_{oct} is octahedral shear stress, P_a is atmospheric pressure; and K_1, K_2, K_3 are regression constants. This model does not take into account moisture variations, and in order to account for changes in resilient modulus due to seasonal effects an empirical equation is applied to resilient modulus

values in MEPDG based on degree of saturation is applied to resilient modulus values. This model is shown in eq. (6), and is part of the enhanced integrated climatic model utilized by MEPDG (Larson and Dempsy 1997).

$$\log \frac{M_r}{M_{r-opt}} = a + \frac{b-a}{1+\exp(\ln \frac{-b}{a} + k_m(S-S_{opt}))} \quad (7)$$

where M_r = resilient modulus at a given degree of saturation; M_{r-opt} = resilient modulus at a reference condition; a = minimum of $\log(\frac{M_r}{M_{r-opt}})$; b = maximum of $\log(\frac{M_r}{M_{r-opt}})$; k_m = regression parameter; and $(S - S_{opt})$ = variation in degree of saturation in decimal form. A set of regression constants for two types of soils, coarse-grained and fine-grained, is used in this model.

CHAPTER 3

MATERIALS, SPECIMEN PREPARATION, AND TESTS METHODS

3.1 Introduction

This chapter highlights the results of these preliminary classification tests and also details the preparation of resilient modulus specimens, the multiple tests performed (resilient modulus, alternate resilient modulus test, and static tests) as well as the deformation measurement techniques. It is standard to characterize soils according to grain-size distribution, plasticity index, and moisture-density relationships. Such tests have been used extensively as standards in determining the quality of a material as a layer beneath a pavement. These customary tests provide pertinent information prior to resilient modulus testing in the interest of fabricating specimens to desired densities and moisture contents, as well as determining the size of specimens for testing according to grain-size distribution of the soil.

3.2 Materials and Classifications

The subgrade soil used in this study was sampled from the right of way of a highway project on U.S. 491 in Northwestern New Mexico. The project extended from Tohatchi to Shiprock, New Mexico. Figure 3.1 is a map of the portion of New Mexico where the soil was taken from, Figure 3.2 shows a backhoe loader excavation soil to a loose state at the ground surface to facilitate bagging and transportation to the laboratory.



Figure 3.1 U.S. 491 Gallup to Shiprock



Figure 3.2 Backhoe Loader Removing Soil Used In This Study

An initial classification of the soil based on project testing of soils near the location it was taken from indicates it is an A-6 soil with a plastic limit of 16%, a liquid limit of 29%, resulting in a PI of 13%. Table 3.1 lists the gradation data of the site soil.

Table 3.1 Gradation Information

Sieve No.	Sieve Size (mm)	% Passing
4	4.75	100
10	2	98.0
40	0.425	96.0
50	0.3	53.7
200	0.075	49.6

The soil collected in this study was sampled using a backhoe, resulting in large chunks of soil that were then hand pulverized until all was passing the No. 4 sieve prior to use for moisture-density characterization and test specimen preparation. Figure 3.3 shows an example of a portion of this soil which passes the No. 4 sieve and Figure 3.4 shows a liquid limit test conducted.



Figure 3.3 Sample of Soil Used in Study



Figure 3.4 Determining Atterberg Limits

3.3 Moisture-Density Relationship

Sufficient quantities of soils passing the No. 4 sieve were obtained in order to determine the moisture-density relationships according to AASHTO T 180 using a modified proctor effort.

Using a manual mechanical mixer, soil and water were mixed in 5 gallon plastic buckets, sealed, and allowed to mellow prior to compaction, Figure 3.5 below shows the equipment used for mixing.



Figure 3.5 Example of Mixing Procedure

Five points for the moisture-density characterization was used to determine the maximum dry density and optimum moisture content. Figure 3.6 is a plot of the moisture-density relationship, the soil used in this study was determined to have an optimum moisture content of 15.1% and a maximum dry density of 120 pcf.

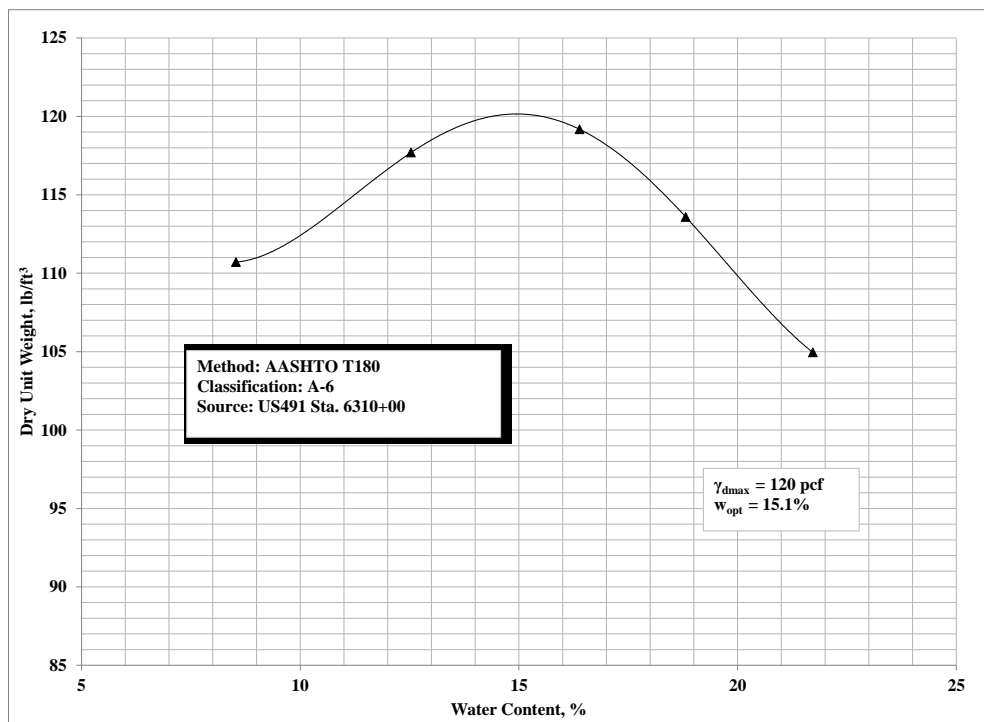


Figure 3.6 Moisture-Density Relationship

3.4 Specimen Preparation

3.4.1 Specimen Compaction

Specimens for this study were prepared using dynamic impact compaction. Impact compaction energy was provided by a modified proctor effort which delivers 56,000 ft-lbf/ft³ (the result of a 10 lbf hammer dropping from 18 inches). The necessary number of blows per layer was calculated using Eq (3.1) from NCHRP 1-28A:

$$n = \frac{CE*V}{N*W*h} \quad \text{Eq. (3.1)}$$

For this study where 2.8 inch and 4 inch diameter specimens are prepared:

n = number of blows

CE = compactive effort of 56,000 ft-lbf/ft³

V = Volume of specimen (approx. 0.058 ft³ for 4 inch diameter specimens, and 0.02 ft³ for 2.8 inch diameter specimens)

N = number of layers (8 layers for 4 inch diameter specimens, and 3 layers for 2.8 inch diameter specimen)

W = weight of drop hammer, 10 lbf

h = drop height in feet, 1.5 ft

It was introduced in Chapter 1 that while moisture-density relationships used for pavement construction are defined by energy delivered by impact compaction, only NCHRP 1-28A allows this as a method for reconstituting resilient modulus specimens. However, only 4 inch and 6 inch diameter specimens are considered in reconstituting specimens in NCHRP 1-28A.

AASHTO T 307 does include 2.8 inch diameter size specimens for reconstitution. In order to consider 2.8 inch diameter specimens reconstituted using impact compaction for this study, a number of lifts needed to be selected to determine the equivalent number of blows using the compaction energy equation shown in Eq. (3.1). Based on equivalent energy delivered by the modified proctor hammer, three lifts of equal height were selected for the 2.8 in. diameter specimens, resulting in approximately 25 blows per lift. Concern may exist over the 2.8 in. mold size relative to the surface area of the modified proctor hammer, i.e. side -wall constraint effects. However, it was found in this study that for this particular soil at the ranges of moisture contents used (about +/- 2-3% relative to optimum), desired densities at 95-100% of maximum dry density were always achieved using the values determined using equivalent energy. Table 3.2 shows the information used for determining the approximate number of blows for each specimen size based on the modified compaction effort. An illustration of the two specimen sizes is displayed in Figure 3.7.

Table 3.2 Equivalent blows per lift using modified compaction effort

Standard	NCHRP 1-28A	N/A
Specimen Diameter (in.)	4.0	2.8
CE (ft-lbf/ft ³)	56,000	56,000
V (ft ³)	0.058	0.02
N (lifts)	8	3
W (lbf)	10	10
h (ft)	1.5	1.5
n (blows per lift)	~27	~25

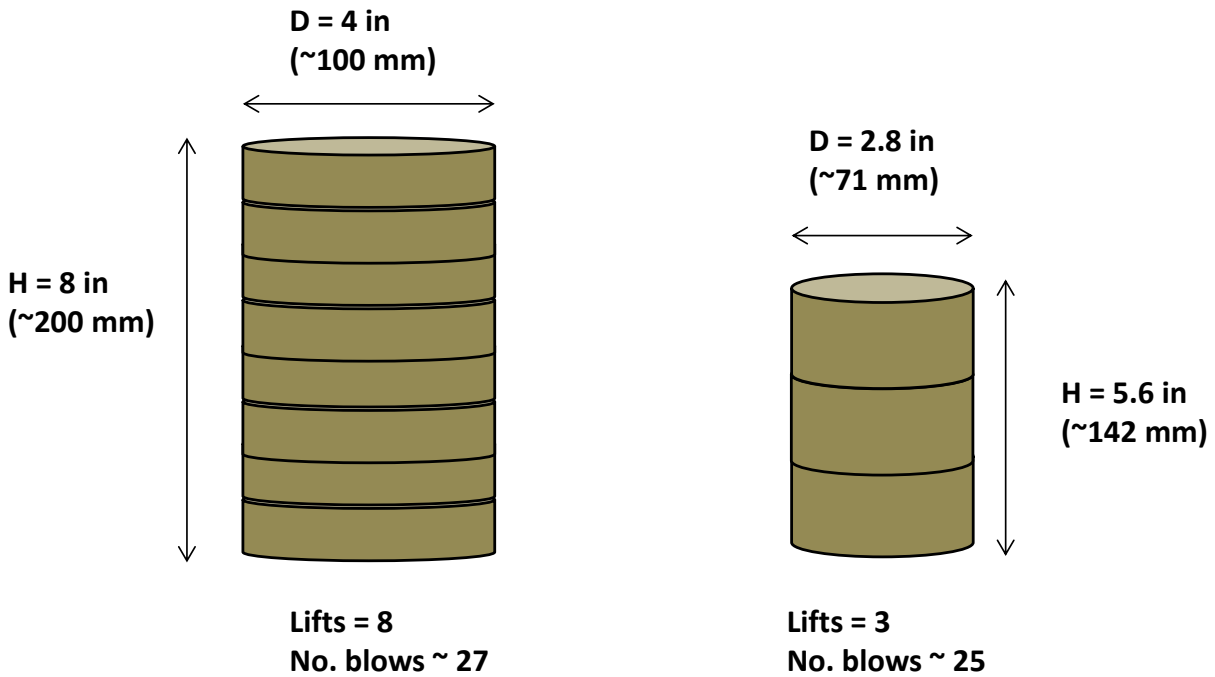


Figure 3.7 Compaction Size and Lift Illustration (Not to Scale)

All specimens were compacted in split molds lined with membranes with vacuum pressure applied. Figure 3.8 shows the two sizes of split molds used in the study. Vacuum ports at two locations, especially at a point near the highest lift, were needed due to the pressure of the soil on the membrane sealing the lower port and cutting off the vacuum. When this happens the membrane becomes loose and can get caught by the proctor hammer and in between lifts causing deformities in specimens. Also multiple reinforcing hose clamps were needed, in this case 3 were found sufficient to keep the split mold closed during compaction. When only one was is, the pressure of the soil can open the mold, vacuum is lost and diameter is varied, which results in losing the specimen, time, and material. In Figure 3.9, the 2.8 inch diameter mold is shown with the membrane attached and vacuum connected to the pressure control panel, additionally the modified proctor hammer used for compaction is displayed in the picture.



Figure 3.8 Split Molds Used for Compaction



Figure 3.9 Mold Setup with Membrane and Applied Vacuum

Weights of each lift were determined based on desired specimen densities and as mixed moisture contents. True moisture contents were then determined from oven drying both the loose mixes at preparation as well as from the test specimens post UCS failure. Densities were kept constant with target dry densities between 95 and 100% of maximum dry density, all specimens were compacted within this range. The optimum moisture content was determined to be 15.1%, for this study the target was 0.5% wet of optimum, while the actual mixed moisture for the 2.8 in. replicate optimum moisture group was 0.9% wet of optimum. For this study the specimens nearest the optimum moisture content are designated to be at optimum. Target ranges for dry and wet specimens were +/- 2-3% relative to optimum. However, it was difficult to prevent specimens from losing moisture during the time between fabrication and unconfined failure when actual specimen moisture contents were determined (between this time specimens were capped and multiple dynamic tests were run requiring time intensive setup). Typical time

between specimen preparation and the last test typically ranged from 18 to 30 hrs. Specimens were sealed in attempts to mitigate moisture losses. However, the range of moistures of replicate groupings always showed the first specimen having the nearest moisture content to the mixture value and the last replicate having the lowest. Table 3.3 shows the moisture content as-mixed during specimen fabrication as well as the values of the replicates after all testing was performed, showing the moisture losses that occurred.

Table 3.3 Moisture Contents at Fabrication and Post-Testing for 2.8 inch Diameter Specimens

Replicate No.	Moisture Content at Fabrication (%)		
	Dry of Optimum	Optimum	Wet of Optimum
	13.7	16.0	18.1
	Moisture Content Post-Testing (%)		
1	13.4	15.8	17.9
2	13.2	15.6	17.6
3	13.0	15.6	17.2

3.4.2 End Treatments

Difficulties were encountered in achieving smooth surfaces when using impact compaction and split molds. Specimens were capped in this study to ensure smooth surfaces in hopes of reducing uneven stress distributions and potential rocking of the specimen during loadings. Only the top end of the specimen directly exposed to the impact hammer was capped, the bottoms had smooth finishes. Since the bottoms finishes were considered good, this made it easy to make a smooth finish on the top with just portions of cylinder molds, hose clamps, and a level for ensuring the

cap finish would be even, pictures of capping are shown in Figure 3.10. The material used for capping was gypsum cement with a 0.45 water to cement ratio. Specimens were capped immediately after compaction and sealed in attempts to prevent moisture loss.



Figure 3.10 Example of Gypsum Cement Capping Method

3.5 Test Methods

Two types of dynamic tests were performed on all specimens, a resilient modulus test according to the AASHTO T 307 Subgrade test sequences, as well as an alternate unconfined method.

Static tests were also performed, which include unconfined compression on all specimens and a modulus of elasticity test performed on the 4 in. diameter specimens. Shown in Tables 3.4 and 3.5 are test matrices and show nominal values for size, moisture condition, and the testing that was conducted for this chapter. Table 3.4 is for 2.8 inch diameter specimens, while Table 3.5 is for 4 inch diameter specimens. The only difference in testing between the two sizes is that a static elastic modulus test was performed on the 4 inch diameter specimens.

Table 3.4 Test Matrix for 2.8 inch Diameter Specimens

Test Matrix for 2.8 in. Diameter Specimens			
Moisture Condition	No. Specimens	Dynamic Testing*	Static Testing
2% Dry of Optimum	3	T 307 Subgrade (+ 15, 20, 25 psi M_r sequences), Alternate M_r testing @ 8, 10 15, 20 psi	UCS
Optimum	3	T 307 Subgrade (+ 15, 20 psi M_r sequences), Alternate M_r testing @ 6, 10, 14 psi	UCS
2% Wet of Optimum	3	T 307 Subgrade (+ 12, 14 psi M_r sequences), Alternate M_r testing @ 4, 8, 12 psi	UCS

*T307 Subgrade testing tested using two internal deformation techniques as well as external LVDTs, higher stress sequences tested using two internal deformation techniques, and sine stress testing was conducted using internal spring type LVDTs

Table 3.5 Test Matrix for 4 inch Diameter Specimens

Test Matrix for 4 in. Diameter Specimens			
Moisture Condition	No. Specimens	Dynamic Testing*	Static Testing
2% Dry of Optimum	1	T 307 Subgrade (+ 15, 20, 25 psi M_r sequences), Alternate M_r testing @ 8, 10 15, 20 psi	UCS, Modulus of Elasticity
Optimum	1	T 307 Subgrade (+ 15, 20 psi M_r sequences), Alternate M_r testing @ 6, 10, 14 psi	UCS, Modulus of Elasticity
2% Wet of Optimum	1	T 307 Subgrade (+ 12, 14 psi M_r sequences), Alternate M_r testing @ 4, 8, 12 psi	UCS, Modulus of Elasticity

*T307 Subgrade testing tested using two internal deformation techniques as well as external LVDTs, higher stress sequences tested using two internal deformation techniques, and sine stress testing was conducted using internal spring type LVDTs

3.5.1 Resilient Modulus Testing

Resilient modulus testing was conducted on two separate GCTS universal testing systems, with the same load cell (500lb. capacity) for controlling stress in all tests. Figure 3.11 shows the two frame/controller combinations used. The system on the left (ATM-025x/SCON2000) was used when testing for internal glued button and external deformation measurement and the system on the right (FRM100/SCON1500) was used for testing with ring clamp LVDT setups. Figure 3.12 shows the controlling load cell used in all dynamic tests conducted in this study.



Figure 3.11 Universal Testing Systems Used in Study



Figure 3.12 Load Cell for Used For Resilient Modulus and Alternate Testing

Stress Sequences

The stress sequences for this method follow AASHTO T 307 Subgrade sequences, which were shown in Table 2.2. Each loading cycle is 0.1 seconds of a haversine pulse followed by 0.9 seconds of a rest period. There is always an axial seating stress applied to the specimen which is 10% of the maximum axial cyclic load. As previously discussed, the resilient modulus for a particular test sequence is determined as the average resilient modulus determined from the last five cycles. Figure 3.13 shows the haversine waveform and comes from the AASHTO T 307 standard. Examples of stress and strain behavior for the last five cycles of an example test sequence are shown in Figures 3.14 and 3.15.

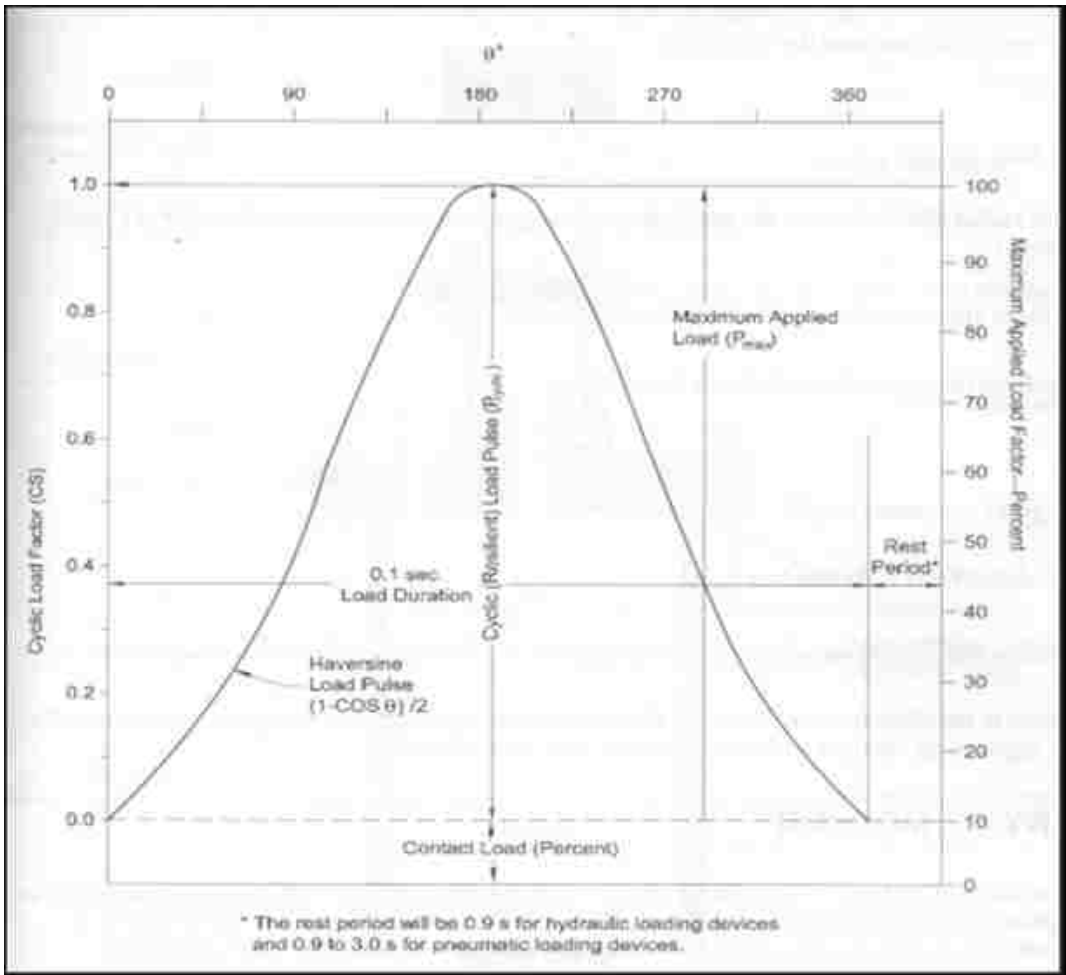


Figure 3.13 Haversine Load Pulse (Source: AASHTO T 307-99 protocol)

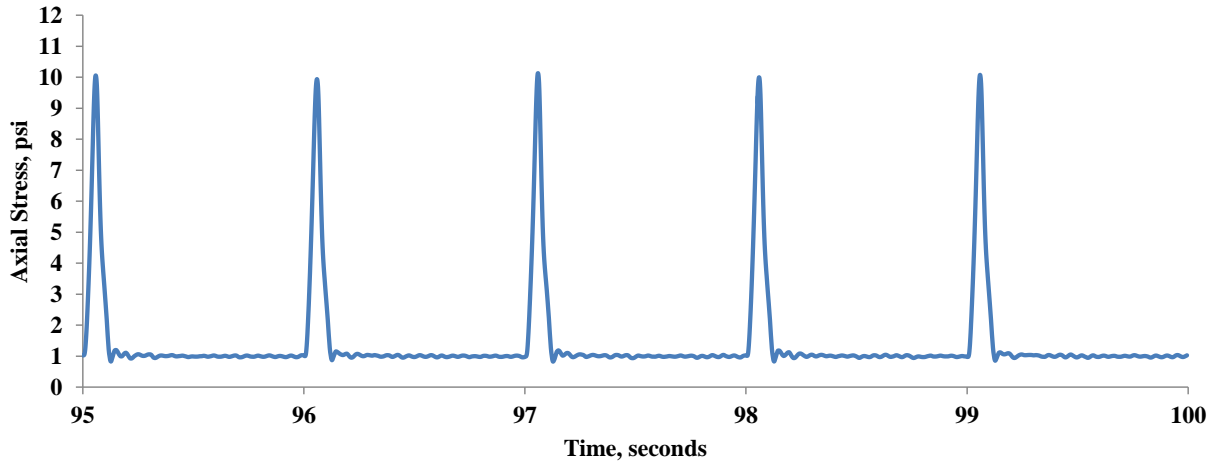


Figure 3.14 Example of Stress during Last Five Resilient Modulus Cycles

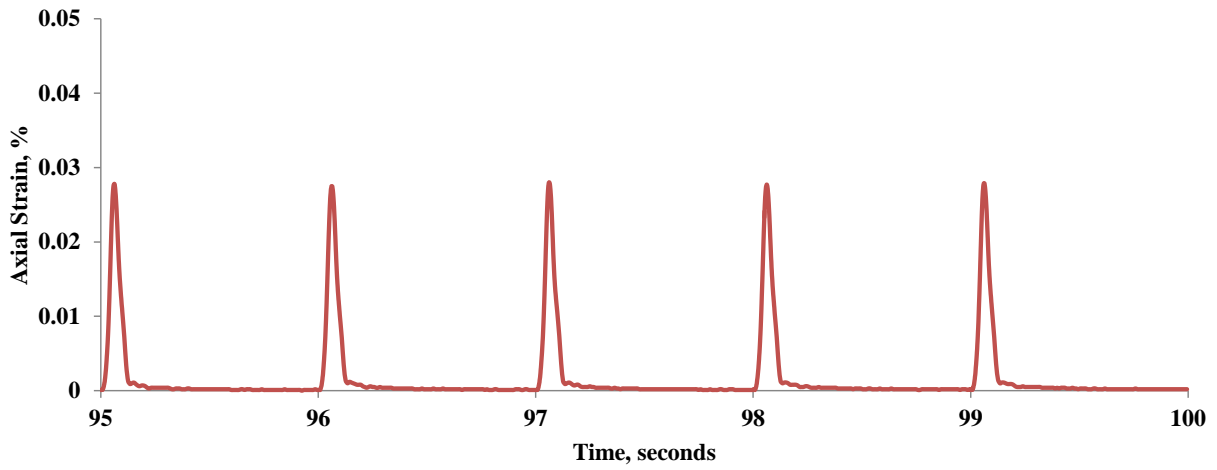


Figure 3.15 Example Strain Behavior during Last Five Resilient Modulus Test Cycles

Axial Deformation Measurements

Three types of deformation measurements were used to determine resilient modulus in this study two internal measurement techniques, and one external measurement techniques. One internal measurement technique used requires epoxying metal buttons to the specimen, this required much more effort than the other internal method due to the time it took to place epoxy and then seal the membrane around the buttons. While this method took longer, based on previous studies as well as the results shown in Chapters 4 and 5, this is considered the method with that results in the truest deformation response compared to others and is used as the reference for comparison and analysis throughout this study (Andrei (2003), Barksdale (1997)). Figure 3.16 shows the buttons (1/4 inch diameter by 3/8 inch height), the Spring Loaded LVDTs (+/- 1 mm range), and the guides for connecting the buttons and LVDTs. This deformation measurement setup is the same as the one used for dynamic modulus testing of asphalt specimens.



Figure 3.16 LVDT Setup for Glued Button Deformation Measurement

In order to glue the buttons into the specimen, a hole is cut in a membrane at the locations of interest, for both sizes a 100 mm central gauge length was used. A membrane with holes cut is placed over a specimen then a small depression (about 1/4 length of the button and slightly larger

than the diameter of the button) is scraped where the button is to be fixed. Note, for the wet of optimum specimens, the buttons are just pushed into the location of interest to make the depression. The depression is then filled with quick setting epoxy glue and the button is then placed inside with the glue filling the entire void. Then a piece of membrane is cut and then placed over the button and hole and glued to keep the covering air tight. Examples of the buttons glued to the specimen are shown in Figure 3.17. Finally, to further ensure proper sealing, the openings that were glued were then covered with electrical tape.



Figure 3.17 Epoxied Button Examples

The other internal deformation measurement method used in this study utilized hollow core LVDTs and a pair of ring clamps that fit around the membrane along with 1-72 threaded rod and small O-rings for fixing the clamps. Figure 3.18 shows an example of the ring clamp setup used in this study as well as the hollow core LVDTs used which have a range of +/- 1 mm.

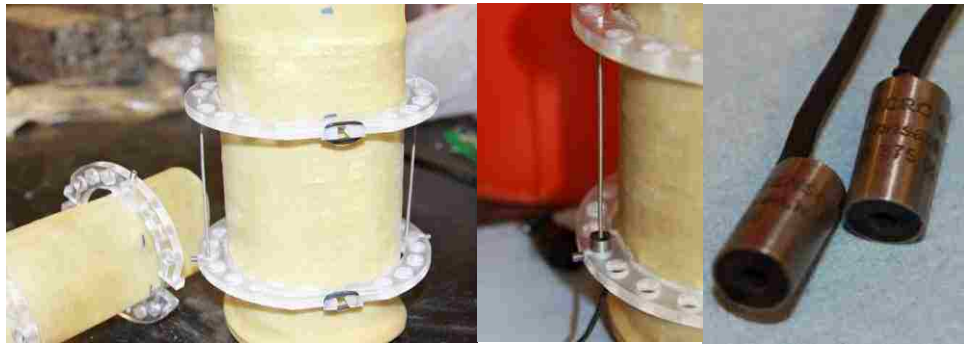


Figure 3.18 Ring Clamp Method Examples

External deformations were determined from an LVDT setup mounted on the loading piston.

The same spring-type LVDTs (± 1 mm) are used for the glued button method were used for the external method. An example of the external deformation measurement setup used in this study is shown in Figure 3.19.



Figure 3.19 External LVDT Setup Clamped to Loading Piston

3.5.2 Alternate Mr Testing Experiment

This experimental test was created using the Universal Test Setup within the GCTS CATS software. Rationale for conducting this experiment is explained in Chapter 5. Characteristics of the testing performed include:

- No confining pressure
- 1 Hz Sinusoidal Loading Form, shifted to have all positive values (minimum zero stress)
- No rest period

The stress sequences were 60 cycles long (i.e. 1 minute total sequence duration), and the magnitudes of the stresses were varied depending on the moisture condition of the soil (these values can be seen in the test matrices shown in Tables 3.4 and 3.5). At the very beginning of a test sequence one half of the maximum axial cyclic stress for that sequence was applied, this was found to make controlling the stress much easier. For this test method, the same glued button method which was introduced in Section 3.5.1 was used to monitor resilient deformations, and calculate equivalent resilient modulus values. Resilient modulus values were determined from the averages of maximum axial stress and recoverable strain values for cycles 20-40 (the middle 1/3 of the test sequence). Data for this test was sampled at 32 points per cycle. This sampling rate was found to be sufficient in characterizing the waveforms as shown in Figure 3.20, showing the consistency in load control from cycle to cycle as well as LVDT response based on the average axial strain plotted on the secondary axis.

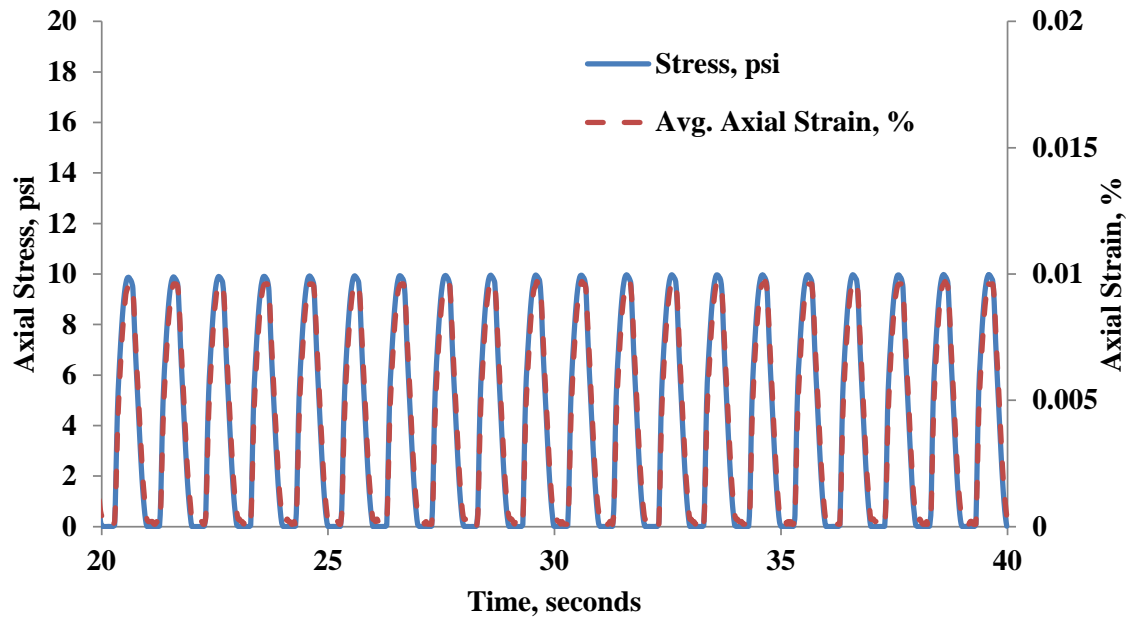


Figure 3.20 Example of Alternate Test Stress-Strain Response Form and Consistency

CHAPTER 4

RESILIENT MODULUS RESULTS AND DISCUSSION

4.1 Introduction

For resilient modulus testing, the AASHTO T 307 subgrade stress sequences for Type 2 soils, presented in tabular form in Chapter 2, were used. Deformation, stress, and resilient modulus values were monitored during testing. Additional test sequences at higher stresses were tested for to examine trends, deformation behaviors, and perform analyses. Results, comparisons, and analyses of resilient modulus with varying deformation measurement methods, moisture contents, and sizes are presented in this chapter.

4.2 Objective

One objective related to this chapter is to evaluate the difference between different axial deformation measurement methods, and to select a method to be used for comparative analysis. Another objective is to compare resilient modulus results from 2.8 in. to 4 in. diameter specimens that have both been impact compacted. Lastly, an attempt is made to generate a predictive equation for this material based on varying moisture contents and stress variables.

4.3 Resilient Modulus Testing

4.3.1 2.8 inch Diameter Specimens

Dry of Optimum

Moisture contents for dry of optimum specimens varied from 13.4% to 13.0%. With internal deformation measurements and consistent with literature on fine-grained soils, specimens showed decreased modulus values with increasing maximum cyclic axial stresses. Values for each test replicate, using each deformation method, and at each testing sequence are shown in Table 4.1. At lower deviator stress sequences, the internal clamp method show consistently larger modulus values than the glued button method. It is noted that as the deviator stresses increase, the difference in resilient modulus between these measurement methods decreases. Confining pressure appears to show little effect in terms of resilient modulus output for these specimens. The largest effects of confining pressure are present at low deviator stresses in the clamp method LVDTs, however here results are inconsistent and LVDT output was a concern. Since the effects of confining pressure are low relative to the effects of deviator stress when using the reference glued button method, plots and analyses are shown for the singular confining stress of 4 psi in this chapter. Figure 4.1 is a plot of all data from Table 4.1 for $\sigma_3 = 4$ psi, and is a graphical representation of resilient modulus results using the different deformation measurement methods. Modulus values using the external LVDTs were lower than the internal measurements as expected. In addition, they show an increasing modulus with increasing deviator stress which is not characteristic of resilient modulus behavior of fine-grained cohesive soils. Using an internal load cell with external LVDTs is one source of error, other sources of error more difficult to quantify are any physical equipment deformations (system compliance).

Table 4.1 2.8 in. Diameter @ 2% Dry of Optimum MC M_r Results

$\sigma_{\text{cyclic max}}$ (psi)	σ_3 (psi)	Replicate 1			Replicate 2			Replicate 3		
		w = 13.4%			w = 13.2%			w = 13.0%		
		Axial Deformation Measurement Method								
		Glued	Clamp	External	Glued	Clamp	External	Glued	Clamp	External
		M_r (ksi)								
1.8	6	125	199	11	138	349	13	138	262	17
3.6	6	114	141	13	129	249	14	131	169	19
5.4	6	102	115	14	125	138	15	124	135	20
7.2	6	92	102	15	121	123	16	119	123	21
9	6	88	96	16	118	119	17	115	114	21
1.8	4	114	213	11	141	265	13	133	253	17
3.6	4	108	147	12	133	215	14	129	165	19
5.4	4	97	116	14	128	159	15	124	139	20
7.2	4	90	103	15	123	131	16	120	124	21
9	4	87	96	16	119	120	17	116	116	22
1.8	2	111	206	12	139	253	14	133	302	17
3.6	2	101	151	13	136	211	14	128	166	19
5.4	2	93	118	14	127	170	16	125	139	20
7.2	2	89	104	15	123	135	16	121	124	21
9	2	86	97	16	118	120	17	117	116	22

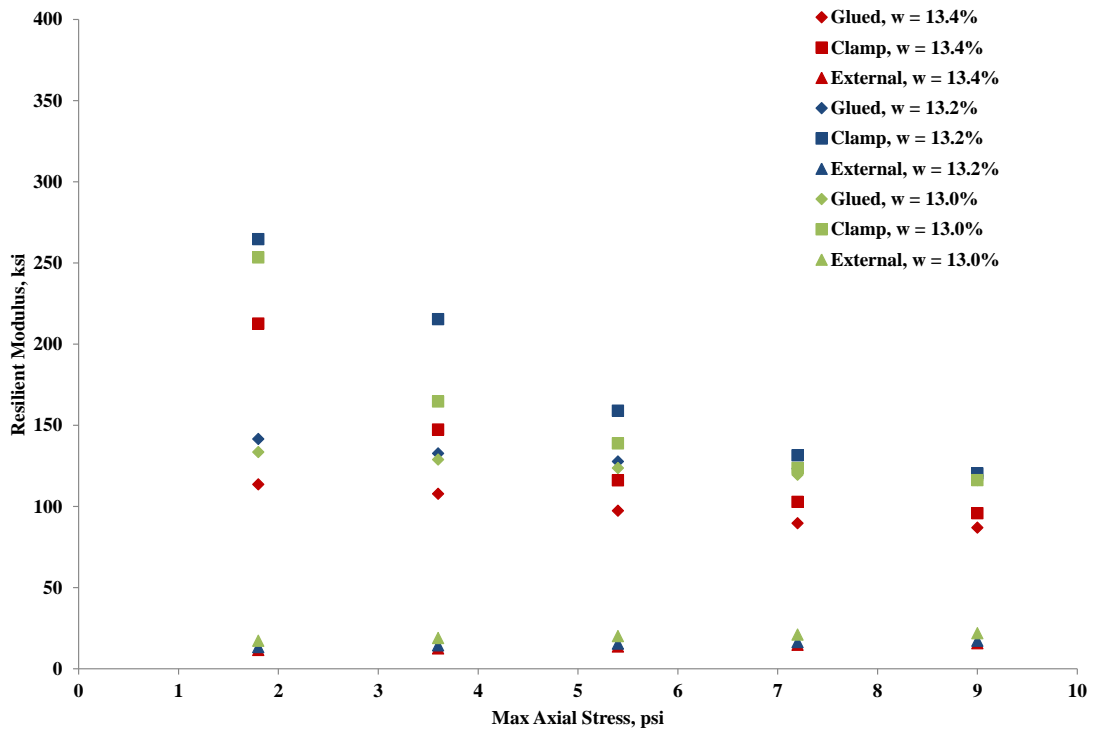


Figure 4.1 M_r Plot 2.8 inch Diameter Dry of Optimum MC, $\sigma_3 = 4$ psi

Optimum

Moisture contents for optimum specimens varied from 15.8% to 15.6%. Again, with internal deformation measurement, specimens showed decreased modulus values with increasing maximum cyclic axial stresses. Values for each test replicate, using each deformation method, and at each testing sequence are shown in Table 4.2. At lower deviator stress sequences, the internal clamped LVDTs show larger modulus values than the internal glued button method for 2 of the 3 replicates.

Modulus values using the external LVDTs were lower than the internal measurements as expected, but the difference is smaller than for the dry of optimum specimens. This makes sense, if the deformations outside the specimen contributing to the difference are near constant when testing specimens of varying stiffness, then the difference in values between external and internal deformation measurement should be smaller for the specimen with a lower stiffness. The trend for external LVDTs is still increasing with increasing deviator stress but at a smaller rate than for the dry specimens. Figure 4.2 is a plot of all data from Table 4.2 for $\sigma_3 = 4$ psi, and is a graphical representation which presents the spread in resilient modulus results when using the different deformation measurement methods.

Table 4.2 2.8 in. Diameter @ Optimum MC M_r Results

$\sigma_{\text{cyclic max}}$ (psi)	σ_3 (psi)	Replicate 1			Replicate 2			Replicate 3		
		w = 15.8%			w = 15.6%			w = 15.6%		
		Axial Deformation Measurement Method								
		Glued	Clamp	External	Glued	Clamp	External	Glued	Clamp	External
M_r (ksi)										
1.8	6	95	70	10	144	177	4	67	103	10
3.6	6	80	59	10	112	76	10	62	63	10
5.4	6	68	53	11	100	61	11	55	54	10
7.2	6	64	50	11	83	54	11	51	47	10
9	6	59	47	11	74	51	11	49	43	10
1.8	4	85	77	10	150	173	5	62	99	10
3.6	4	72	60	10	125	76	10	57	62	10
5.4	4	65	53	10	95	58	10	54	51	10
7.2	4	62	49	11	81	53	11	53	45	10
9	4	59	46	11	72	50	11	51	44	10
1.8	2	83	132	10	151	184	5	65	100	10
3.6	2	72	60	10	116	76	10	57	65	10
5.4	2	65	52	11	89	58	10	55	51	10
7.2	2	62	49	11	77	53	11	53	45	10
9	2	59	46	11	72	50	11	51	43	11

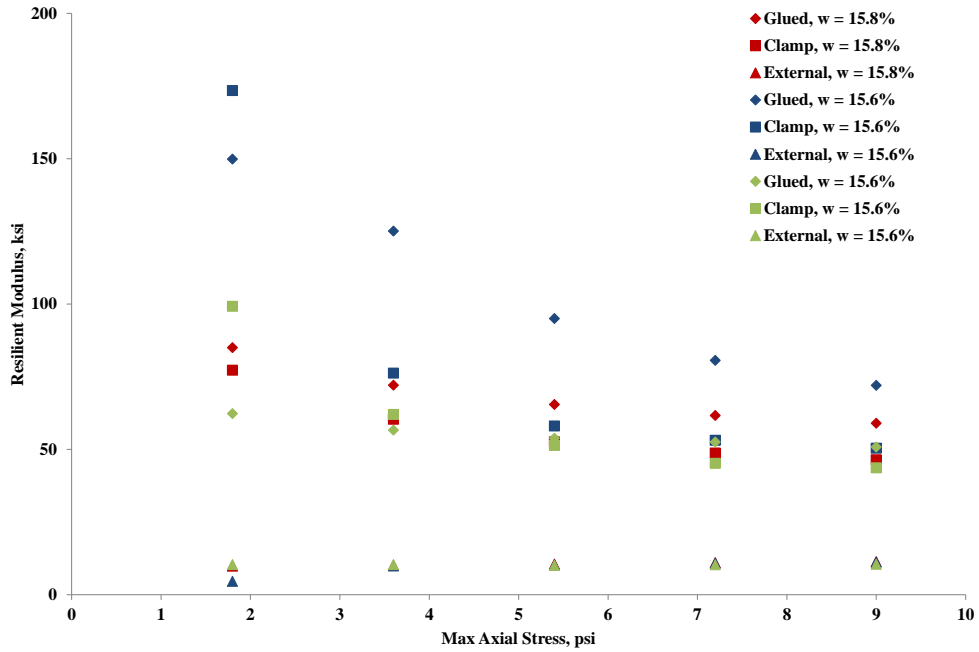


Figure 4.2 M_r Plot 2.8 in. Diameter @ Optimum MC, $\sigma_3 = 4$ psi

Wet of Optimum

Moisture contents for wet of optimum specimens varied from 17.9% to 17.2%. Similar to the dry of optimum and wet of optimum groupings, with internal deformation measurement, specimens showed decreased modulus values with increasing maximum cyclic axial stresses. Values for each test replicate, using each deformation method, and at each testing sequence are shown in Table 4.3. At lower deviator stress sequences, the internal hollow core LVDTs show larger modulus values than the internal spring type LVDTs for 1 of the 3 replicates. It is noted that for this group of specimens, the results from the two internal deformation measurement techniques are nearest to one another than the other moisture contents tested. Figure 4.3 is a plot of all data from Table 4.3 for $\sigma_3 = 4$ psi, and is a graphical representation which presents the spread in resilient modulus results when using the different deformation measurement methods. The general agreement of results using the two internal methods at max cyclic stresses of 5.4 psi and higher is encouraging. Similar to the dry of optimum and optimum groupings, as the deviator stresses increased, this difference in resilient modulus between the measurement methods decreases. Modulus values using the external LVDTs were again significantly lower than the internal measurements. The difference is smaller than for the both the optimum and dry of optimum specimens. As discussed previously this makes sense, if the deformations outside the specimen contributing to the difference are near constant when testing specimens of varying stiffness, then the difference in values between external and internal deformation measurement should be, and is, smaller for the specimen with a lower stiffness.

Table 4.3 2.8 in. Diameter Wet of Optimum MC M_r Results

$\sigma_{\text{cyclic max}}$ (psi)	σ_3 (psi)	Replicate 1			Replicate 2			Replicate 3		
		w = 17.9%			w = 17.6%			w = 17.2%		
		Axial Deformation Measurement Method								
		Glued	Clamp	External	Glued	Clamp	External	Glued	Clamp	External
		M_r (ksi)								
1.8	6	29	27	8	39	57	8	68	68	10
3.6	6	27	25	7	34	42	8	58	41	9
5.4	6	24	23	7	31	37	8	46	36	9
7.2	6	22	21	7	30	32	8	37	32	9
9	6	21	19	7	28	30	8	33	30	9
1.8	4	29	27	8	39	58	8	66	59	10
3.6	4	25	23	7	33	39	8	50	40	9
5.4	4	23	22	7	31	33	8	40	35	9
7.2	4	22	21	7	29	30	8	35	32	9
9	4	20	20	7	28	29	8	33	30	9
1.8	2	29	28	8	38	54	8	66	56	10
3.6	2	25	24	7	33	38	8	50	41	9
5.4	2	23	22	7	31	33	8	40	35	9
7.2	2	22	21	7	29	30	8	35	32	9
9	2	20	20	7	29	29	8	33	31	10

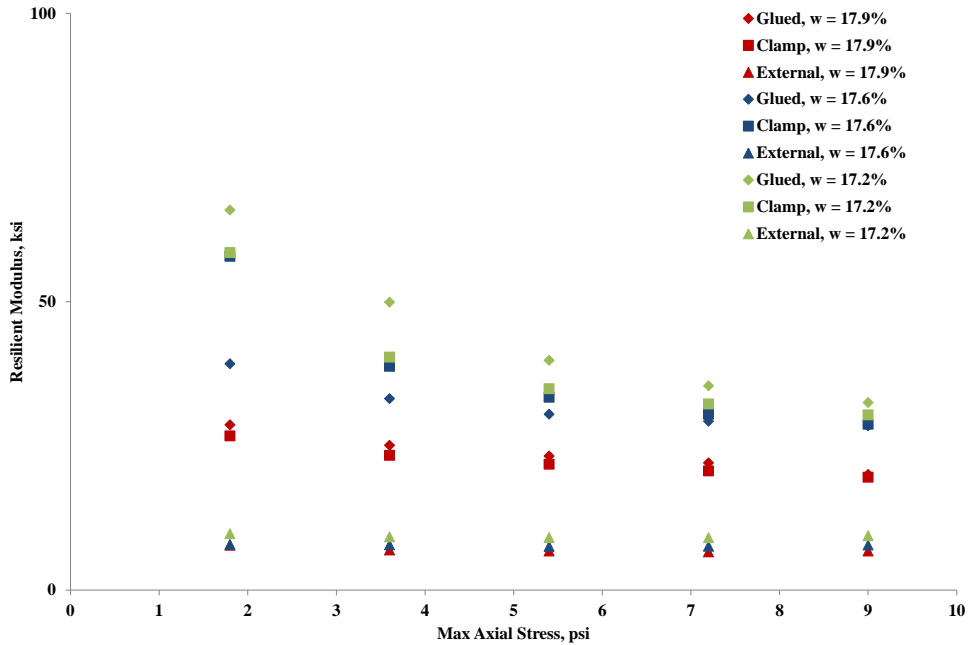


Figure 4.3 M_r Plot 2.8 in. Diameter Wet of Optimum MC, $\sigma_3 = 4$ psi

2.8 inch Diameter Resilient Modulus at Higher Deviator Stresses

For the internal deformation measurement methods, specimens were tested at maximum cyclic stresses higher than those reached in the AASHTO T 307 subgrade standard. These tests were performed separately after the initial subgrade sequences were run. This higher stress testing was performed to evaluate if the trends shown at the higher deviator stresses (i.e. better agreement between the two deformation measurement methods at high compared to low deviator stresses) continued. Figure 4.4 shows the results for the dry of optimum replicates, 2 of the 3 replicates appear to follow the subgrade sequence trend well while one replicate shows a deviation from the trend. For all replicates the agreement between the two deformation methods are better at the higher deviator stresses than the lower, this was expected based on the initial trends from the subgrade sequence testing. Figure 4.5 shows continuation of trends and good agreement between the two methods for all comparison replicates at the higher deviator stresses for 2.8 inch diameter specimens at optimum moisture contents. Figure 4.6 is a plot of specimens at wet of optimum moisture content, consistent with the results shown in Figures 4.4 and 4.5, this figure shows good improving agreement between deformation measurement methods for each replicate as the maximum cyclic stress increases.

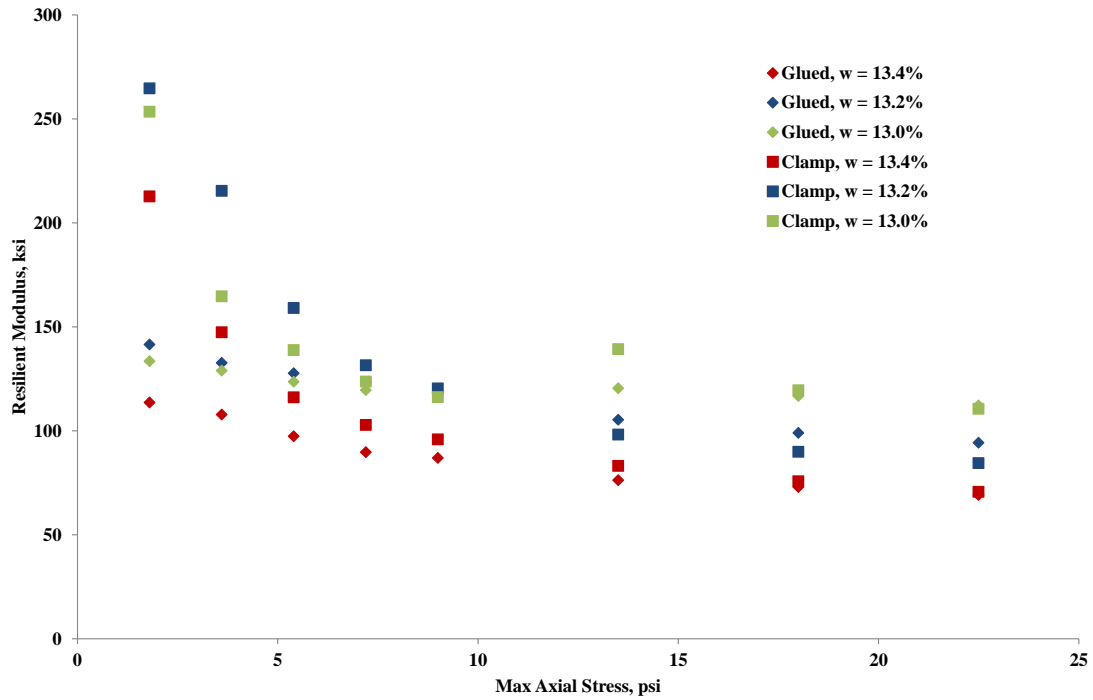


Figure 4.4 Dry of Optimum M_r , including Higher Stress Sequences 2.8 inch Diameter Specimens

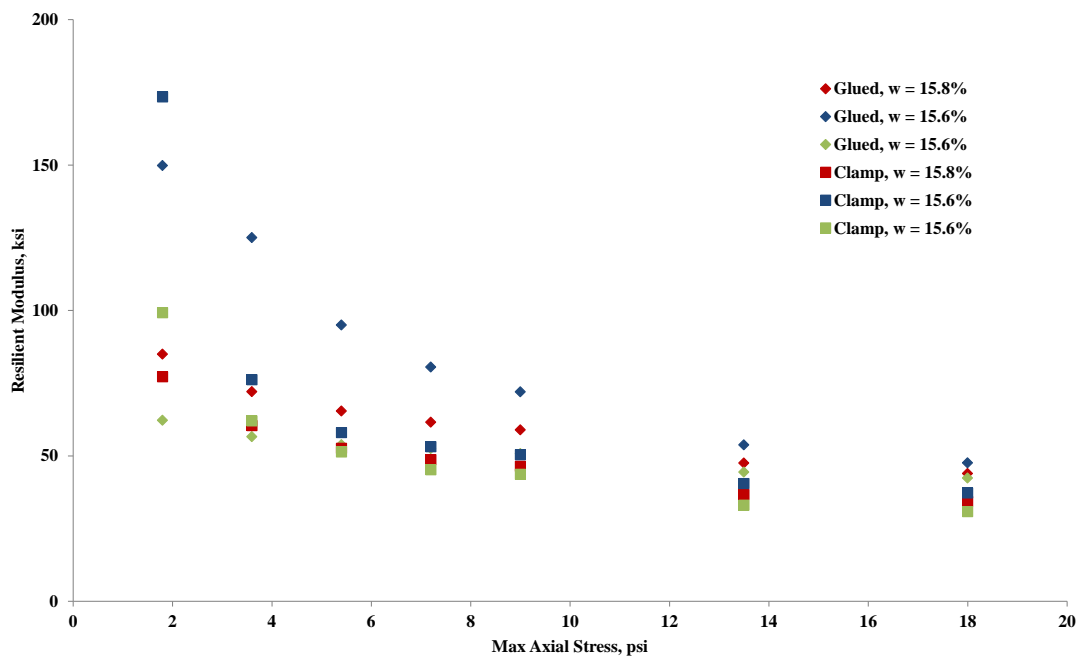


Figure 4.5 Optimum M_r , including Higher Stress Sequences 2.8 inch Diameter Specimens

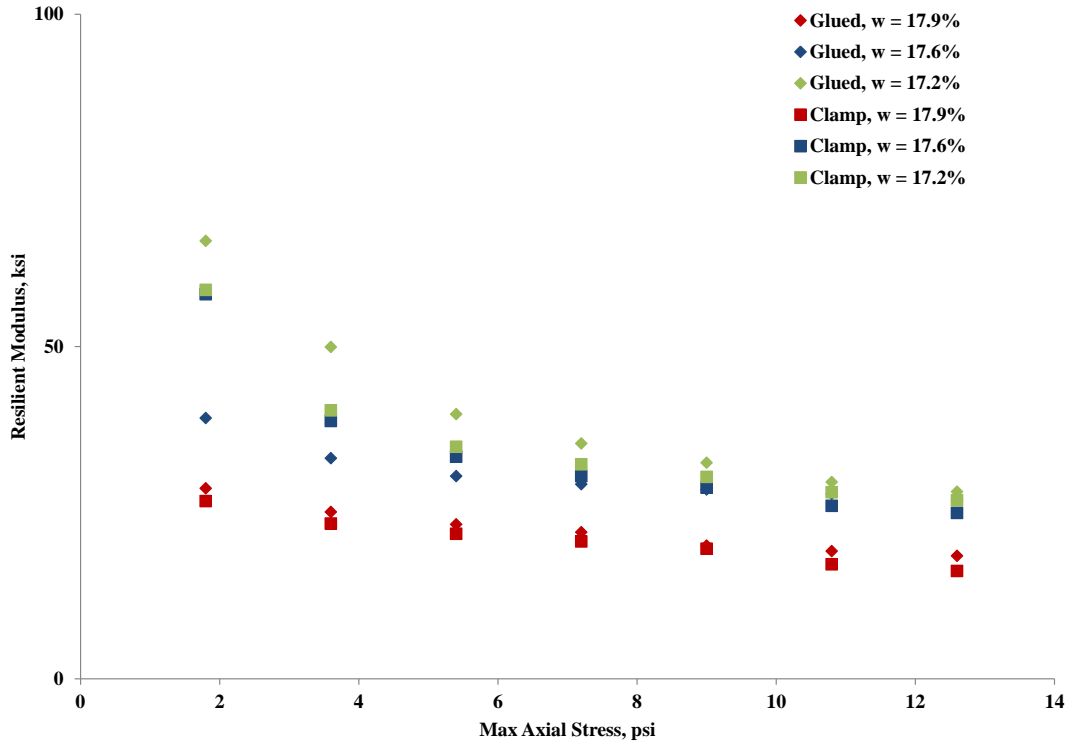


Figure 4.6 Wet of Optimum M_r , including Higher Stress Sequences 2.8 inch Diameter Specimens

4.3.2 4 inch Diameter Specimens

All results from resilient modulus testing on 4 in. diameter specimens using the T 307 subgrade sequences are presented in Table 4.4. Similar to the 2.8 inch diameter specimens the internal glued button method showed the most consistent results. For example, notice the differences in values between the two internal deformation measurement methods at the lower stress sequences. The inflated values for the dry of optimum and optimum specimens stick out at over 1,400 and 600 ksi. It is noted that these are not characteristic of the material deformation and are considered erroneous and is likely due to the physical clamp setup and one LVDT not deforming with the specimen. These are values correspond to deformations much smaller than the precision of the transducers based on the 0.25% non-linearity error. Also, while the ring

clamp setup for 4 in. specimens fit tightly around the membrane/specimen, it was noticed it did not feel like it gripped as firmly as the 2.8 in. diameter clamp rings did. Again, similar to the results of section 4.2, the gaps in resilient modulus values between the two methods closes as the maximum cyclic axial stress magnitudes increase. Figure 4.7 is a plot of all data from Table 4.6 for $\sigma_3 = 4$ psi, and is a graphical representation which presents the spread in resilient modulus results when using the different deformation measurement methods. Looking at values after the 5.4 psi stress, the trend of decreasing resilient modulus with increasing moisture content becomes clearer.

Table 4.4 4 inch Diameter M_r Results

$\sigma_{\text{cyclic max}}$ (psi)	σ_3 (psi)	4 inch Diameter Specimens								
		w = 13.4%			w = 15.5%			w = 17.8%		
		Glued	Clamp	External	Glued	Clamp	External	Glued	Clamp	External
		M_r (ksi)								
1.8	6	147	1441	14	110	632	12	31	69	9
3.6	6	128	1162	13	103	216	12	28	28	8
5.4	6	110	206	13	100	81	12	25	19	8
7.2	6	97	128	14	97	62	12	21	15	8
9	6	89	102	15	92	55	13	19	12	8
1.8	4	140	1454	14	105	754	12	30	77	9
3.6	4	113	1207	13	101	162	12	25	29	8
5.4	4	102	239	13	97	80	12	21	18	8
7.2	4	94	131	14	95	62	13	20	15	8
9	4	89	104	15	92	55	13	19	12	8
1.8	2	140	1623	14	105	844	12	30	79	9
3.6	2	112	655	13	100	174	12	25	29	8
5.4	2	100	224	14	96	80	12	21	18	8
7.2	2	95	134	14	94	63	13	20	14	8
9	2	89	108	15	89	57	13	19	13	8

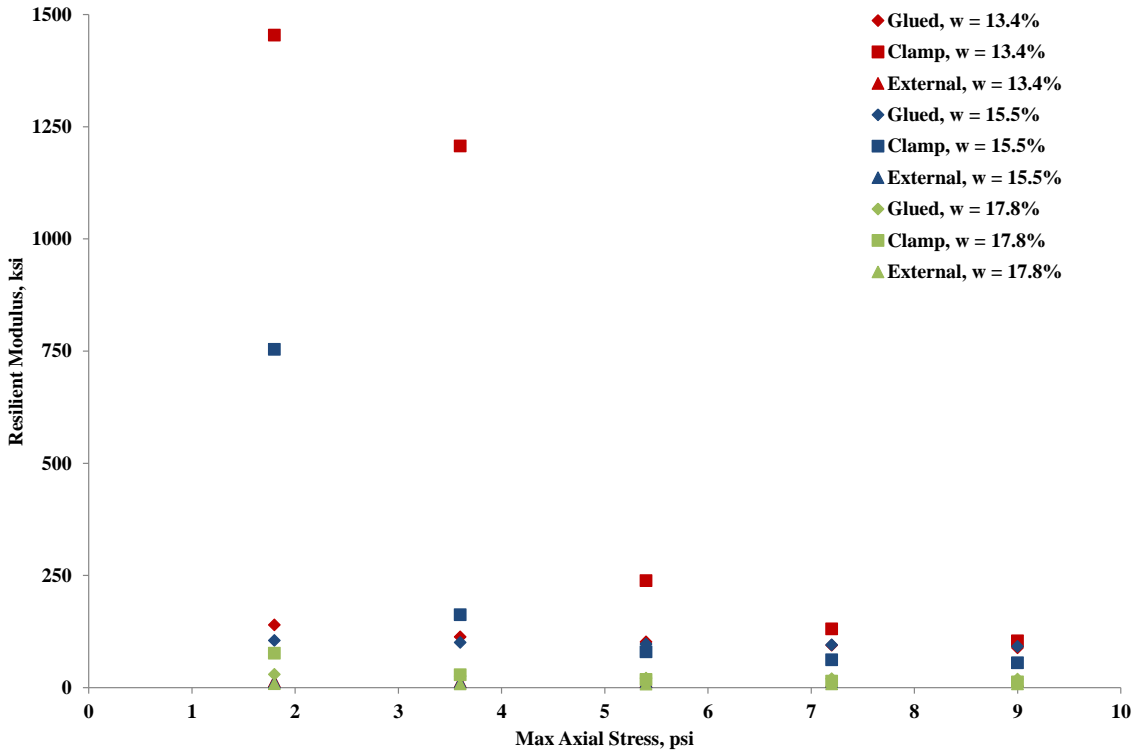


Figure 4.7 M_r Plot 4 inch Diameter, $\sigma_3 = 4$ psi

4.3.3 Resilient Modulus Results Discussion

Confining Pressure Effects

In order to examine the effects of confining pressure on these resilient modulus results, a comparison of M_r values at the same maximum cyclic axial stresses are compared to one another as percent differences between the 2 and 4 psi confining stresses, and the 2 and 6 psi confining stresses relative to the 2 psi M_r value. An example of how this comparison method was done is shown below in Eqns. (4.1) and (4.2).

$$\%Difference_{2to4psi} = \left(\frac{M_{r,4 psi} - M_{r,2 psi}}{M_{r,2 psi}} \right) * 100 \quad \text{Eqn. (4.1)}$$

$$\%Difference_{4to6psi} = \left(\frac{M_{r,4 psi} - M_{r,2 psi}}{M_{r,2 psi}} \right) * 100 \quad \text{Eqn. (4.2)}$$

For the 2.8 inch diameter specimens, the average difference across cyclic axial stresses for 14 of the 18 specimens showed a small increase (all less than 10%) in resilient modulus relative to the 2 psi confining pressure value. For 4 of the 18 comparisons, average percent differences of -1.9% to -0.5% were observed. It is understood the effect of increasing confining pressure should not result in decreasing resilient modulus, and it would be of greater concern if the decreasing values were larger or the majority of comparisons showed this behavior. However, this is not the case and with the differences so small that they are not really a concern, the results support studies that have found cohesive fine-grained specimens not significantly affected by small confining pressures. In Table 4.5, 4.6 and 4.7 the percent difference results comparisons are shown for all 2.8 inch diameter specimens at dry of optimum, optimum and wet of optimum moisture states respectively.

Table 4.5 Confining Pressure Effect 2.8 inch Diameter Dry of Optimum

$\sigma_{\text{cyclic max}}$ (psi)	w = 13.4%		w = 13.2%		w = 13.0%	
	% Difference of M_r Values					
	$\sigma_3, 2$ to 4 psi	$\sigma_3, 2$ to 6 psi	$\sigma_3, 2$ to 4 psi	$\sigma_3, 2$ to 6 psi	$\sigma_3, 2$ to 4 psi	$\sigma_3, 2$ to 6 psi
1.8	2.4	12.9	1.8	-0.6	0.2	3.8
3.6	7.0	12.7	-2.7	-5.7	0.6	1.9
5.4	4.3	9.1	0.3	-1.5	-1.0	-0.6
7.2	0.2	2.6	0.4	-1.2	-1.5	-1.5
9	1.1	2.5	0.4	-0.4	-0.6	-1.6
Avg.	3.0	8.0	0.0	-1.9	-0.5	0.4

Table 4.6 Confining Pressure Effect 2.8 inch Diameter Optimum

$\sigma_{\text{cyclic max}}$ (psi)	w = 15.8%		w = 15.6%		w = 15.6%	
	% Difference of M_r Values					
	$\sigma_3, 2$ to 4 psi	$\sigma_3, 2$ to 6 psi	$\sigma_3, 2$ to 4 psi	$\sigma_3, 2$ to 6 psi	$\sigma_3, 2$ to 4 psi	$\sigma_3, 2$ to 6 psi
1.8	2.0	13.8	-0.8	-4.4	-3.5	4.2
3.6	0.4	11.0	7.7	-3.8	-0.7	8.3
5.4	0.5	4.4	6.5	11.7	-1.3	0.9
7.2	-0.1	3.5	4.8	8.0	-0.1	-3.2
9	-0.2	0.3	-0.4	2.7	-0.8	-4.4
Avg.	0.5	6.6	3.6	2.8	-1.3	1.2

Table 4.7 Confining Pressure Effect 2.8 inch Diameter Wet of Optimum

$\sigma_{\text{cyclic max}}$ (psi)	w = 17.9%		w = 17.6%		w = 17.2%	
	% Difference of M_r Values					
	$\sigma_3, 2$ to 4 psi	$\sigma_3, 2$ to 6 psi	$\sigma_3, 2$ to 4 psi	$\sigma_3, 2$ to 6 psi	$\sigma_3, 2$ to 4 psi	$\sigma_3, 2$ to 6 psi
1.8	-1.1	1.6	2.3	2.0	0.4	3.5
3.6	-1.4	4.1	0.9	3.9	0.7	17.4
5.4	-0.9	2.8	-0.7	2.2	0.7	16.4
7.2	-0.8	0.3	-0.5	0.5	0.2	5.6
9	-0.9	2.7	-0.3	-0.3	-0.3	0.3
Avg.	-1.0	2.3	0.3	1.7	0.3	8.6

For the 4 in. diameter specimens, confining pressure showed less than 10% average effect with all three test specimens showing average percent increases. Table 4.8 shows comparison values

for the 4 in. diameter specimens, it is noted that the average percent increase in M_r are smaller from 2 to 4 psi than from 2 to 6 psi for all specimens, though again the effect is small.

Table 4.8 Confining Pressure Effect 4 inch Diameter

$\sigma_{\text{cyclic max}}$ (psi)	w = 13.4%		w = 15.5%		w = 17.8%	
	% Difference of M_r Values					
	$\sigma_3, 2$ to 4 psi	$\sigma_3, 2$ to 6 psi	$\sigma_3, 2$ to 4 psi	$\sigma_3, 2$ to 6 psi	$\sigma_3, 2$ to 4 psi	$\sigma_3, 2$ to 6 psi
1.8	-0.2	5.3	0.1	4.9	0.2	4.5
3.6	1.5	14.9	0.7	3.0	1.3	10.2
5.4	1.3	9.5	0.9	4.2	1.4	20.5
7.2	-0.2	2.6	0.8	2.2	1.4	6.6
9	-0.9	-0.6	3.3	3.9	0.7	2.1
Avg.	0.3	6.3	1.1	3.6	1.0	8.8

To put into perspective the differences in M_r values presented, take the largest magnitude percentage increase and decrease seen in all the values shown in Tables 4.5 through 4.8, this is 20.5% in Table 4.10 and -5.7% in Table 4.7. For the 20.5% difference, this corresponds to a pair of M_r values of 20.6 ksi at 2 psi confining pressure and 24.9 ksi at 6 psi confining pressure. At the 5.4 psi max cyclic axial stress which this pair comes from, this corresponds to a deformation difference of approximately 1.76×10^{-4} inches (about 4.5 microns). For the -5.7% difference, this corresponds to a pair of M_r values of 128.6 ksi at 2 psi confining pressure and 136.3 ksi at 6 psi confining pressure. At the 3.6 psi max cyclic axial stress which this pair comes from, this corresponds to a deformation difference of approximately 6.2×10^{-6} inches (< 1 micron). In Chapter 2 it was introduced that researchers have found the range of confining pressures applied during a subgrade resilient modulus test, have showed little influence on the M_r values. Results from this study agree that confining pressure has little effect on resilient modulus, especially relative to deviator stress or moisture content.

Axial Deformation Measurement Methods

Internal vs. External LVDTs

For all sizes of specimens across all moisture contents, the resilient modulus values determined using internal deformation measurements was consistently much higher than for the external deformation measurements. For the majority of specimens the M_r values determined using internal LVDTs were 5 to 10 times the M_r values determined external, exceptions to this were for the specimens with the lowest stiffness at the higher stress sequences. One certain source of error is due to the internal load cell, as it is a strain gauge device and located within the triaxial cell, below the external LVDTs that are located on the actuator. The load cell deformation contributes to the resilient strain thereby reducing the magnitude of resilient modulus. The load cell used in this study has a rated deflection of 0.002 inches at maximum output. The load cell deflection curve is shown in Figure 4.8, with the corresponding nominal load deflections for a 2.8 in. and 4 in. specimen subjected to AASHTO T 307 subgrade stress sequences.

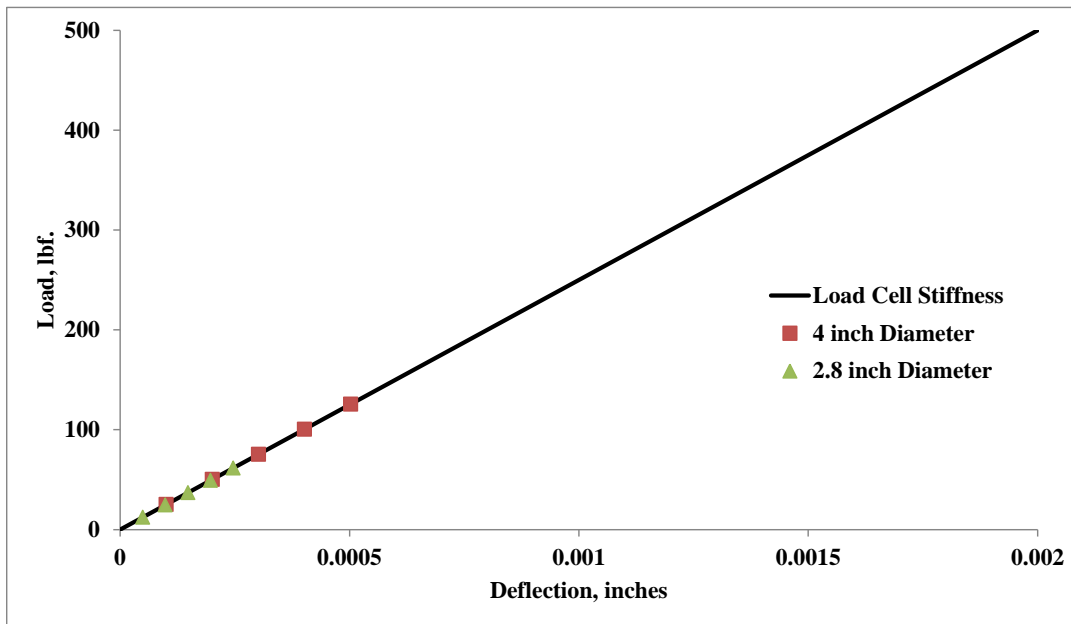


Figure 4.8 Load Cell Output vs. Deflection

With knowledge of the load cell deflection to output behavior it may be possible to remove this strain from the test results, however other contributing factors such as unfixed connections and any other deformations are not as easy to quantify nor are they expected to be as consistent as a load cells deflection to output (or consistent at all for that matter when comparing two different systems or making changes to a test setup). In order to get an idea of the contributions of load cell and other compliance related deformations a comparison was performed on the resilient modulus results of various specimen sizes and moisture contents at the middle stress sequence of 5.4 psi maximum axial stress and 4 psi confining pressure. Using the deformation differences between the internal and external LVDT modulus results as considered errors, and then subtracting the amount of load cell deformation based on load output at the reference sequence, an estimate of the amount of compliance related erroneous deformations is then quantified. Table 4.9 displays the results from this analysis, showing the majority of deformations seen when measuring externally are extraneous.

Table 4.9 Extraneous Deformation Estimation 2.8 inch Diameter Specimens

		Size = 2.8 inch Diameter					
		Deformation (in. x 10 ⁻³)					% Error (Other/External Deformations)
Moisture Condition	Specimen No.	Specimen		Difference	Load Cell	Other Deformations	
		Internal	External				
Dry of Optimum	1	0.23	1.62	1.39	0.15	1.24	77
	2	0.17	1.42	1.25	0.15	1.10	78
	3	0.18	1.10	0.92	0.15	0.77	70
Optimum	4	0.34	2.10	1.77	0.15	1.62	77
	5	0.23	2.16	1.93	0.15	1.78	82
	6	0.41	2.18	1.77	0.15	1.62	74
Wet of Optimum	7	0.95	3.26	2.31	0.15	2.17	66
	8	0.72	2.91	2.19	0.15	2.04	70
	9	0.55	2.42	1.87	0.15	1.72	71

Figure 4.9 is a plot of the equivalent deformations for the nine 2.8 inch diameter specimens tested, note the increasing trend in deformations from Specimen 1 to 9, where 1-3, 4-6, and 7-9 are dry, optimum, and wet of optimum respectively. This makes sense based on the resilient modulus values showing decreasing values with moisture content. It is also noted that though the magnitudes of the external and internal deformations are very different, the trends are similar.

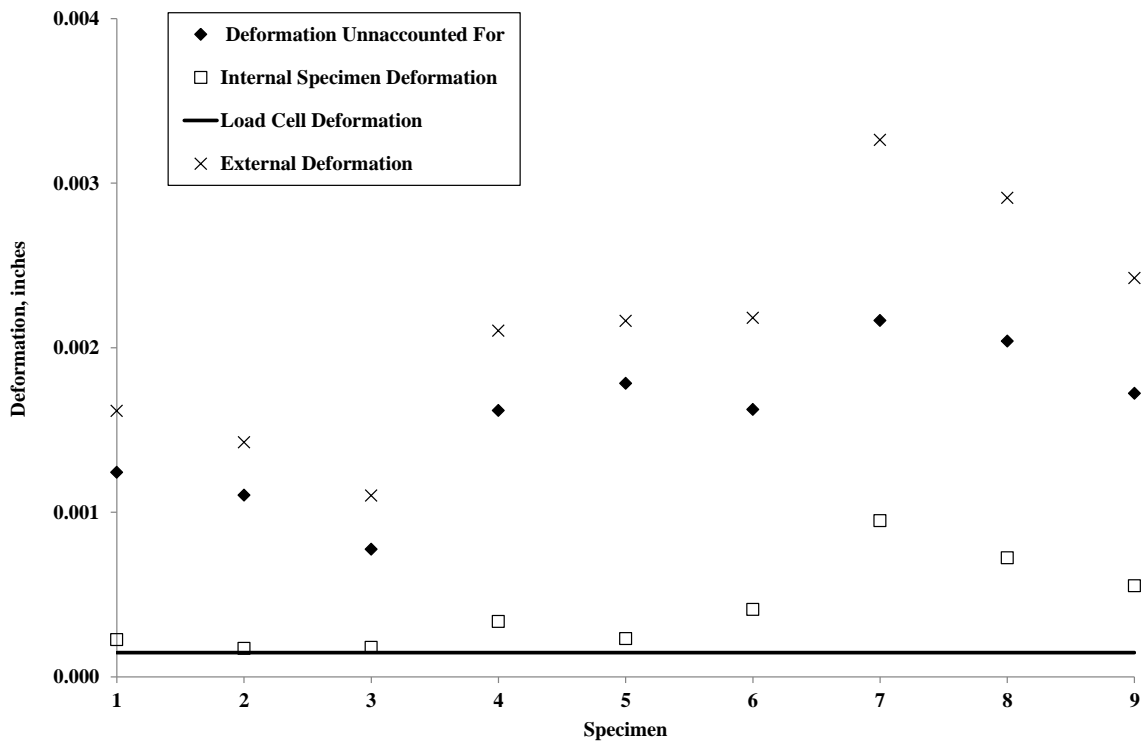


Figure 4.9 Example of Deformation Accounts 2.8 inch Diameter Specimens

In Chapter 2 it was presented that numerous researchers have expressed concern regarding external transducers being used for determining resilient modulus, i.e. system compliance influencing M_r results when using external LVDTs. Additionally, when researchers attempted to mitigate error by factoring out compliance or fixing specimen ends to platens, threshold values of M_r were still encountered where compliance significantly influenced results. Barksdale et al.

(1997) found that reliable resilient modulus values cannot be determined using external LVDTs for specimens stiffer than 10 ksi, and that to account for the compliance using checks and calibration standards can be “tedious and time consuming,” and even then a threshold of 60 ksi was found limiting when using external LVDTs. Kim and Drabkin (1994) found that by grouting the end platens to the specimen, external deformation measurement could only accurately determine M_r for values below 50 ksi. An attempt was made during this study to determine compliance related deformations using a very stiff check specimen that should be unresponsive (should not show measureable deformations) within the LVDT range at the subgrade axial stresses of 2-10 psi. In reference to the example shown in Table 4.9 and Figure 4.9, the compliance check specimen yielded a deformation of 0.67×10^{-3} inches at a 5.4 psi deviator stress, which still does not account for the majority of compliance deformations seen in this study when using external LVDTs. The amount of time and effort that can be exerted testing check standard specimens to account for compliance, as well as the fact that other researchers have found threshold values well below values of M_r that can be reached by subgrade specimens, supports the fact that internal deformation measurements should be used for determining resilient modulus.

Internal Deformation Measurement Comparison

A comparison of the glued button and ring clamp deformation methods is conducted using the glued button as a reference. In initial results discussion, it was introduced that the differences between the two methods became smaller as the axial stresses increased.

Tables 4.10-4.13 show the percent differences between the two internal methods, where the general trend is that agreement between the two deformation methods improved as maximum

axial cyclic stresses increased. Figures 4.10 and 4.11 are plots of the tabulated data where percent difference and max cyclic axial stress are the axes, these plots show the agreement between the two methods improves at the higher stresses.

Table 4.10 Internal Deformation Measurement Comparison 2.8 in. Dry of Optimum

$\sigma_{\text{cyclic max}}$ (psi)	σ_3 (psi)	Replicate 1			Replicate 2			Replicate 3			
		w = 13.4%			w = 13.2%			w = 13.0%			
		Deformation Measurement Method									
		Glued	Clamp	Difference	Glued	Clamp	Difference	Glued	Clamp	Difference	
M_r (ksi)		(%)	M_r (ksi)		(%)	M_r (ksi)		(%)			
1.8	6	125	199	59	138	349	153	138	262	89	
3.6	6	114	141	24	129	249	94	131	169	29	
5.4	6	102	115	13	125	138	10	124	135	9	
7.2	6	92	102	11	121	123	1	119	123	3	
9	6	88	96	8	118	119	1	115	114	-1	
1.8	4	114	213	87	141	265	87	133	253	90	
3.6	4	108	147	37	133	215	62	129	165	28	
5.4	4	97	116	19	128	159	25	124	139	12	
7.2	4	90	103	15	123	131	7	120	124	3	
9	4	87	96	10	119	120	1	116	116	0	
1.8	2	111	206	85	139	253	82	133	302	127	
3.6	2	101	151	50	136	211	55	128	166	30	
5.4	2	93	118	27	127	170	33	125	139	11	
7.2	2	89	104	16	123	135	10	121	124	2	
9	2	86	97	12	118	120	2	117	116	-1	

Table 4.11 Internal Deformation Measurement Comparison 2.8 in. Optimum

$\sigma_{\text{cyclic max}}$ (psi)	σ_3 (psi)	Replicate 1			Replicate 2			Replicate 3		
		w = 15.8%			w = 15.6%			w = 15.6%		
		Deformation Measurement Method								
		Glued	Clamp	Difference (%)	Glued	Clamp	Difference (%)	Glued	Clamp	Difference (%)
M_r (ksi)		M_r (ksi)			M_r (ksi)					
1.8	6	95	70	-26	144	177	23	67	103	54
3.6	6	80	59	-26	112	76	-32	62	63	2
5.4	6	68	53	-22	100	61	-39	55	54	-3
7.2	6	64	50	-22	83	54	-34	51	47	-8
9	6	59	47	-21	74	51	-32	49	43	-13
1.8	4	85	77	-9	150	173	16	62	99	59
3.6	4	72	60	-16	125	76	-39	57	62	10
5.4	4	65	53	-20	95	58	-39	54	51	-5
7.2	4	62	49	-21	81	53	-34	53	45	-14
9	4	59	46	-21	72	50	-30	51	44	-14
1.8	2	83	132	59	151	184	22	65	100	55
3.6	2	72	60	-16	116	76	-34	57	65	15
5.4	2	65	52	-20	89	58	-35	55	51	-7
7.2	2	62	49	-21	77	53	-31	53	45	-15
9	2	59	46	-22	72	50	-30	51	43	-17

Table 4.12 Internal Deformation Measurement Comparison 2.8 in. Wet of Optimum

$\sigma_{\text{cyclic max}}$ (psi)	σ_3 (psi)	Replicate 1			Replicate 2			Replicate 3		
		w = 17.9%			w = 17.6%			w = 17.2%		
		Deformation Measurement Method								
		Glued	Clamp	Difference (%)	Glued	Clamp	Difference (%)	Glued	Clamp	Difference (%)
M_r (ksi)		M_r (ksi)			M_r (ksi)					
1.8	6	29	27	-8	39	57	45	68	68	-1
3.6	6	27	25	-7	34	42	23	58	41	-30
5.4	6	24	23	-5	31	37	16	46	36	-22
7.2	6	22	21	-6	30	32	10	37	32	-13
9	6	21	19	-7	28	30	4	33	30	-8
1.8	4	29	27	-7	39	58	48	66	59	-11
3.6	4	25	23	-7	33	39	17	50	40	-19
5.4	4	23	22	-6	31	33	10	40	35	-12
7.2	4	22	21	-6	29	30	4	35	32	-9
9	4	20	20	-2	28	29	1	33	30	-7
1.8	2	29	28	-5	38	54	40	66	56	-15
3.6	2	25	24	-7	33	38	14	50	41	-18
5.4	2	23	22	-7	31	33	6	40	35	-11
7.2	2	22	21	-7	29	30	3	35	32	-8
9	2	20	20	-3	29	29	2	33	31	-6

Table 4.13 Internal Deformation Measurement Comparison 4 in. Specimens

$\sigma_{\text{cyclic max}}$ (psi)	σ_3 (psi)	Dry			Optimum			Wet		
		w = 13.4%			w = 15.5%			w = 17.8%		
		Deformation Measurement Method								
		Glued	Clamp	Difference	Glued	Clamp	Difference	Glued	Clamp	Difference
M_r (ksi)		(%)	M_r (ksi)		(%)	M_r (ksi)		(%)		
1.8	6	147	1441	878	110	632	475	31	69	123
3.6	6	128	1162	806	103	216	110	28	28	2
5.4	6	110	206	87	100	81	-19	25	19	-24
7.2	6	97	128	32	97	62	-36	21	15	-29
9	6	89	102	14	92	55	-41	19	12	-36
1.8	4	140	1454	942	105	754	618	30	77	159
3.6	4	113	1207	966	101	162	61	25	29	13
5.4	4	102	239	134	97	80	-18	21	18	-14
7.2	4	94	131	39	95	62	-35	20	15	-27
9	4	89	104	18	92	55	-40	19	12	-34
1.8	2	140	1623	1060	105	844	705	30	79	166
3.6	2	112	655	487	100	174	74	25	29	14
5.4	2	100	224	124	96	80	-17	21	18	-12
7.2	2	95	134	42	94	63	-34	20	14	-26
9	2	89	108	21	89	57	-36	19	13	-33

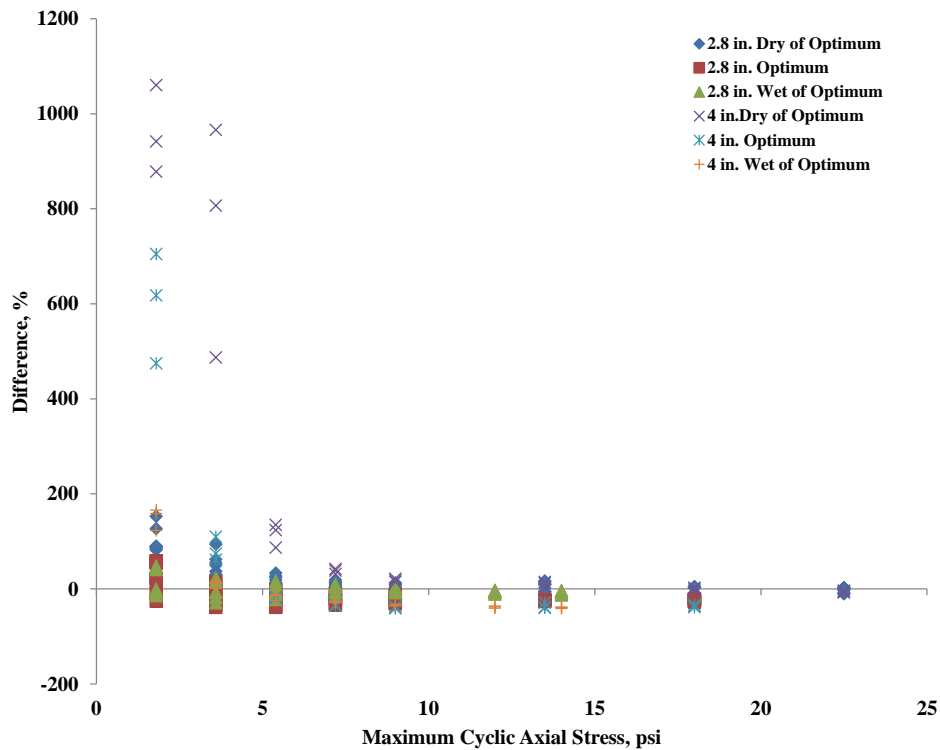


Figure 4.10 Internal Deformation Measurement Comparison Plot

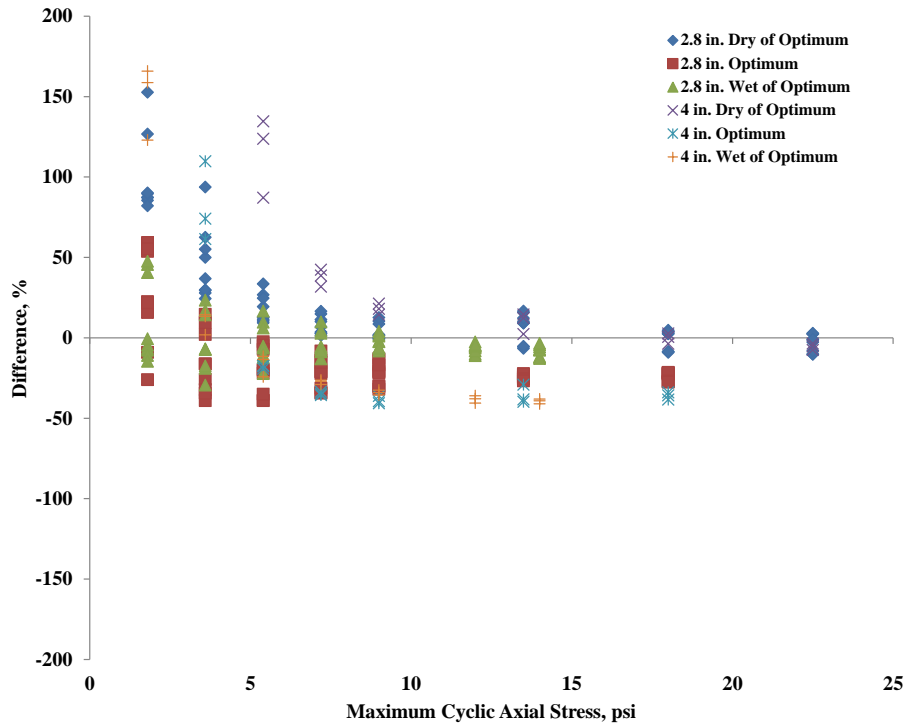


Figure 4.11 Internal Deformation Measurement Comparison Plot 2

2.8 inch Diameter vs. 4 inch Diameter Specimens

While groups of replicates were made for 2.8 in. diameter specimens at different moisture conditions, it is difficult to consider any specimen a true replicate of another considering potential variations introduced when reconstituting soils. One obvious variation that is shown is moisture content within the groupings, whereas it was difficult to prevent moisture loss considering specimens were capped and time between testing. For comparison of 2.8 in. diameter to 4 in. diameter, it was decided to compare the 4 inch specimens to the 2.8 in. specimen with the nearest moisture content. This is because 1 specimen at each moisture condition was tested for 4 in. diameter specimens compared to 3 for each moisture condition for the 2.8 in. specimen. For comparative purposes Tables 4.14-4.16 show the replicate of 2.8 in.

diameter specimens chosen to compare to the respective 4 in. diameter specimen as well as the percent difference in modulus value of 4 in. to 2.8 in. Figures 4.13-4.15 are the plots of the tabulated data for a comparison of the values and trends for dry of optimum, optimum, and wet of optimum size parings. Dry of optimum and wet of optimum specimens show good agreement, with the dry of optimum specimens showing particularly close results between sizes at higher deviator stresses. The optimum moisture content comparison did not yield good results. The behavior of all the specimens compared can be seen in Figure 4.12 plotted against a line of unity. Again this shows the similar behavior between the size couples for the dry and wet of optimum, and the poor uniformity for the optimum moisture content pair. It is recognized the data points are fairly limited, considering only one specimen of each moisture content for 4 in. specimens was tested, however considering the difficulty known in generating consistent resilient modulus results even among replicate specimens, having 2 out of 3 pairs of different size specimens behave within 10% of one another at the majority of deviator stresses is encouraging.

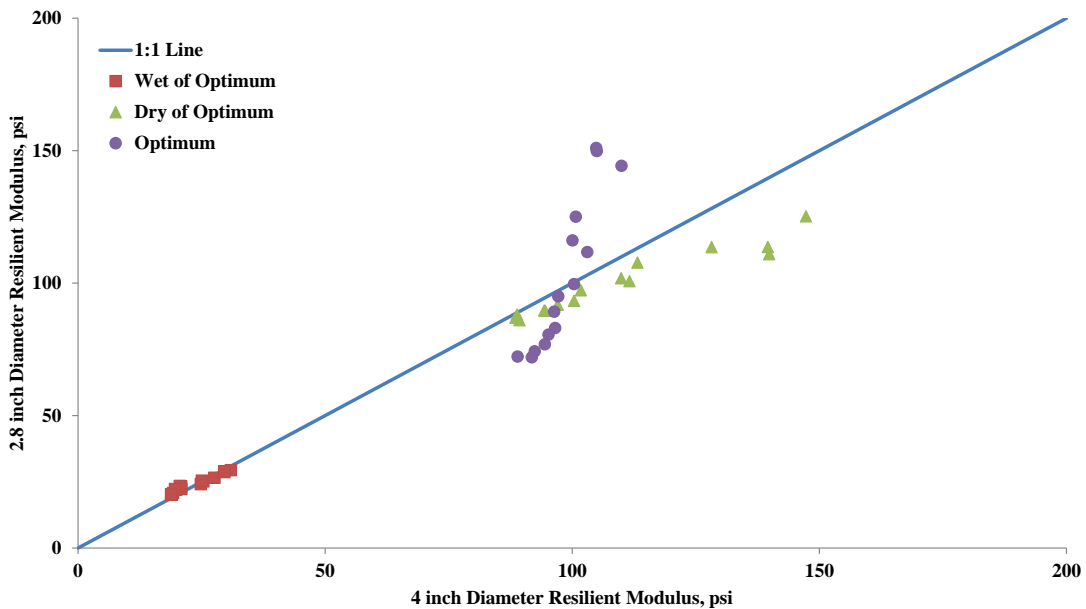


Figure 4.12 Resilient Modulus Size Comparison

Table 4.14 Dry of Optimum 2.8 inch vs. 4 inch Diameter Comparison

Dry of Optimum					
w (%)					
		13.4	13.4		
Diameter (inches)					
		2.8	4		
σ_3 (psi)	$\sigma_{\text{cyclic max}}$ (psi)	M_r (ksi)		% Difference	
6	1.8	125	147	-15	
6	3.6	114	128	-11	
6	5.4	102	110	-7	
6	7.2	92	97	-5	
6	9	88	89	-1	
4	1.8	114	140	-19	
4	3.6	108	113	-5	
4	5.4	97	102	-4	
4	7.2	90	94	-5	
4	9	87	89	-2	
2	1.8	111	140	-21	
2	3.6	101	112	-10	
2	5.4	93	100	-7	
2	7.2	89	95	-5	
2	9	86	89	-4	

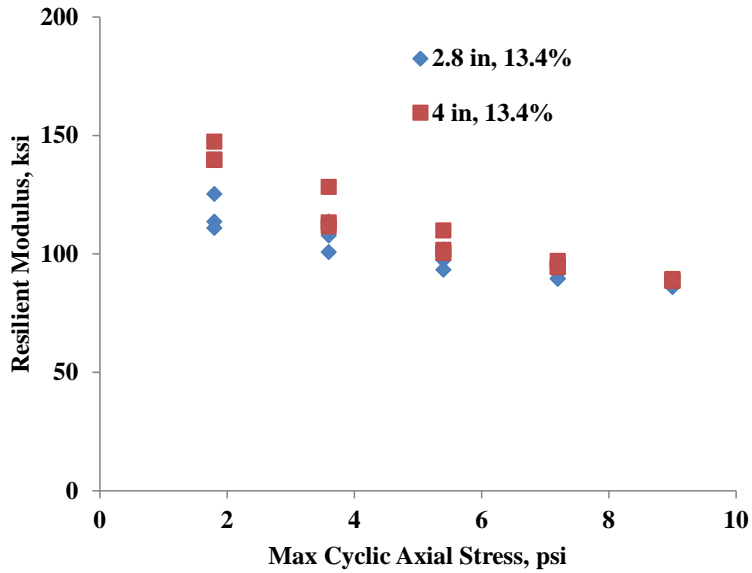


Figure 4.13 Dry of Optimum 2.8 inch vs. 4 inch Plot

Table 4.15 Dry of Optimum 2.8 inch vs. 4 inch Diameter Comparison

		Optimum		
		w (%)		
		15.6	15.5	
		Diameter (inches)		
		2.8	4	
σ_3 (psi)	$\sigma_{\text{cyclic max}}$ (psi)	M_r (ksi)		% Difference
6	1.8	144	110	31
6	3.6	112	103	8
6	5.4	100	100	-1
6	7.2	83	97	-14
6	9	74	92	-20
4	1.8	150	105	43
4	3.6	125	101	24
4	5.4	95	97	-2
4	7.2	81	95	-15
4	9	72	92	-22
2	1.8	151	105	44
2	3.6	116	100	16
2	5.4	89	96	-7
2	7.2	77	94	-19
2	9	72	89	-19

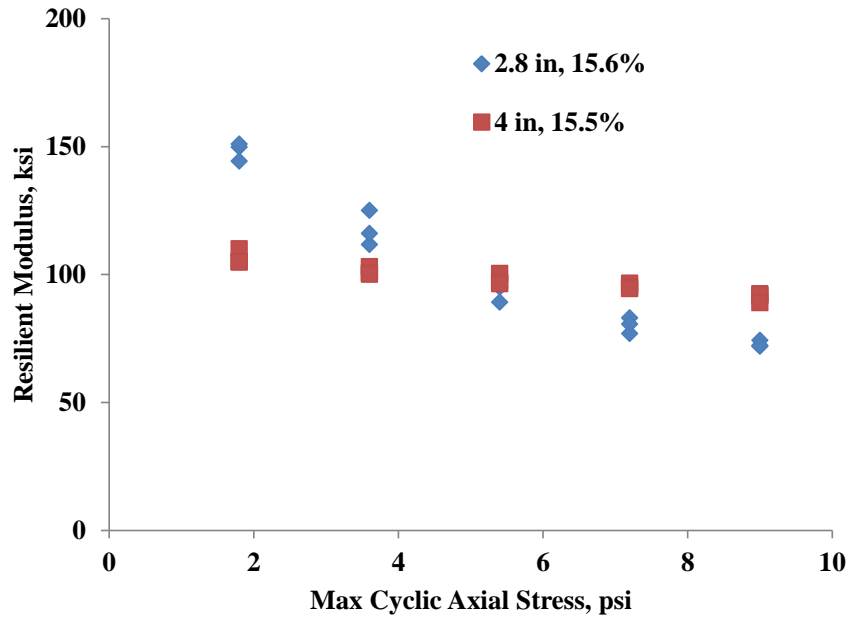


Figure 4.14 Optimum 2.8 inch vs. 4 inch Plot

Table 4.16 Wet of Optimum 2.8 inch vs. 4 inch Diameter Comparison

Wet of Optimum					
w (%)					
		17.9	17.8		
Diameter (inches)					
		2.8	4		
σ_3 (psi)	$\sigma_{\text{cyclic max}}$ (psi)	M_r (ksi)		% Difference	
6	1.8	29	31	-5	
6	3.6	27	28	-4	
6	5.4	24	25	-3	
6	7.2	22	21	6	
6	9	21	19	8	
4	1.8	29	30	-3	
4	3.6	25	25	-1	
4	5.4	23	21	11	
4	7.2	22	20	11	
4	9	20	19	6	
2	1.8	29	30	-2	
2	3.6	25	25	2	
2	5.4	23	21	14	
2	7.2	22	20	13	
2	9	20	19	7	

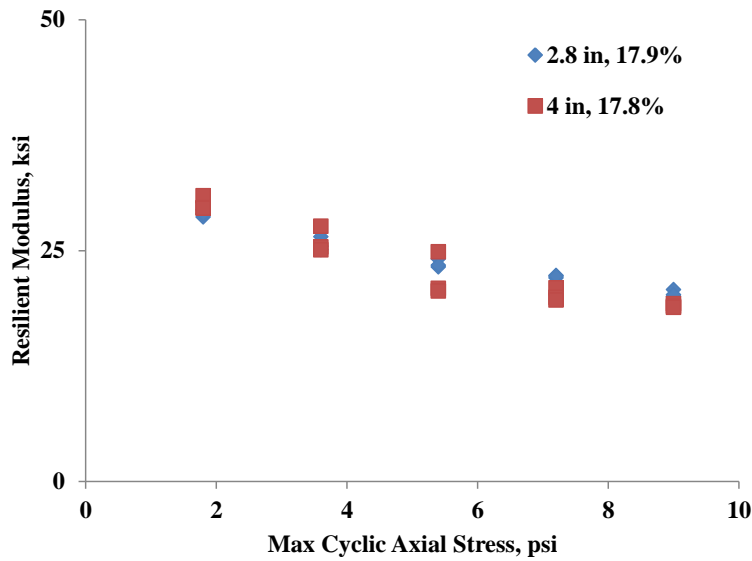


Figure 4.15 Wet of Optimum 2.8 inch vs. 4 inch Plot

4.4 Static Testing Results

Static testing included unconfined compression testing on all specimens and sizes, in addition and elastic modulus test was performed on 4 in. diameter specimens.

4.4.1 Unconfined Compression Testing Results

Unconfined compression results showed increasing strength with decreasing moisture content. For 2.8 inch diameter specimens, Table 4.17 lists uncorrected UCS values for all replicates, where the average for dry of optimum is 190 psi, for optimum is 90 psi, and for wet of optimum is 62 psi. Figure 4.16 shows a plot of axial stress and axial strain, however the axial strain was measured using a low precision (± 2 inch) frame mounted LVDT, therefore modulus values should not be determined from these plots, they are presented to show the trends of the various replicates and different moisture contents. The larger range LVDT was used because the specimen was taken to failure which meant the LVDTs used for resilient modulus testing would have not been adequate and likely destroyed during UCS testing.

Table 4.17 2.8 inch Diameter UCS Values

	Dry of Optimum		
	Replicate No.		
	1	2	3
UCS (psi)	175	185	210
	Optimum		
	Replicate No.		
	1	2	3
UCS (psi)	86	93	92
	Wet of Optimum		
	Replicate No.		
	1	2	3
UCS (psi)	59	62	64

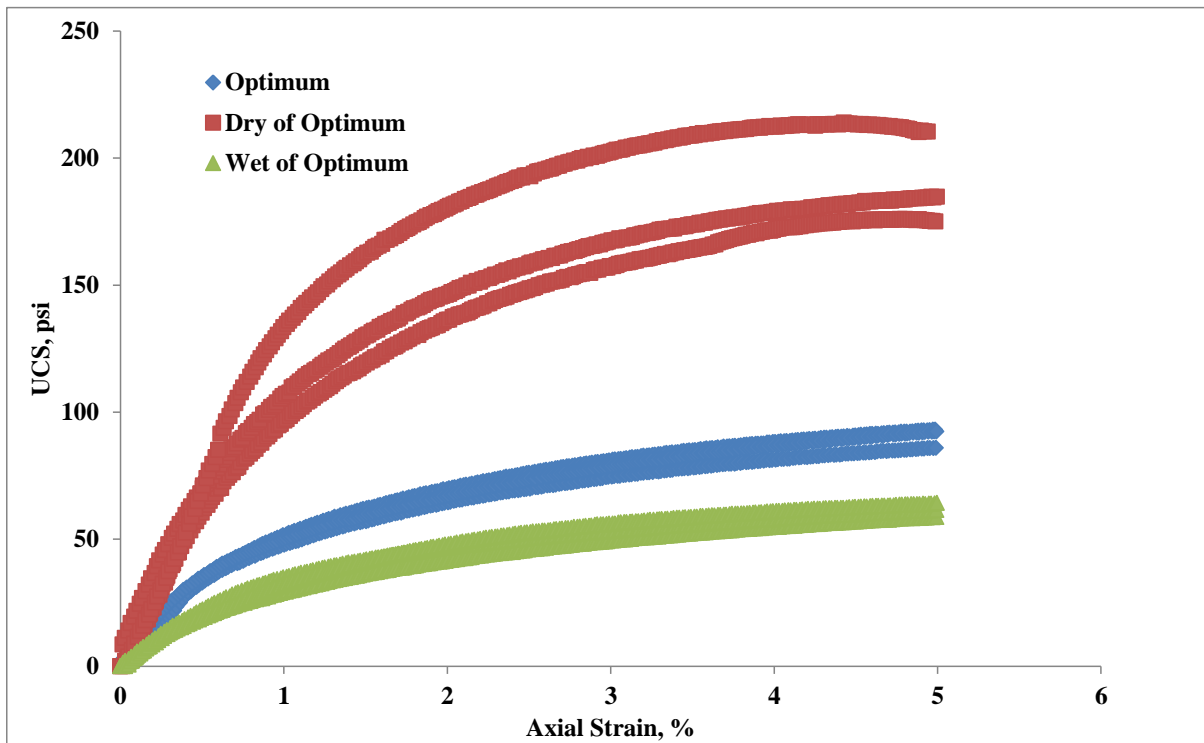


Figure 4.16 2.8 inch Diameter UCS Plot

For the 4.0 inch diameter specimens, the same trend of UCS relating to moisture content was seen as in the 2.8 inch diameter specimens. Table 4.18 and Figure 4.17 show results from 4.0

inch diameter UCS testing. Again, note the use of actuator mounted deformation measurement used to determine strain values in reference to the plot shown in Figure 4.17.

Table 4.18 4 inch Diameter UCS Results

	Dry of Optimum
UCS (psi)	136
	Optimum
UCS (psi)	98
	Wet of Optimum
UCS (psi)	47

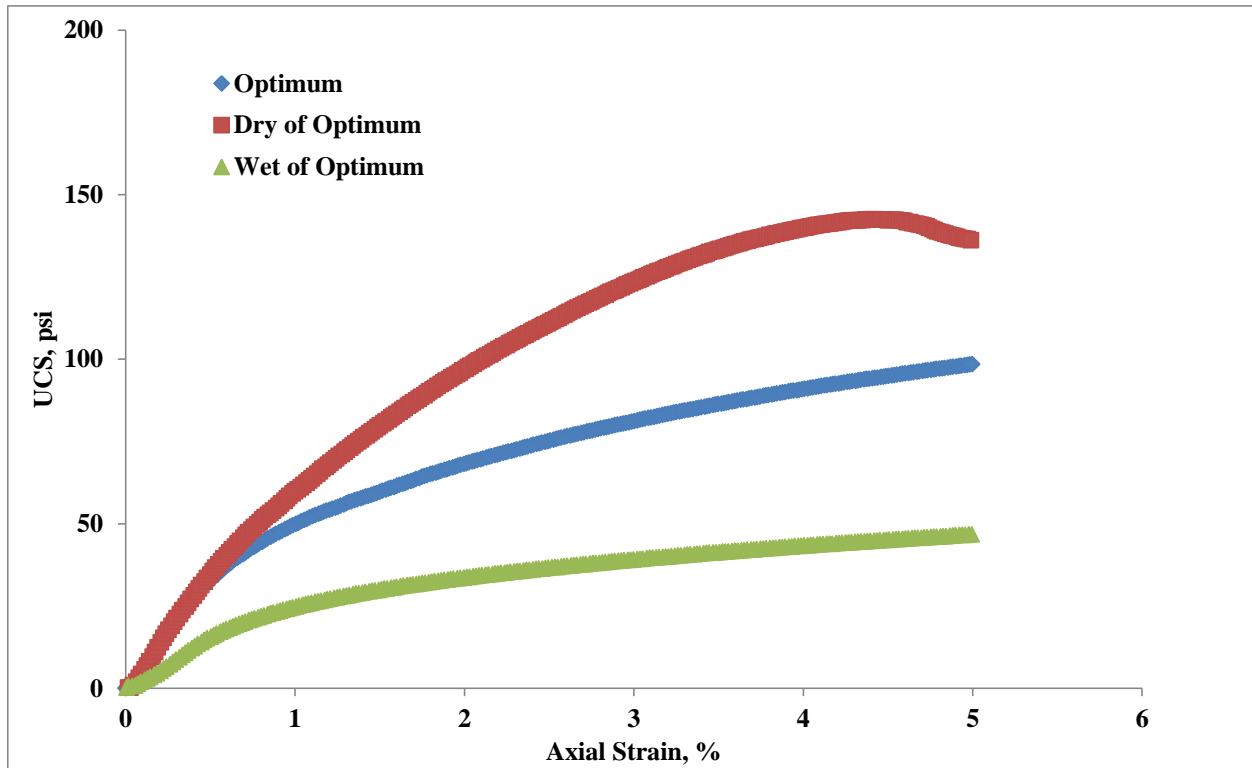


Figure 4.17 4 inch Diameter UCS Plot

4.4.2 Elastic Modulus Testing

A modified elastic modulus test was performed on the 4 in. diameter specimens using the internal glued button deformation measurement method to check the variation in modulus compared to the UCS testing performed using the frame LVDT. For this testing the specimens were loaded up to values approaching the highest value they experienced during resilient modulus tests for an average duration of 4 minutes, then secant modulus values were calculated based on the final stress and strain values. It is clear from comparing the results shown in Table 4.19 that the modulus values determined from using on specimen deformation measurement are significantly higher than those using the frame LVDT. Figure 4.18 shows plot of results from this testing.

Table 4.19 Elastic Modulus Values from Static Test on 4 inch Diameter Specimens

	Dry of Optimum
Elastic Modulus (ksi)	51.0
	Optimum
Elastic Modulus (ksi)	46.7
	Wet of Optimum
Elastic Modulus (ksi)	12.5

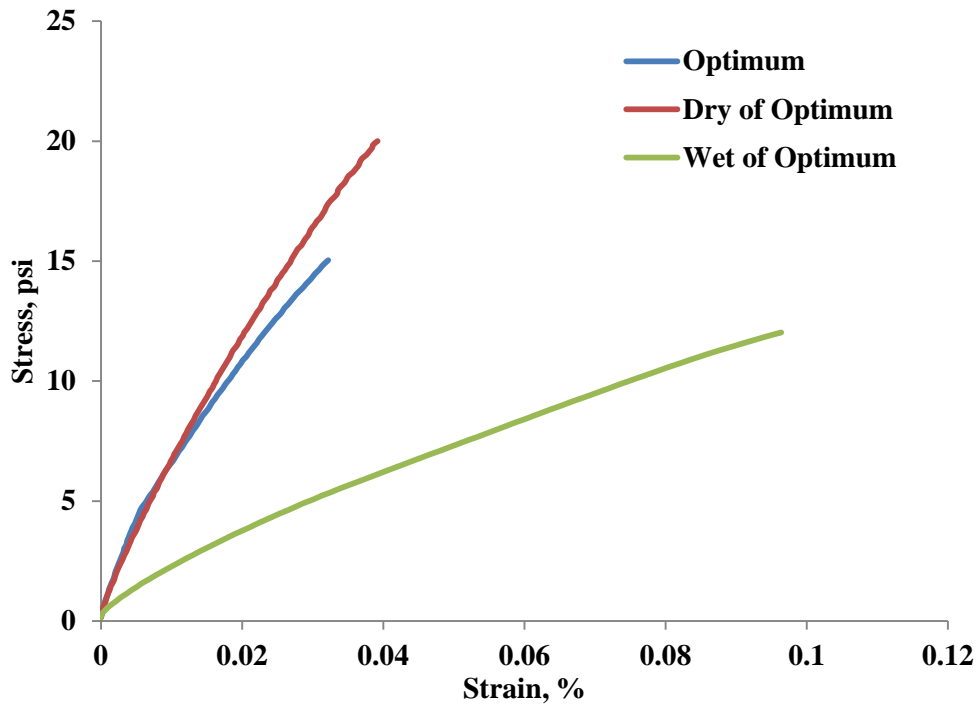


Figure 4.18 Elastic Modulus Results 4 in. Diameter Specimens

4.5 Multivariate Linear Regression

Based on initial reduction of results it was shown that the maximum cyclic stress and moisture contents effect on resilient where cyclic stress and moisture content increase, M_r decreases. The effects of these variables appear to be generally linear based on the results. To a lesser degree resilient modulus values are affected by confining stress, where increasing confining pressure results in increasing resilient modulus, though it was shown that the influence is small based on percent difference comparisons. To further examine the influence of these variables, a multivariate linear regression analysis was performed using *Minitab15* software. The confidence interval for the regression is 95%, thus P values for variables examined that are below 0.05 are accepted as significant and values greater than 0.05 are considered insignificant. Independent variables examined include maximum cyclic stress, moisture content, confining stress, and

unconfined compression. Some examples of the regression analyses results are shown in Tables 4.20-4.23. It is noted by the prediction equations in Tables 4.20 and 4.21, resilient modulus prediction begins with a constant value then cyclic stress and moisture content decreases the M_r values (are subtracted) while confining pressure increases the value (is added in the case of table 4.21). This makes sense based on past studies as well as what has been presented in these results, moisture content and cyclic stress increases result in decreases in resilient modulus while confining pressure, though insignificant, in this case results in increasing resilient modulus. The best predictive equation was found using two predictor variables, maximum cyclic stress (psi) and gravimetric moisture content (%), the selected prediction methods results are presented in Table 4.21. The results from values predicted using the equation are shown in Figures 4.19 and 4.20, and include all subgrade sequence predicted resilient modulus results plotted against the measured M_r value and a line of unity. Although this predictive equation is unique to this soil tested, the benefit of having a predictive equation that takes into account the two variables discussed, is that it can be used to build up a state level material database for different moisture and deviator stress conditions.

Table 4.20 Prediction Equation and ANOVA Table Using 3 Predictors (Cyclic Stress, Moisture Content, and Confining Pressure)

The regression equation is:					
Mr = 394 - 3.67 *CyclicStress (psi) - 19.4*Moisture Content (%) + 0.645*Confining Stress (psi)					
Predictor	Coef	SE Coef	T	P	
Constant	393.55	10.76	36.59	0.000	
CyclicStress	-3.6688	0.4563	-8.04	0.000	
Moisture Content	-19.3589	0.6457	-29.98	0.000	
Confining Stress	0.6453	0.7112	0.91	0.365	
S = 15.5824 R-Sq = 84.6% R-Sq(adj) = 84.3%					
<u>Analysis of Variance</u>					
Source	DF	SS	MS	F	P
Regression	3	234128	78043	321.41	0.000
Residual Error	176	42735	243		
Total	179	276862			

Table 4.21 Prediction Equation and ANOVA Table Using 2 Predictors (Cyclic Stress and Moisture Content)

The regression equation is:					
Mr = 394 - 3.67 *CyclicStress (psi) - 19.4*Moisture Content (%)					
Predictor	Coef	SE Coef	T	P	
Constant	396.13	10.37	38.21	0.000	
CyclicStress	-3.6688	0.4560	-8.05	0.000	
Moisture Content	-19.3589	0.6454	-29.99	0.000	
S = 15.5746 R-Sq = 84.5% R-Sq(adj) = 84.3%					
<u>Analysis of Variance</u>					
Source	DF	SS	MS	F	P
Regression	2	233928	116964	482.19	0.000
Residual Error	177	42934	243		
Total	179	276862			

Table 4.22 Prediction Equation and ANOVA Table Using 4 Predictors (Cyclic Stress, Moisture Content, Confining Pressure, and UCS)

The regression equation is:					
$Mr = 443 - 3.67 \cdot \text{Cyclic Stress (psi)} - 21.9 \cdot \text{Moisture (\%)} + 0.645 \cdot \text{Confining Stress (psi)} - 0.0921 \cdot \text{UCS (psi)}$					
Predictor	Coef	SE Coef	T	P	
Constant	442.97	38.94	11.37	0.000	
Cyclic Stress	-3.6688	0.4553	-8.06	0.000	
Moisture	-21.900	2.030	-10.79	0.000	
Confining Stress	0.6453	0.7097	0.91	0.364	
UCS	-0.09213	0.06979	-1.32	0.189	
S = 15.5496 R-Sq = 84.7% R-Sq(adj) = 84.4%					
<u>Analysis of Variance</u>					
Source	DF	SS	MS	F	P
Regression	4	234549	58637	242.51	0.000
Residual Error	175	42313	242		
Total	179	276862			

Table 4.23 Prediction Equation and ANOVA Table Using 4 Predictors (Cyclic Stress, Moisture Content, Confining Pressure, and UCS)

The regression equation is:					
$Mr = 28.3 - 3.67 \cdot \text{Cyclic Stress (psi)} + 0.622 \cdot \text{UCS (psi)}$					
Predictor	Coef	SE Coef	T	P	
Constant	28.332	4.670	6.07	0.000	
Cyclic Stress	-3.6688	0.5850	-6.27	0.000	
UCS	0.62192	0.02847	21.84	0.000	
S = 19.9802 R-Sq = 74.5% R-Sq(adj) = 74.2%					
<u>Analysis of Variance</u>					
Source	DF	SS	MS	F	P
Regression	2	206203	103101	258.27	0.000
Residual Error	177	70660	399		
Total	179	276862			

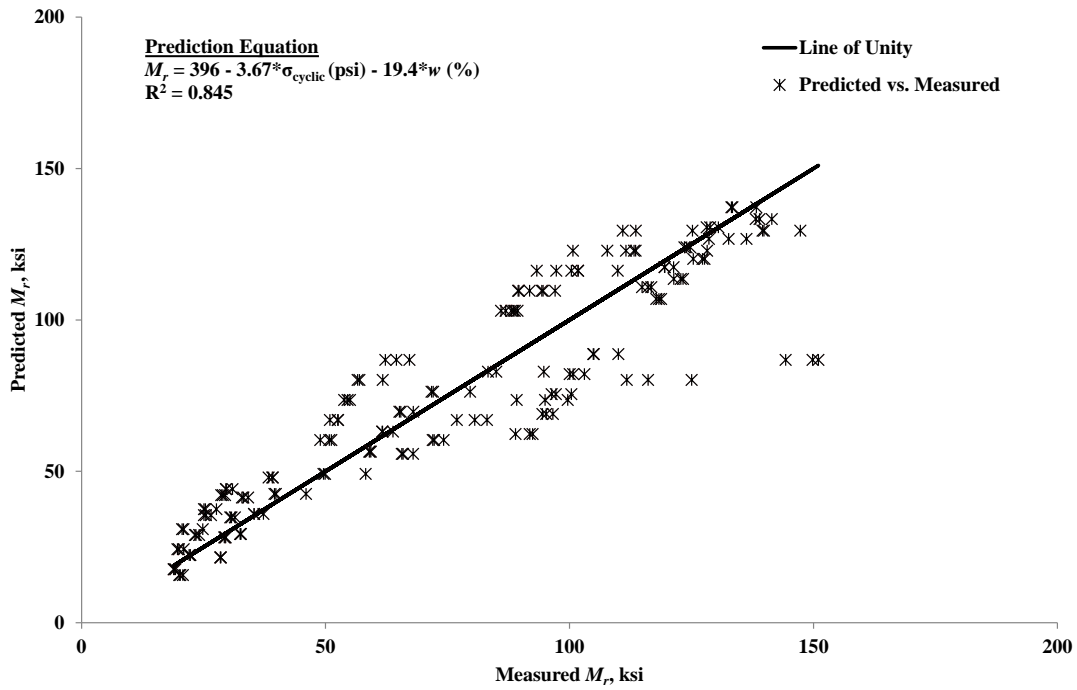


Figure 4.19 Predicted vs. Measured M_r as a function of $\sigma_{\text{maxcyclic}}$ and Moisture Content

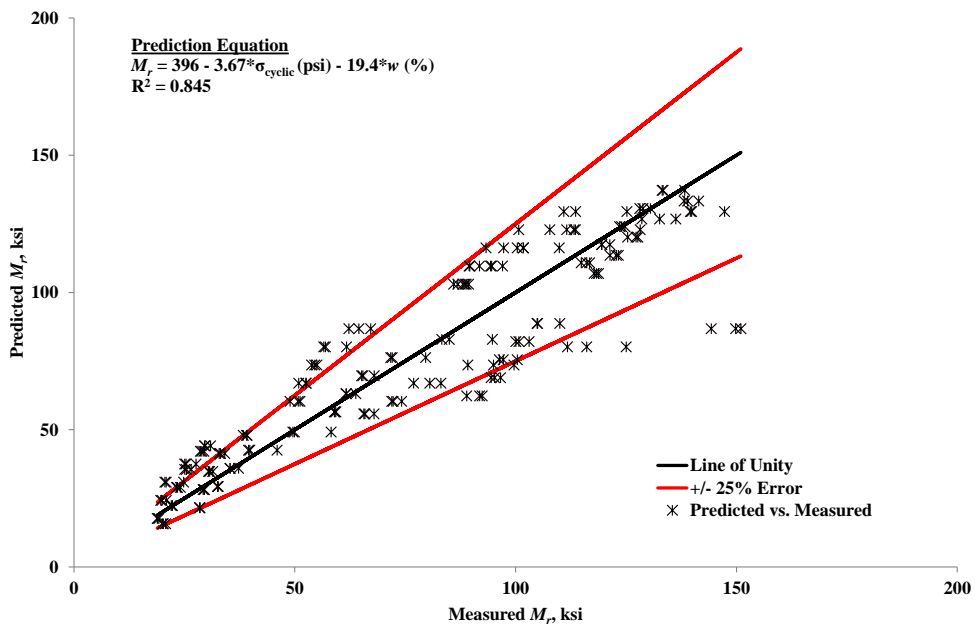


Figure 4.20 Predicted vs. Measured M_r as a function of $\sigma_{\text{maxcyclic}}$ and Moisture Content

4.6 Resilient Modulus Testing Summary

In this chapter resilient modulus testing was conducted on an A-6 soil at moisture contents dry of optimum, optimum, and wet of optimum. Multiple resilient modulus tests were conducted using different deformation methods namely: on-specimen glued button, on-specimen ring clamp, and external actuator mounted. Comparisons of these results showed the external deformation method yielded the lowest results consistently, while the differences between the internal on-specimen deformation methods was more pronounced at lower cyclic stresses and improved as the stress magnitudes increased. Analysis of confining pressure showed negligible effects on resilient modulus relative (often less than 10%), especially relative to cyclic stresses and moisture content. A multivariate predictive equation was developed with variables of gravimetric moisture content (%) and max cyclic axial stress (psi) with an R^2 of 84.5% and the majority of data points falling within a $\pm 25\%$ over/under-predicted envelope. The implications of generating such an equation is that it has the potential to build up state level material input databases for Mechanistic-Empirical design at different seasonal moisture conditions.

CHAPTER 5

EXPERIMENTAL ALTERNATE M_r TEST RESULTS

5.1 Introduction

An experimental study was conducted using an alternate dynamic test. The goal of this experiment was to evaluate the potential determining resilient modulus of fine-grained cohesive soils using less time-consuming, unconfined test method.

Rationale for Unconfined Experiment

Based on previous studies, confining pressure has been shown to have little effect on resilient modulus of fine grained cohesive soils in the ranges of confining stresses typically applied for subgrade testing (Muhanna et al. (1999), Thompson and Robnett (1979), Freudland (1977)). The results of this study, presented in Chapter 4, support the small confining pressure effect where in Section 4.3.3, it was shown that confining pressure was shown to have on average less than a 10% effect on resilient modulus results between the smallest and largest confining stresses applied (2 and 6 psi respectively). Barksdale (1997) recommended an unconfined dynamic test for cohesive subgrade soils as a part of the NCHRP 1-28 findings, noting Illinois DOT uses unconfined testing in design. In a joint study by Purdue and the Indiana DOT, M_r testing at a single confining stress (2 psi) was conducted to simplify the multi-confining stress test procedures (Kim and Siddiki (2006)).

In addition to the little effect confining pressure has on resilient modulus, Muhanna et al. 1999 found that the number of load applications, rest period, or stress sequencing do not significantly affect resilient modulus of A-5 and A-6 soils they tested (Huang (2004)).

In consideration of Chapter 4 results and the previous studies listed, a sinusoidal stress with 1 Hz frequency is applied for 60 seconds with no confining pressure, contact stress, or rest period.

Selection of this loading form and duration was based on several factors including:

- Based on this experiment, sinusoidal loading yielded good results in comparison to standard resilient modulus tests load forms. Though it is noted that load pulses experienced in subgrades may generally be characterized as haversine or triangular (Huang 2004).
- The 1 Hz frequency, though larger in pulse duration than those based on what subgrade should experience in the field (based on subgrade depth and vehicle speed), did not show significant effect relative to 10 Hz pulse. In addition, it was easy to control and quickly reached target peak stresses (stabilized) well into a 60 second test sequence using the PID tuner within the GCTS CATS software.
- Rest period was eliminated because it is believed to have little effect on resilient modulus of cohesive fine-grained soils based previous studies which were introduced in Chapter 2 as well as in this experimental rationale section.
- Finally, a 1 Hz Sinusoidal loading lasting 60 seconds seemed a good baseline study given the notable parameters (i.e. 1 cycle lasts 1 second, sine wave, 1 minute total test duration).

It is noted that the decision to run this alternate test at the stresses and conditions described above is based on cohesive fine grained soils tested within approximately $\pm 2\%$ of optimum moisture content. The moisture effects in these ranges show significant effect on resilient modulus, however it was not believed that they would show significant effects due to a longer loading pulse (reduced frequency), like what might be expected of a similar soil at a much higher moisture content relative to optimum.

Resilient modulus values were determined for this testing method by dividing the maximum cyclic axial stress by the resilient strain for cycles 20-40 of a 60 cycle test. Stress and strain (load cell and LVDT) output data sampled at 32 points per cycle provided sufficient data for characterizing the sinusoidal control and response forms. A higher stress range was tested for according to the moisture condition of the specimens. This was selected because during standardized resilient modulus testing at higher stresses, the LVDT output was always larger than the non-linearity range and the trends with regards to deviator stress stabilized. Also, based on the stress-strain behavior at the cycles used to determine resilient modulus, the higher stresses selected indicate the elastic behavior intended for resilient modulus testing. The epoxied buttons and spring-type LVDTs were used for determining M_r of this alternate method, and then compared to their equivalent standardized resilient modulus results.

5.2 Objective

The objective of this Chapter is to present the results of this experimental alternative resilient modulus test and perform a comparative analysis with the standardized results from Chapter 4 to

determine how well the alternative method performs compared to the standard. In chapter 2 it was detailed that previous studies have found that portions of the resilient modulus testing sequences have little effect on the resilient modulus results of cohesive fine-grained subgrade soils, namely confining pressure, rest period, load applications, and load sequence. Strictly speaking in terms of testing time with regards to the AASHTO T 307 Subgrade test sequences, eliminating the rest period would take out 90% of the test time, reducing number of load applications would decrease it according to the number of sequences taken out, and only testing at a single or no confining pressure would cut the test time in half assuming the pre-conditioning sequence were left in. For this alternate method testing, the potential influence due to a sine pulse lasting 1 second (experimental method) and a haversine pulse lasting 0.1 second (AASHTO T 307) is another difference introduced.

5.3 Alternate Method Results of 2.8 inch Diameter Specimens

5.3.1 Dry of Optimum

Cyclic stresses for dry of optimum specimens varied from 8 to 20 psi. Table 5.1 shows the results for the 3 dry of optimum 2.8 inch diameter specimens. Corresponding modulus values varied from 106 to 63 ksi, with a general decreasing trend in moduli with increasing stress magnitudes. Figures 5.1 and 5.2 are example plots of stress-strain behavior of replicate No. 2. Noting that these figures represent 20 stress-strain cycles, the figures show the agreement between the stresses and deformation waveforms as well as the consistent behavior of the loading and deformations at peaks, i.e. no increasing or decreasing strains, or load control issues.

Table 5.1 Dry of Optimum Alternate Experiment Test Results

Dry of Optimum			
Replicate No.			
	1	2	3
Gravimetric Moisture Content (%)			
	13.4	13.2	13.0
$\sigma_{cyclicmax}$ (psi)	M_r (ksi)	M_r (ksi)	M_r (ksi)
8	79	106	102
10	81	103	106
15	72	97	100
20	63	89	97

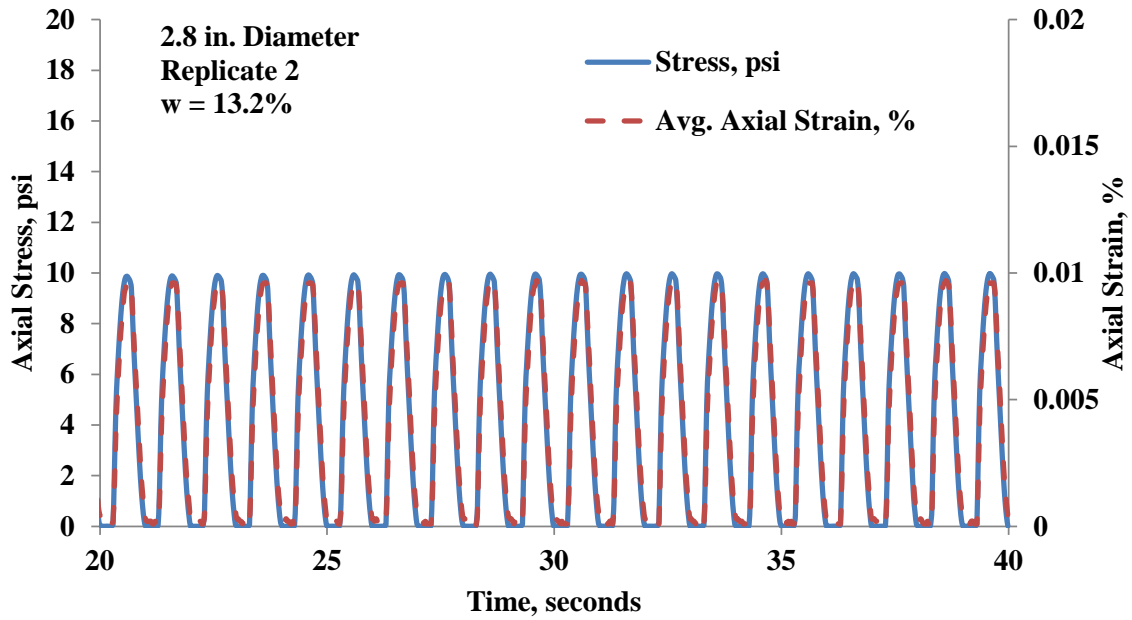


Figure 5.1 Stress and Strain vs. Time

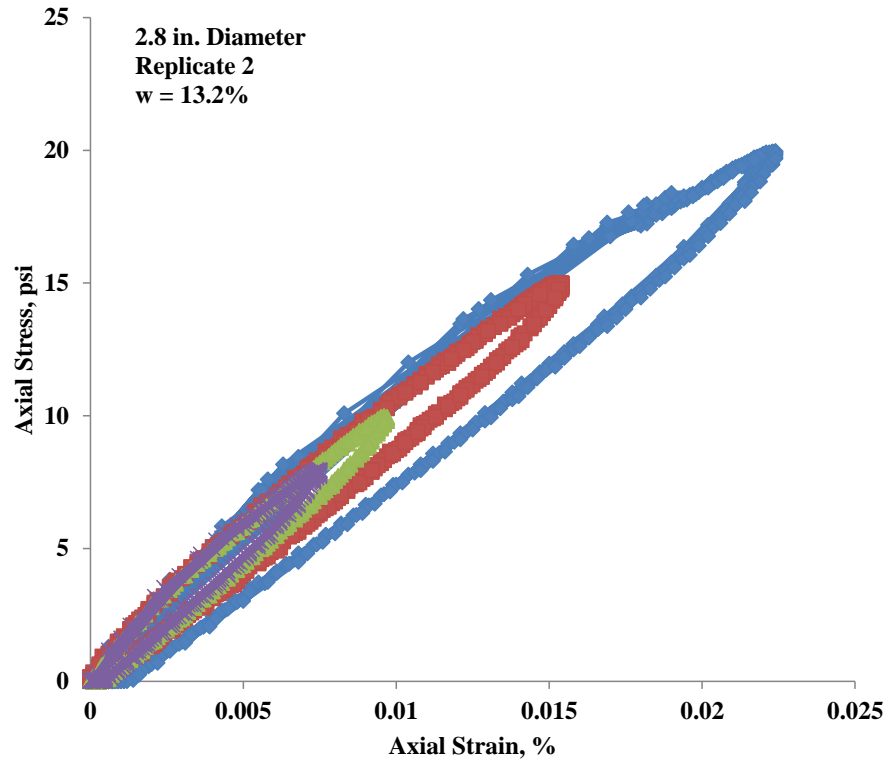


Figure 5.2 Alternate Experimental Test Stress-Strain Plot

5.3.2 Optimum

Cyclic stresses for optimum specimens varied from 6 to 14 psi, while modulus values ranged from 71 to 44 ksi. Table 5.2 shows moduli for all stresses and replicates tested at optimum for 2.8 inch diameter specimens.

Table 5.2 Optimum Alternate Experiment Test Results

Optimum			
Replicate No.			
Gravimetric Moisture Content (%)			
$\sigma_{\text{cyclicmax}}$ (psi)	M_r (ksi)	M_r (ksi)	M_r (ksi)
6	56	71	56
10	53	60	49
14	45	50	44

5.3.3 Wet of Optimum

Cyclic stresses for wet of optimum specimens varied from 4 to 12 psi. Table 5.3 lists the corresponding modulus results for each stress and replicate tested wet of optimum for 2.8 inch diameter specimens. Modulus values range from 52 to 20 ksi, and show a decreasing behavior with increasing cyclic stress magnitude, as well as an increasing behavior with decreasing moisture content.

Table 5.3 Wet of Optimum Experiment Test Results

Wet of Optimum			
Replicate No.			
Gravimetric Moisture Content (%)			
$\sigma_{\text{cyclicmax}}$ (psi)	M_r (ksi)	M_r (ksi)	M_r (ksi)
4	23	31	52
8	20	28	33
12	20	26	28

5.3.4 Discussion of 2.8 inch diameter Alternate Mr Method Results

Similar to the resilient modulus testing according to the standardized methods, modulus results for this method showed a decreasing trend with increasing moisture content, consistent with literature. Figure 5.3 illustrates the modulus results of all alternate method testing on the 2.8 inch diameter specimens versus moisture content. The spread seen in resilient modulus values for specific moisture contents in this figure is largely due to the effect of maximum cyclic axial stress magnitudes.

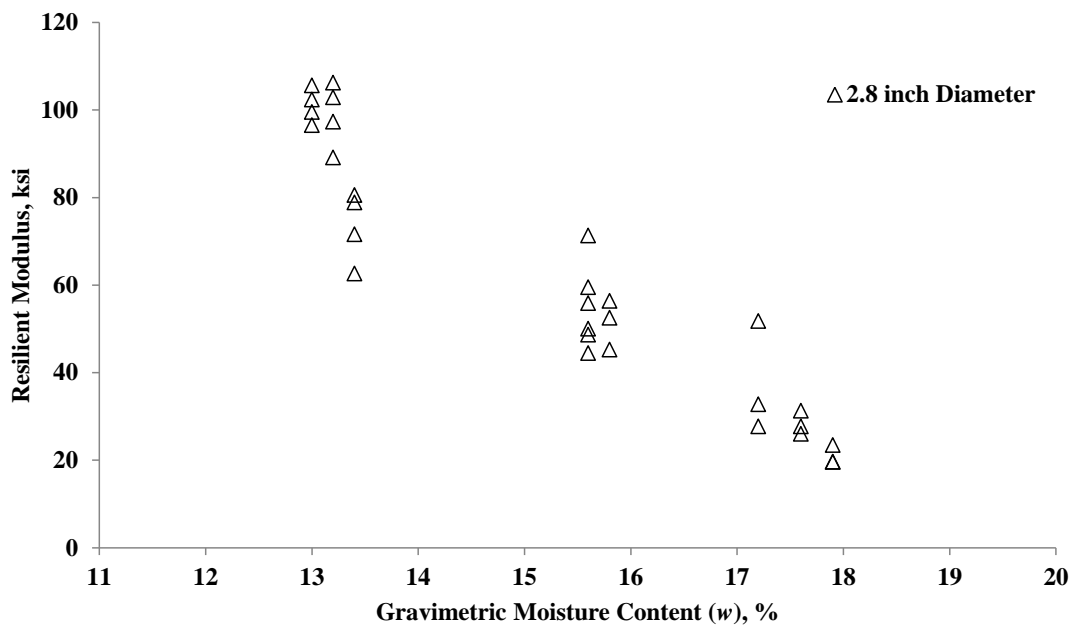


Figure 5.3 Alternate Experiment Resilient Modulus vs. Moisture Content

An initial comparison of the standardized resilient modulus results for 2.8 inch diameter specimens showed that the modulus values determined from the alternate test method fit well

with the standardized trends. Figure 5.4 shows examples results from standardized and alternate resilient modulus tests of dry, optimum, and wet of optimum specimens. Since, the maximum axial cyclic stress of each alternate method test fell within points of the standardized test, modulus values could not be compared one-to-one between the tests. Regression analysis was performed to determine standardized modulus values at the stress amplitudes corresponding to the alternate stress test sequences. Results from these comparisons are found in Section 5.6.

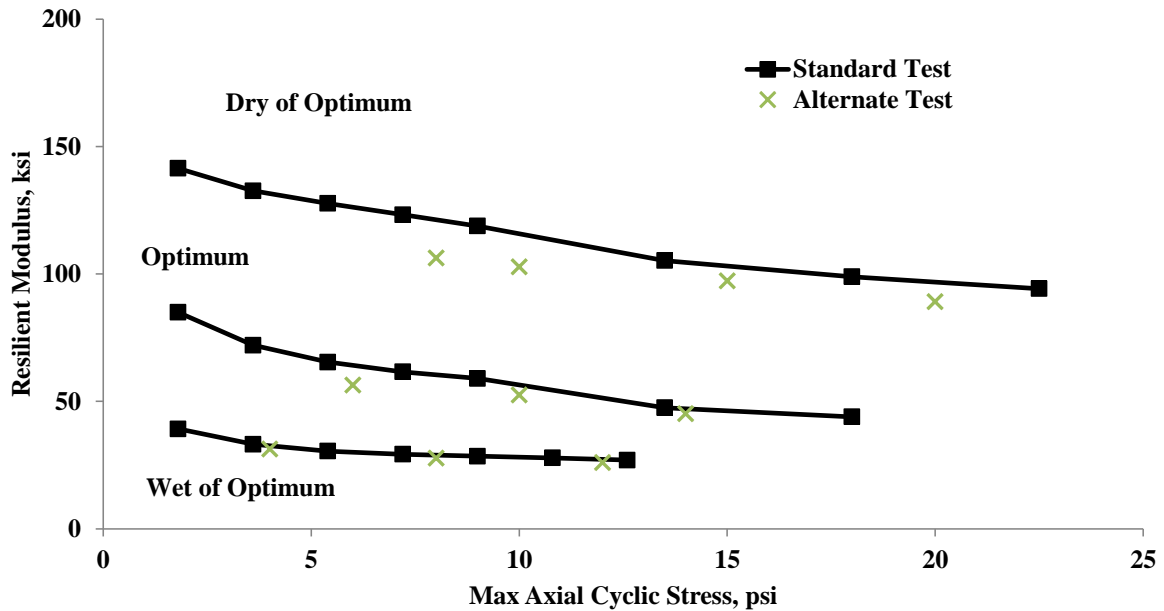


Figure 5.4 2.8 inch Diameter Alternate Experiment and Standard Resilient Modulus Results

5.4 Alternate Experiment Results of 4 inch Diameter Specimens

Maximum cyclic axial stresses for 4 in. diameter specimens were the same magnitudes as those tested for the 2.8 in. diameter specimens. One replicate each was tested at dry, optimum, and wet of optimum conditions. Figures 5.5 and 5.6 show examples of the stress and strain behavior for Cycles 20-40 for the 4 in. diameter wet of optimum tested using the alternate method.

Similar to results shown for the 2.8 in. specimens, the consistent behavior is noted of controlled stresses and response of the strain during loading and unloading for all 20 cycles.

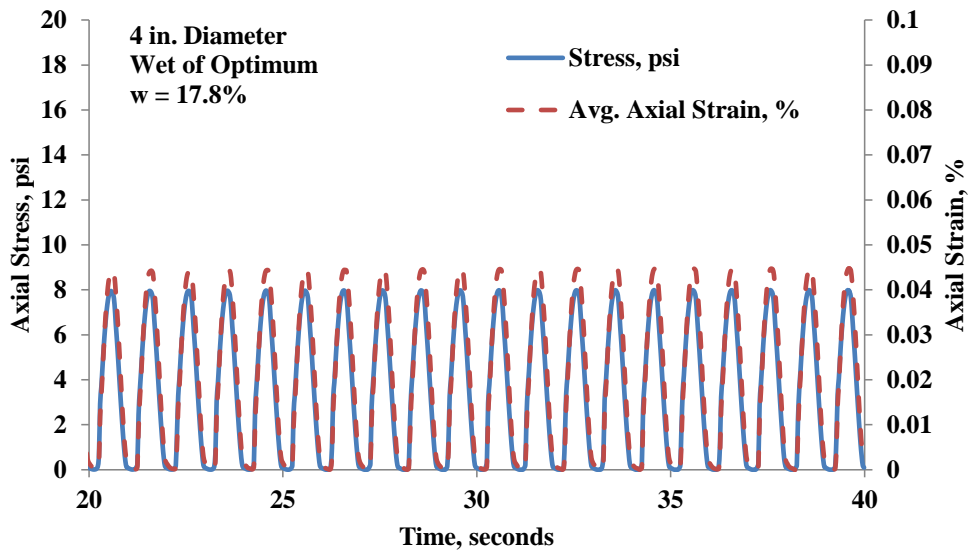


Figure 5.5 Alternate Experiment Method Stress and Strain versus Time

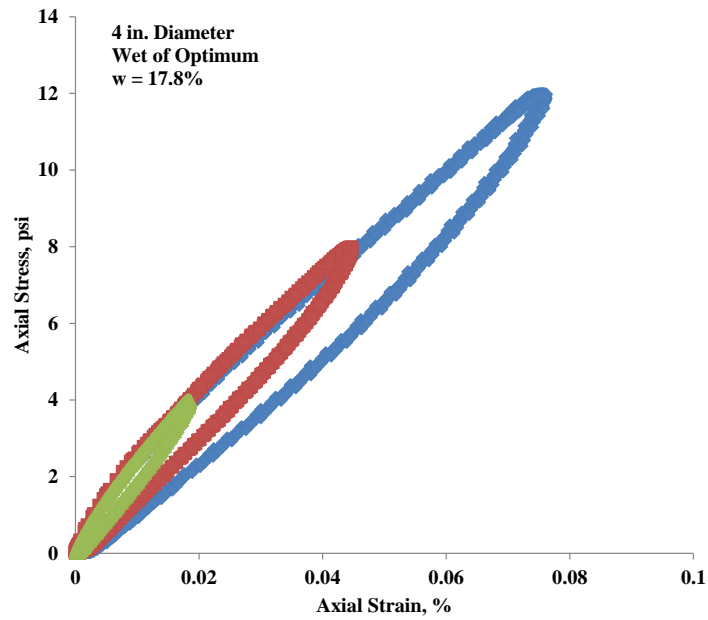


Figure 5.6 4 inch Diameter Wet of Optimum Stress-Strain Plot

5.4.1 Dry of Optimum

Results for the dry of optimum specimen showed modulus values varying from 78 to 64 ksi, decreasing with increasing deviator stress. Table 5.4 shows the results from alternate method testing on the 4 inch diameter dry of optimum specimen.

Table 5.4 Alternate Method Results for 4 inch Diameter Dry of Optimum

Dry of Optimum	
Gravimetric Moisture Content (%)	
13.4	
$\sigma_{\text{cyclicmax}}$ (psi)	M_r (ksi)
8	78
10	75
15	68
20	64

5.4.2 Optimum

Results for the optimum test specimen showed modulus values varying from 79 to 55 ksi, decreasing with increasing deviator stress. Table 5.5 shows the results from alternate method testing on the 4 inch diameter optimum specimen.

Table 5.5 Alternate Method Results for 4 inch Diameter at Optimum

Optimum	
Gravimetric Moisture Content (%)	
15.5	
$\sigma_{\text{cyclicmax}}$ (psi)	M_r (ksi)
6	79
10	59
14	55

5.4.3 Wet of Optimum

Results for the wet of optimum test specimen showed modulus values varying from 21 to 16 ksi, decreasing with increasing deviator stress. Table 5.6 shows the results from alternate method testing on the 4 inch diameter optimum specimen.

Table 5.6 Alternate Method Results for 4 inch Diameter Wet of Optimum

Wet of Optimum	
Gravimetric Moisture Content (%)	
17.8	
$\sigma_{\text{cyclicmax}}$ (psi)	M_r (ksi)
4	21
8	18
12	16

5.4.4 Discussion of 4 inch diameter Alternate M_r Experiment Results

Similar to the resilient modulus testing according to the standardized methods and the alternate method for 2.8 inch diameter specimens, modulus results for this method showed a decreasing trend with increasing moisture content. However, with less test specimens than the 2.8 inch specimens the trend is not as pronounced due to the modulus values seen at the optimum moisture content. Figure 5.7 illustrates the modulus results of all alternate method testing on the 4 inch diameter specimens versus moisture content. The spread seen in resilient modulus for specific moisture contents is due to the effect of deviator stress. The data is limited in Figure 5.7 so in Figure 5.8 the alternate method M_r results of all test specimens versus moisture content, with more data points this gives better indication of how the results change with moisture and how the different specimen sizes compare to one another.

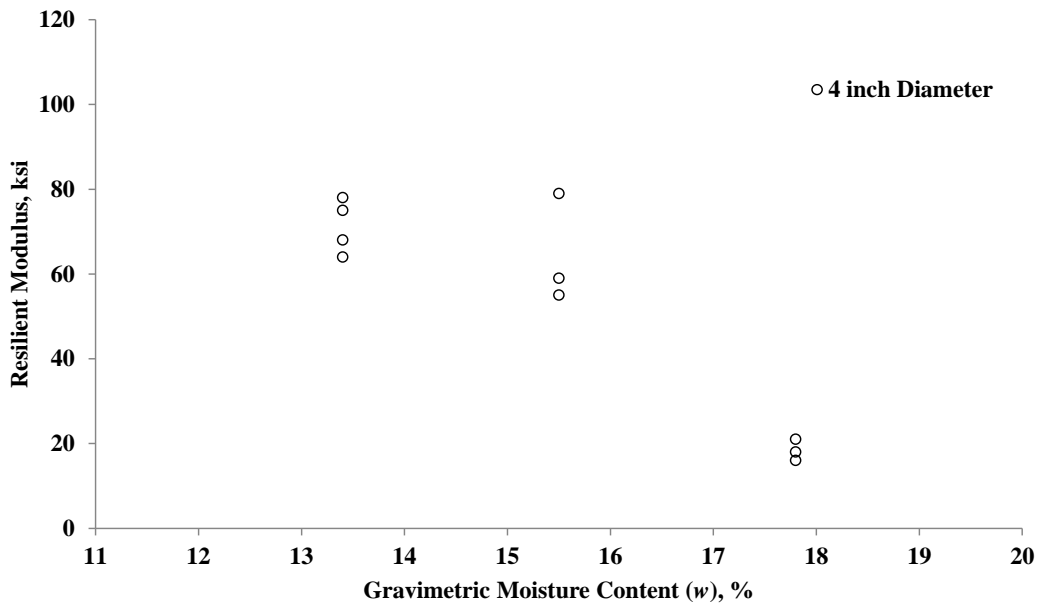


Figure 5.7 Alternate Method Resilient Modulus vs. Moisture Content for 4 in. Diameter

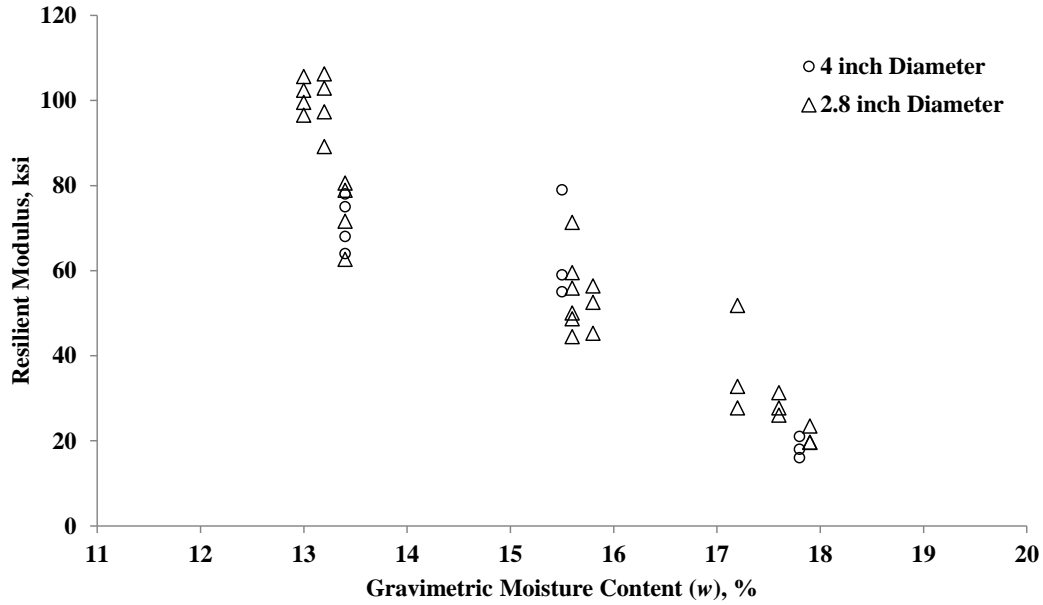


Figure 5.8 Alternate Method Resilient Modulus vs. Moisture Content for All Specimens

5.5 Comparison of 2.8 and 4 inch Diameter Alternate M_r Method Results

The same method of comparison used for the standard resilient modulus results is used to compare alternate method test results of 2.8 inch and 4 inch diameter specimens. Each 4 inch diameter specimen is compared to a 2.8 inch diameter specimen with the nearest moisture content. Table 5.7 lists the comparison results showing the compared groupings moisture contents and percent difference where the 4 inch diameter specimen is used as the reference. For a comparison of 10 test point pairs, 9 of 10 pairings showed a percent difference magnitude of 10% or less. Figure 5.9 shows the results plotted against a line of unity.

Table 5.7 Size Comparison of Alternate Method Resilient Modulus Results

Dry of Optimum			Optimum			Wet of Optimum		
Diameter (in.), Moisture Content (%)		%	Diameter (in.), Moisture Content (%)		%	Diameter (in.), Moisture Content (%)		%
2.8, 13.4	4.0, 13.4		2.8, 13.4	4.0, 13.4		2.8, 13.4	4.0, 13.4	
M_r (ksi)		difference	M_r (ksi)		difference	M_r (ksi)		difference
79	78		-1	71		79	10	
81	75	-7	60	59	-1	20	18	-10
72	68	-5	50	55	9	20	16	-25
63	64							

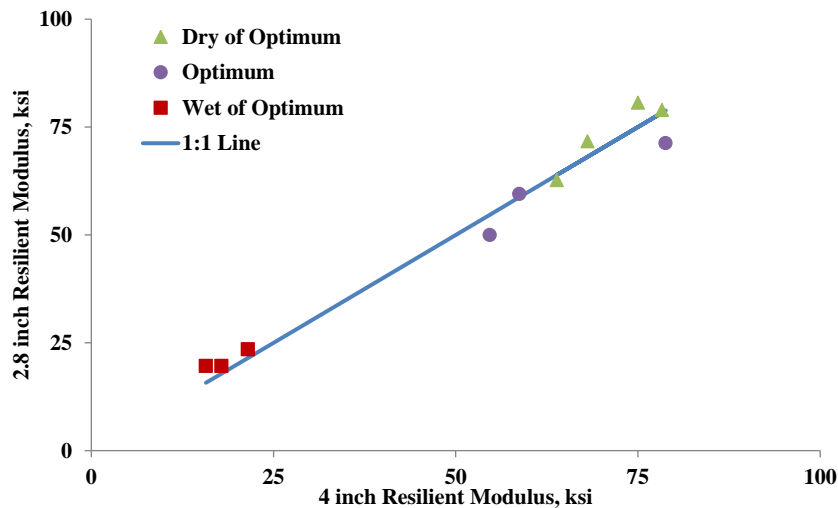


Figure 5.9 Alternate Method Resilient Modulus Specimen Size Comparison

5.6 Comparison of M_r Results Using Alternate and Standard Method

Two methods of regression were used to determine values based on the standard resilient modulus results which were presented in Chapter 4 to compare to the resilient modulus results measured from the alternate testing method. This is done because the alternate method maximum cyclic axial stresses fall between cyclic axial stress values tested using the standard test methodology. Method 1 determines a standard resilient modulus based on a linear

regression of all standard test results for respective specimen. Method 2 also determines a standard resilient modulus for comparison based on standard test results, but does it in a segmented approach. In this method, two points on either side (respective of max cyclic stress) of an alternate method point are interpolated. All values used for comparison originate from testing performed using the spring loaded LVDTs mounted on the specimen.

5.6.1 Comparison to Standardized M_r Using Linear Regression of Test Sets

The first method used to determine comparison resilient modulus results for the alternate results was a linear regression of the full data sets. The resilient modulus results for all specimen moisture contents and sizes largely followed a linear trend as a function of the maximum cyclic stress; therefore linear equations for each specimen as a function of this seemed sufficient for individual comparisons. An example of a set of regression fits is shown in Figure 5.10. In Table 5.8 a list of predicted M_r values, the R^2 of the fit used as a predictor, and the alternate test method modulus as well as the percent differences are presented.

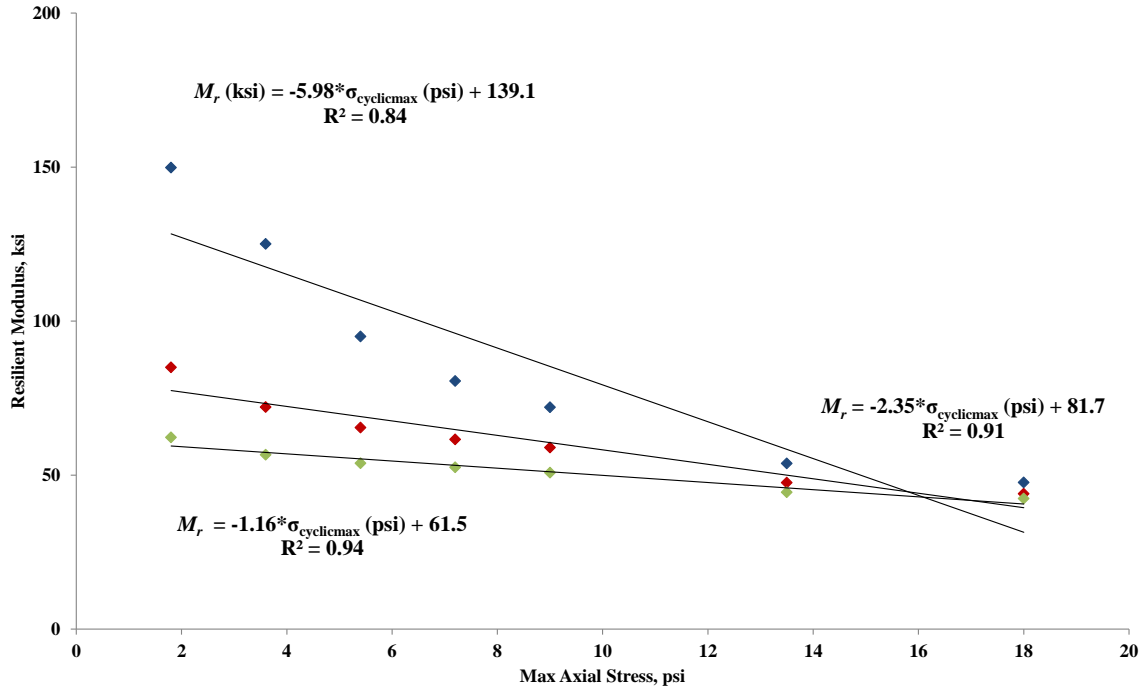


Figure 5.10 Example of Method 1 Prediction Fits for Standard M_r Results

Table 5.8 Standard vs. Alternate Experiment Test Results Method 1 Comparison

Dry of Optimum				Optimum				Wet of Optimum			
Standard M_r Trend R^2	Trend Predicted Standard M_r (ksi)	Alternate Test M_r (ksi)	% Difference	Standard M_r Trend R^2	Trend Predicted Standard M_r (ksi)	Alternate Test M_r (ksi)	% Difference	Standard M_r Trend R^2	Trend Predicted Standard M_r (ksi)	Alternate Test M_r (ksi)	% Difference
0.89	94	79	-15.8	0.91	68	56	-16.6	0.94	25	23	-7.2
	90	81	-10.0		58	53	-9.8		22	20	-9.6
	79	72	-9.3		49	45	-7.3		18	20	8.6
	68	63	-8.4		103	71	-30.9		34	31	-7.7
0.96	123	106	-13.4	0.84	79	60	-24.9	0.81	30	28	-7.5
	118	103	-12.9		55	50	-9.7		26	26	-0.2
	107	97	-8.8		55	56	2.5		50	52	2.7
	95	89	-6.6		50	49	-2.4		38	33	-12.8
0.72	119	102	-14.0	0.94	45	44	-1.7	0.85	25	28	11.7
	117	106	-10.0		95	79	-16.9		25	21	-13.7
	113	100	-12.1		82	59	-28.0		20	18	-11.6
	109	97	-11.6		68	55	-20.0		16	16	1.3
0.81	100	78	-21.9	0.95				0.90			
	94	75	-20.4								
	79	68	-14.0								
	64	64	-0.5								

From Table 5.8 it is seen that the majority of results (31 of 40 test comparisons) show a percent difference magnitude of less than 15%. The average absolute value of percent difference is about 11% for all specimen results compared. A plot of the predicted vs. alternate modulus method against a line of unity is shown in Figure 5.11. In this figure it is shown that modulus values from both methods show good agreement, particularly below values of about 60 ksi.

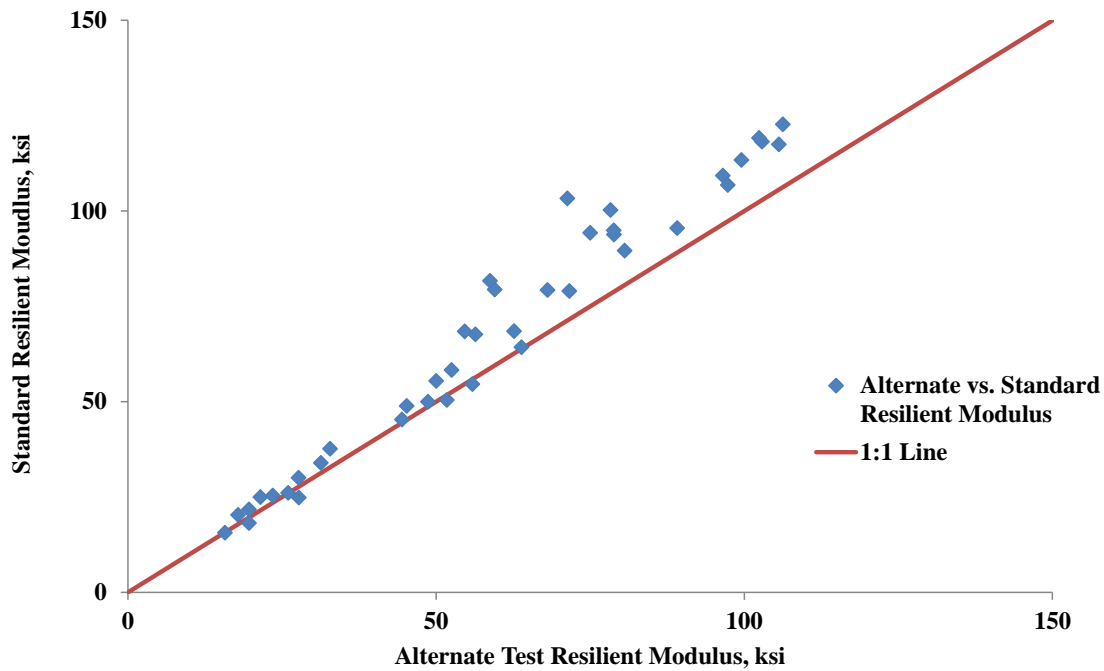


Figure 5.11 Test Method Comparison Plot 1

5.6.2 Comparison to Standardized Mr Using Segmented Regression Prediction

The second method used to determine comparison resilient modulus results for the alternate results used two segmented (piecewise) regression to predict values between two standardized test data points based on the variable of maximum cyclic stress. It was believed since each alternate method data point was tested at a stress level between two result points from the standard resilient modulus test, that this method of interpolation could yield better comparative

results due to the fact that it would eliminate influence of points at stresses further from the test point for comparison, like those at the lower deviator stresses. As expected this method improved the results, however since the first method compared well and majority of the fits were linear with generally good coefficient of determination values the improvement is not enormous. Table 5.9 shows the predicted and alternate modulus values as well as the percent differences between the two. In this case 35 of 40 test comparisons are within 15% difference, and the average of the absolute magnitude of differences is about 9%.

Table 5.9 Standard vs. Alternate Experiment Test Results Method 2 Comparison

Dry of Optimum			Optimum			Wet of Optimum		
Trend Predicted Standard M_r (ksi)	Alternate Test M_r (ksi)	% Difference	Trend Predicted Standard M_r (ksi)	Alternate Test M_r (ksi)	% Difference	Trend Predicted Standard M_r (ksi)	Alternate Test M_r (ksi)	% Difference
88	79	10.8	64	56	12.1	25	23	4.9
85	81	4.7	56	53	6.9	21	20	7.3
75	72	4.7	47	45	4.0	19	20	-4.9
71	63	12.0	90	71	20.9	33	31	4.0
121	106	12.4	68	60	12.4	29	28	4.2
116	103	11.2	53	50	5.9	27	26	4.7
103	97	5.6	53	56	-4.7	48	52	-8.5
97	89	8.0	49	49	1.4	34	33	3.9
117	102	12.6	44	44	-0.6	29	28	3.2
117	106	9.8	97	79	18.4	24	21	12.0
119	100	16.5	86	59	31.6	20	18	8.5
115	97	15.8	64	55	14.5	16	16	4.6
92	78	14.7						
86	75	12.4						
74	68	7.8						
69	64	7.9						

Figure 5.12 is a plot of the compared values as well as a line of unity. Again the best agreement is generally shown when modulus values are below about 60 ksi. Overall based on these

prediction methods the alternate test method seems to generate a similar modulus value to that of the standard resilient modulus value, with the exception that at higher modulus values (above about 75 ksi) it is conservative by about 10-20%. A couple reasons why the alternate test could yield lower results would be because it is unconfined and uses a longer loading time, however the softer (less stiff) specimens show good agreement.

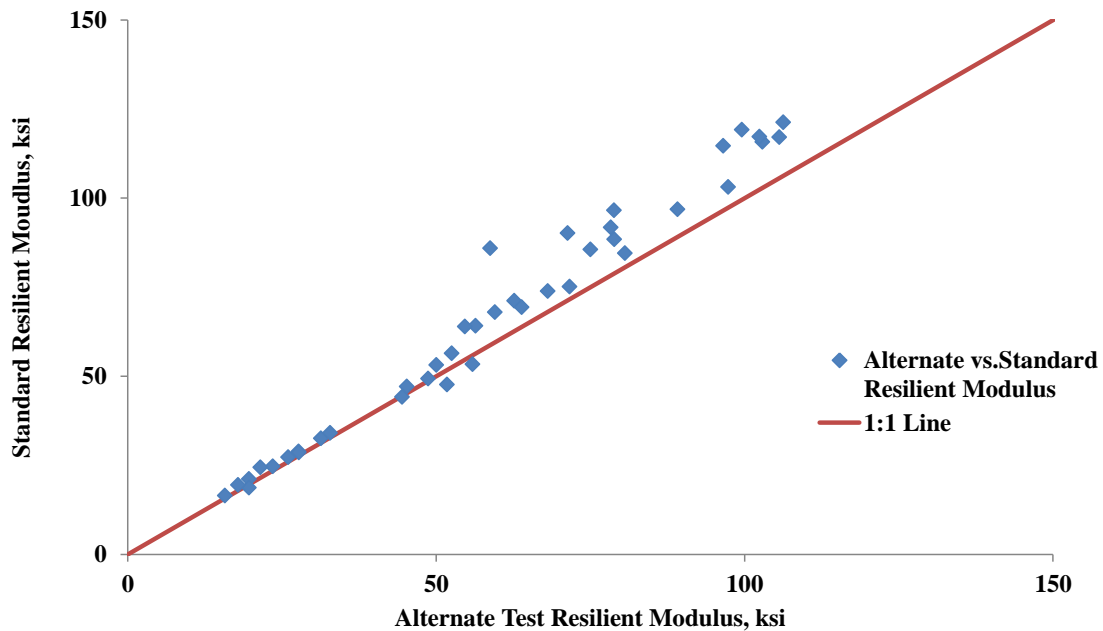


Figure 5.12 Test Method Comparison Plot 2

5.7 Alternate M_r Test Summary

In this chapter an alternate dynamic laboratory test was introduced, which attempts to more efficiently determine resilient modulus of cohesive fine-grained subgrade soils. Some of the differences between the alternate method and the standard standard M_r test sequences included: loading form and duration, number of cycles, and lack of confining stress. Comparisons between moisture contents, specimen sizes, and most importantly alternate test method and standard test

results were introduced. As expected, the M_r values determined from the alternate test showed decreasing behavior with increasing moisture content and max cyclic stresses. Specimen size results were compared in three pairs, for 9 of 10 test sequence results the magnitude of difference between the pairs was 10% or less, where 1 test sequence showed a 25% difference. The M_r results from the alternate testing shows promise as an alternative for determining resilient modulus in the laboratory, where one analysis showed 35 of 40 tests resulting in a magnitude difference of 15% or less.

CHAPTER 6

CONCLUSIONS AND RECOMMENDATIONS

6.1 General

In this study 12 specimens of A-6 soil were reconstituted using modified impact compaction at varying moisture contents while maximum dry density was not varied. Nine 2.8 inch diameter specimens were fabricated in replicates of three at dry of optimum, optimum, and wet of optimum conditions. Three 4.0 inch diameter specimens were fabricated, one each at dry of optimum, optimum, and wet of optimum conditions. Dynamic testing included resilient modulus testing and an experimental unconfined test. Resilient modulus testing was conducted using two methods of internal deformation measurement and one method of external deformation measurement, while the alternate method was conducted using one internal deformation measurement method. The deformation measurement method used in analysis and comparison as a reference for this study was the epoxy glued button method. Effects on resilient modulus were evaluated based on deformation measurement method, moisture content, specimen size, and test method (standard sequences vs. alternate method).

6.2 Conclusions

Based on this study, the following conclusions were made:

- M_r values determined using external deformation measurement were consistently lower than when internal deformations were measured. A comparison example showed the magnitudes of extraneous deformations (correcting for the internal load cell deformations) when using external LVDTs was larger than the deformations experienced

by the specimen according to the internal LVDT readings. This is consistent with results and concerns presented in the literature review concerning system compliance affecting resilient modulus.

- Comparison of the glued button and ring clamp LVDT methods show agreement between the two methods improve as maximum axial cyclic stresses increase, however at lower stress sequences the differences are very large.

- Using the internal reference deformation method, M_r variations were examined due to maximum cyclic stress amplitudes, moisture content, and confining pressure. Trends showed resilient modulus decreased significantly with increase in maximum cyclic stress amplitude and moisture content in an approximately linear fashion. While increases in confining pressure generally resulted in an increase in resilient modulus, the changes are considered insignificant in comparison to the other factors described. A predictive equation for this soil as a function of maximum axial cyclic stress and moisture content was developed using multivariate regression analysis that may have the potential to be used for Level 2 MEPDG design.

- Though limited, the results of the size comparison may warrant potential for future study. 6 specimens (3 pairs of 2.8 inch diameter and 4.0 inch diameter at dry of optimum, optimum, and wet of optimum moisture states) were compared. It was found that using equivalent compaction energy, 2.8 inch diameter specimens for this soil in the moisture ranges tested could be compacted to the desired 95-100% of maximum dry density using

3 equal lifts and approximately 25 blows per lift. In terms of magnitude of percent difference in M_r values between the sizes, 2 of 3 pairings behaved within 10 percent of one another on average across all maximum cyclic stresses for the reference confining pressure.

- A comparison in results from the experimental unconfined test and standard resilient modulus test showed good agreement, with 35 of 40 comparisons tests showing less than 15% difference between the two methods. The experimental test method is much faster because it eliminates test sequences and does not require a triaxial cell.

6.3 Recommendations

Based on the findings of this study, the following recommendations are made:

- Concern in literature and past research results have been presented in this paper which indicate the influence of system compliance on resilient modulus values. The results from this study support this concern. Since compliance varies from system to system and can easily change due to modifications to equipment used in testing (attachments to load rods, connections, etc.) and specimen end effects, it is recommended deformations be measured internally on the specimen.
- Currently NCHRP 1-28A requires internal sensors. While AASHTO T 307 calls for external sensors, this results in underestimation of resilient modulus by factors which can be highly variable. Also, NCHRP 1-28A has higher maximum axial stress values in its

testing sequence which based on this researcher's experience are more desirable in determining resilient modulus values, because it reduces the chance of deformation values recording below the typical 0.25% non-linearity range which is not uncommon (results at lower deviator stresses for dry of optimum and optimum specimens in this study). Subsequently, it is recommended that the NCHRP 1-28A standard be used as a protocol when conducting laboratory resilient modulus testing due to the on-specimen deformation method and higher stress values. However, given that NCHRP 1-28A subgrade sequences have 4 confining pressures and past studies as well as results from this study found confining pressure to have little effect on resilient modulus, it is recommended an option for unconfined testing of cohesive fine-grained subgrades be further studied.

- Also, based on the agreement in results of the experimental method with the standard test sequences it is recommended that for cohesive fine-grained subgrade soils, it is recommended that unconfined testing should be further examined as a potential MEPDG Level 2 test for such subgrade soils.

Recommendations for future studies:

- It is recommended that a pavement design study be performed investigating the effects of subgrade M_r with respect to system compliance influence. For a given subgrade, how much thicker would an asphalt surface layer need to be to achieve the same design life based on the differing resilient modulus results determined using internal and external LVDTs. This could further support or refute the recommendation for using a single protocol which calls for on specimen deformation measurement.

- The comparison of specimen sizes using modified impact compaction was limited. It is recommended more testing be performed pursuant to introducing impact compaction of reconstituted 2.8 inch diameter fine grained cohesive specimens. Impact compaction should be examined as an option for reconstituting specimens in the AASHTO T 307 standard due to the fact that moisture-density relationships are defined by this method of compaction.

- Reconstituting specimens using a split mold may not have been the most expedient method in regards to cohesive fine-grained soils. The top end of specimens was often quite uneven due to the hammer impact, and capping was required to create a smooth surface. A mold and jack extrusion method similar to that used for determining moisture-density relationships would provide the opportunity to create an even finish on the top end. This can eliminate time needed to cap, and since cohesive specimens can retain their shape a membrane could easily be placed over after extrusion. However, extra care would need to be taken during extrusion not to damage the specimen, this is one area where the split mold may be better.

- Due to the time and effort it takes to determine resilient modulus in the laboratory, it desirable to determine parameters which can be determined quickly in the field and correlated to the lab. A future study using an in-situ modulus measurement device on laboratory constituted specimens. One such instrument, the Clegg-Hammer has a model that delivers a dynamic impact resulting from a 10 lbf. free falling 18 inches, like the

impact delivered to by a modified proctor hammer. It would be interesting to see how Clegg Hammer results correlate with resilient modulus values determined in this study.

- Current constitutive models have incorporated water potential (or suction) as a stress parameter included for predicting resilient modulus behavior of cohesive fine-grained soils. Many methods exist for determining potential of soil water, the least time intensive may be to find a closed form solution or moisture characteristic curve for this soil type, moisture content, and density. Total potential or matric potential can also be determined via the filter paper method test. One or two lifts can be compacted and provide a sufficient quantity of soil for performing such a test. Additionally advanced dewpoint based potential measurement devices exist. Once a water potential is determined, a study can then be conducted to see how this soil and its resilient modulus values compare with the existing suction models, if the model can be calibrated for this soil, or a new model developed.

REFERENCES

- American Association of State Highway and Transportation Officials. "Determining the Resilient Modulus of Soils and Aggregate Materials." Specification Number T307-99. Standard Specifications for Transportation Materials and Methods of Sampling and Testing: Part 2B Tests.
- American Association of State Highway and Transportation Officials. "Moisture Density Relations of Soils Using a 4.54-kg (10-lb) Rammer and a 457-mm (18-in) drop." Specification Number T 180 (04). Standard Specifications for Transportation Materials and Methods of Sampling and Testing
- Andrei, D., M.W. Witzak, C.W. Schwartz, and J. Uzan. "Harmonized Resilient Modulus Test Method for Unbound Pavement Materials." *Transportation Research Record 1874*, pp. 29-37; Transportation Research Board.
- Andrei, D. *Development of a Predictive Model for the Resilient Modulus of Unbound Materials*. Phd. Dissertation. Arizona State University, 2003.
- Andrei, D. *Development of a Harmonized Test protocol for the Resilient Modulus of Unbound Materials Used in Pavement Design*. M.S. thesis. Department of Civil and Environmental Engineering, University of Maryland, College Park, 1999.

Barksdale, R.D., et al. *Laboratory Determination of Resilient Modulus For Flexible Pavement Design*. NCHRP Final Report 1-28 (NCHRP Web Document 14). Georgia Institute of Technology, 1997.

Barksdale, R.D., et al. *Laboratory Determination of Resilient Modulus For Flexible Pavement Design*. Interim Report, Georgia Institute of Technology, 1990.

Bejarano, M.O., A.C. Heath, and J.T. Harvey, “A Low-Cost High-Performance Alternative for Controlling a Servo-Hydraulic System for Triaxial Resilient Modulus Apparatus,” *Resilient Modulus Testing for Pavement Components*, ASTM STP 1437, G.N. Durham, W.A. Marr, and W.L. De Groff, Eds., ASTM International, West Conshohocken, PA, 2003.

Boudreau, R., and J. Wang, “Resilient Modulus Test – Triaxial Cell Interaction,” *Resilient Modulus Testing for Pavement Components*, ASTM STP 1437, G.N. Durham, W.A. Marr, and W.L. De Groff, Eds., ASTM International, West Conshohocken, PA, 2003.

Burczyk, J.M., K. Ksaibati, R. Anderson-Sprecher, and M.J. Farrar, 1994. “Factors Influencing Determination of a Subgrade Resilient Modulus Value,” *Transportation Research Record 1462*, pp.72-78; Transportation Research Board.

Durham G.N., Marr, W.A., and De Grof W.L., Eds., *Resilient Modulus Testing for Pavement Components*, ASTM International, West Conshocken, PA, 2003.

Drumm, E.C. et al., “Estimation of Subgrade Resilient Modulus From Standard Tests,” *ASCE Journal of Geotechnical Engineering*, Volume 116 No. 5, 1990.

Fredlund, D. G., A.T. Bergan, and P.K. Wong. Relation Between Resilient Modulus and Stress Conditions for Cohesive Subgrade Soils. Transportation Research Record 642; Transportation Research Board.

Groeger, J.L., G.R., Rada, and A. Lopez, “AASHTO T307 – Background and Discussion,” *Resilient Modulus Testing for Pavement Components, ASTM STP 1437*, G.N. Durham, W.A. Marr, and W.L. De Groff, Eds., ASTM International, West Conshohocken, PA, 2003.

Huang, Y.H., *Pavement Analysis and Design 2nd Edition*, Pearson Prentice Hall, Upper Saddle River, NJ, 2004.

Kim, Dong-Soo, and S. Drabkin, 1994. “Accuracy Improvement of External Resilient Modulus Measurements Using Specimen Grouting to End Platens,” *Transportation Research Record 1462*, pp.65-71; Transportation Research Board.

Kim, D., and N.Z. Siddiki. “Simplification of Resilient Modulus Testing For Subgrades,” FHWA/IN/JTRP-2005/23, Indiana DOT and Purdue University, West Lafayette Indiana, 2006.

Konrad, J., and C. Robert, “Resilient Modulus Testing Using Conventional Geotechnical Triaxial Equipment,” *Resilient Modulus Testing for Pavement Components, ASTM STP 1437*, G.N. Durham, W.A. Marr, and W.L. De Groff, Eds., ASTM International, West Conshohocken, PA, 2003.

Larson, G., and B.J. Dempsy. “Integrated Climatic Model, Version 2.0.” Report No. DTFA MN/DOT 72114, University of Illinois at Urbana Champaign, Urbana, Illinois, 1997.

Li, D., and E.T. Selig, “Resilient Modulus For Fine-Grained Subgrade Soils,” *ASCE Journal of Geotechnical Engineering*, Volume 120 No. 6, 2004.

Li, M.O., and B.S. Qubain, “Resilient Modulus Variations with Water Content,” *Resilient Modulus Testing for Pavement Components, ASTM STP 1437*, G.N. Durham, W.A. Marr, and W.L. De Groff, Eds., ASTM International, West Conshohocken, PA, 2003.

Liang, R.Y. et al., “Predicting Moisture-Dependent Resilient Modulus of Cohesive Soils Using Soil Suction Concept”, *ASCE Journal of Transportation Engineering*, Volume 134 No. 1, 2008.

Marr, W.A. et al., "A Fully Automated Computer Controlled Resilient Modulus Testing System," *Resilient Modulus Testing for Pavement Components, ASTM STP 1437*, G.N. Durham, W.A. Marr, and W.L. De Groff, Eds., ASTM International, West Conshohocken, PA, 2003.

MEPDG. "Guide for Mechanistic-Empirical Design of New and Rehabilitated Pavement Structures." (http://onlinepubs.trb.org/onlinepubs/archive/mepdg/Part2_Chapter2_Materials.pdf), (2004). 85pp.

Mohammad, L.N., A.J. Puppala, and P. Alavilli, "Influence of Testing Procedure and LVDT Location on Resilient Modulus of Soils," *Transportation Research Record 1462*, pp.91-101; Transportation Research Board, 1994

Mohammad, L.N., A.J. Puppala, and P. Alavilli. "Resilient Modulus of Laboratory Compacted Subgrade Soils," *Transportation Research Record 1504*, pp.87-102; Transportation Research Board, 1996.

Muhanna, A.S., M.S. Rahman, and P.C. Lambe, 1999. "Resilient Modulus Measurement of Fine-Grained Subgrade Soils," *Transportation Research Record 1687*, pp.1-12; Transportation Research Board.

NCHRP. <<Mechanistic-Empirical Design of New and Rehabilitated Pavement Structures.>>

National Cooperative Highway Research Program, NCHRP Project 1-37A Report,

National Research Council, Washington, D.C., 2004.

NCHRP, "Laboratory Determination of Resilient Modulus for Flexible Pavement Design."

NCHRP Research Results Digest No. 285, (January 2004) 52pp.

Pezo R.F., et al.. "Development of a Reliable Resilient Modulus Test For Subgrade and Non-

Granular Subbase Materials For Use in Routine Pavement Design." University of Texas at

Austin, 1992.

Tutumuler, E. and M. Thompson, "Progress Report on Laboratory Soil Test Results" Center of

Excellence for Airport Technology, University of Illinois, Urbana-Champaign, 2005.

Thompson, M.R., and Q.L Robnett. "Resilient Properties of Subgrade Soils." *Transportation*

Engineering Journal, Vol. 105, No. TE1, 1979.

Wolfe, W.E., and T.S. Butalia. "Continued monitoring of SHRP pavement instrumentation

including soil suction and relationship with resilient modulus." *Report No. FHWA/OH-*

2004/007, USDOT, FHWA, Washington D.C